# Fourth Image Guided Therapy Workshop

# WORKSHOP PROCEEDINGS




## October 12-13, 2011
## Arlington, VA

**www.ncigt.org**

# Welcome

Welcome to the Fourth Image-Guided Therapy workshop sponsored by the National Center for Image Guided Therapy (NCIGT), the Neuroimage Analysis Center (NAC) and the National Institutes of Health (NIH). The topic for this workshop is "Advanced Imaging Technologies and Methods for Image Guided Therapy" and the goal is to learn about state of the art and future trends in imaging for therapy. The program for this workshop includes a single track of invited scientific talks by thought-leaders in the field, as well as a poster session based on abstract submissions. The talks are divided into sessions that focus on imaging advances for prostate, cardiac, abdominal, and gynecological interventions, as well as on techniques for optical and thermal imaging across clinical specialties.

The overall goal of this workshop series is to assess the current needs and opportunities in the field of image-guided interventions and the role of NCIGT as a national center serving the greater IGT community. Similar to previous workshops in this series, we are honored to have in attendance our colleagues from academia, industry, as well as the National Institutes of Health.

We are pleased to announce that the next workshop in the series will be held on September 21, 2012 in Boston in conjunction with the Interventional MRI Symposium, which will be held on September 22-23. The 2013 workshop in this series will be in partnership with the Society for Minimally Invasive Therapy (SMIT).

We hope that you continue to contribute to the success of this workshop by your participation.

Sincerely,

Members of the Program Committee

## Program Committee

Ferenc Jolesz, MD, Chair

Clare Tempany, MD, Chair

Tina Kapur, PhD, Program Chair

Ron Kikinis, MD

Alexandra Golby, MD

William Wells, PhD

Nathan McDannold, PhD

Greg Clement, PhD

Ehud Schmidt, PhD

Kemal Tuncali, MD

Nobuhiko Hata, PhD

Akila Viswanathan, MD, MPH

Abraham Levy, PhD

John Haller, PhD

Keyvan Farahani, PhD

## Organizing Committee

Ferenc Jolesz, MD

Clare Tempany, MD

Tina Kapur, PhD

Danielle Chamberlain, BS, RT

Marianna Jakab, MS

# Program for Wednesday, October 12

| | | | |
|---|---|---|---|
| 10:00- 10:30 AM | Welcome | Advanced Multimodality Image Guided Operating (AMIGO) Suite | **Ferenc Jolesz, MD,** PI NCIGT, Brigham and Women's Hospital and Harvard Medical School |
| 10:30 AM- 12:00 PM | Session I: Prostate Interventions<br><br>Session Chair: Clare Tempany, MD | Tandem-Robot Assisted Laparoscopic Radical Prostatectomy (T-RALP) | **Misop Han, MD** John Hopkins University |
| | | Biopsy Tracking And MRI Fusion To Enhance Imaging Of Cancer Within The Prostate | **Daniel Margolis, MD** UCLA |
| | | MR-Guided Prostate Biopsy And Brachytherapy | **Kristy Brock, PhD** Princess Margaret Hospital, Toronto |
| 12:00 -1:00 PM | Working Lunch For NIH Program Officers And Investigators | | |
| 1:00-3:00 PM | Session II: Optical Imaging<br><br>Session Chair: David Boas, PhD | Intraoperative Optical Coherence Tomography For Assessing Tumor Margins And Lymph Node Status During Breast Cancer Surgery | **Stephen Boppart, MD, PhD,** University of Illinois Urbana-Champaign |
| | | Reflectance Confocal Microscopy Of Shave Biopsy Wounds In Patients With Skin Cancer: Feasibility Of Intra-Operative Mapping Of Tumor Margins | **Milind Rajadhyaksha, PhD,** Sloan-Kettering Institute for Cancer Research |
| | | 3D Optical Imaging And Digital X-Ray Of Breast Lesions | **David Boas, PhD,** Massachusetts General Hospital |
| | | In Vivo Detection Of Neoplasia In The Digestive Tract | **Thomas D. Wang, MD, PhD,** University of Michigan |
| 3:00-3:30 PM | Break | | |
| 3:30-4:30 PM | Session III: Small Business Innovations in Image Guided Therapy<br><br>Session Chair: Keyvan Farahani, PhD | MR-Guided Laser Ablation | **Roger McNichols, PhD** (Vice President, Visualase, Houston, TX) |
| | | Fast, Easy, And Accurate 3D Ultrasound Guidance For Surgical Needle Ablation | **Sharif Razzaque, PhD** (Chief Technology Officer, InnerOptic Technology, Inc., Chapel Hill, North Carolina) |
| | | Image Guided Interventional Ultrasound Ablation And Radiation Therapy | **Clif Burdette, PhD** (CEO Acoustic MedSystems) |
| 4:30-6:00 PM | Session IV: Thermal Imaging<br><br>Session Chair: Nathan McDannold, PhD | Prospective 3-D Treatment Planning For MR-Guided Laser Induced Thermal Therapy | **Jason Stafford, PhD,** University of Texas MS, Anderson Cancer Center |
| | | Improved MRI Temperature Imaging Using A Subject-Specific Biophysical Model | **Dennis Parker, PhD,** University of Utah |
| | | Noninvasive Estimation Of Temperature Change Using Pulse-Echo Ultrasound: In Vivo Results | **Emad Ebbini, PhD,** University of Minnesota Twin Cities |
| | | Focused Ultrasound Of The Liver During Free Breathing | **Kim Butts-Pauly, PhD,** Stanford |
| 6:15 PM | Poster Session & Reception | | |

# Program for Thursday, October 13

| | | | |
|---|---|---|---|
| 8:30-10:00 AM | Session V: Cardiac Imaging for Intervention<br><br>Session Chair: Ehud Schmidt, PhD | Real-time MRI-Guided Cardiovascular Intervention | **Robert Lederman, PhD,** NHLBI |
| | | Clinical Evaluation Of An Ultrasound Based Imaging System For Guiding Cardiac Ablation | **Patrick Wolf, PhD,** Duke |
| | | MRI Guided EP Ablation | **Henry Halperin, MD,** Johns Hopkins |
| | | 5-D Image Guided Cardiac Ablation Therapy | **Richard Robb, PhD,** Mayo Clinic |
| 10:00-10:30 AM | Break | | |
| 10:30 AM- 12:00 PM | Session VI: Abdominal Interventions<br><br>Session Chair: Kemal Tuncali, MD | 3T MRI For Abdominal Interventions And Computerized Monitoring Of Cryoablation | **Kemal Tuncali, MD**, Brigham & Women's Hospital & Harvard Medial School |
| | | US-Guided Liver Surgery | **Michael Choti, MD**, Johns Hopkins Surgery |
| | | Development Of An Intrabiliary MRI-Monitored Local Agent Delivery Technique: Toward MR/RF-Enhanced Chemotherapy Of Malignant Biliary Obstructions | **Xiaoming Yang, MD, PhD,** University of Washington |
| 12:00-1:00 PM | Poster Session and Lunch | | |
| 1:00-2:00 PM | KEYNOTE | Molecular Medicine and Imaging Science: Focus on Image-Guided Interventions | **Belinda Seto, PhD**, Deputy Director NIBIB |
| 2:00-2:30 PM | | Stimulated Raman Scattering Microscopy: Label Free Molecular Imaging for Medicine | **Sunney Xie, PhD**, Harvard University |
| 2:30-3:00 PM | Break | | |
| 3:00-3:30 PM | | NCI Programs in Image-Guided Interventions | **Keyvan Farahani, PhD,** NCI |
| 3:30-5:00 PM | Session VII: Image Guided Gynecologic Radiation Therapy<br><br>Session Chair: Akila Viswanathan, MD | Image Guided Gynecologic Brachytherapy | **Akila Viswanathan, MD,** Brigham & Women's Hospital/Dana Farber Cancer Institute & Harvard Medial School |
| | | Intra-Tumoral Metabolic Heterogeneity Of Cervical Cancer | **Perry Grigsby, MD**, Washington University, St Louis Metabolic Activity of Cervical Cancer |
| | | IGT For Cervix Cancer Using Diffusion Weighted And Dynamic Contrast Enhanced Magnetic Resonance Imaging (MRI) | **Nina Mayr, MD,** Ohio State University |
| | | Utility Of Preoperative Ferumoxtran-10 MRI To Evaluate Retroperitoneal Lymph Node Metastasis In Advanced Cervical Cancer: Results Of ACRIN 6671/GOG 0233 | **Mostafa Atri, MD,** University of Toronto |
| 5:00 PM | Adjourn | | |

## Table of Contents

## SESSION 7: IMAGE-GUIDED GYNECOLOGIC RADIATION THERAPY.
## CHAIR: AKILA VISWANATHAN, MD, MPH 83

**INVITED SPEAKERS**



**POSTERS**

# Advanced Multi-Modality Image Guided Operating (AMIGO) Suite

Ferenc Jolesz, MD
Brigham and Women's Hospital and Harvard Medical School

Imaging has become essential not only for the detection and monitoring of disease but also for therapeutic interventions. The overall goal of Image-guided Therapy (IGT) is to improve efficacy and reduce the morbidity of minimally invasive procedures by providing the physician with image-based anatomic and physiologic information in real time, intra-operatively or intra-procedurally.

The Advanced Multimodality Image Guided Operating Room (AMIGO) is an innovative surgical and interventional suite that is the clinical arm of the National Center for Image Guided Therapy (NCIGT) at the Brigham and Women's Hospital and Harvard Medical School. Since 1993 the Brigham's IGT Program has been an internationally recognized pioneer in real-time intraoperative MRI-guided interventions with 3,000+ surgical and interventional procedures performed. AMIGO, envisioned in 2002-2003 and completed in 2011, is a continuation of these prior efforts but with multimodal image guidance. AMIGO is a highly integrated, 5700 square foot, completely sterile, fully functional three room procedural suite that allows a multidisciplinary team of physicians to operate on patients with the benefit of intraoperative images from advanced imaging modalities. In AMIGO, real-time anatomical imaging modalities like x-ray and ultrasound are combined with cross sectional digital imaging systems CT and MRI. AMIGO also takes advantage of the most of advanced molecular imaging technologies like PET/CT and optical imaging to provide "molecular imaging-guided therapy". The use of multiple molecular probes increases the sensitivity and specificity of cancer detection with improved


definition of tumor margins. This will result in more complete surgical resection or thermal ablations of tumors. In addition to these multiple imaging modalities, AMIGO has guidance or navigational devices that can help the physicians to localize tumors or other targeted abnormalities that can be identified in the images but may not be visible on the patient. It is also possible to track the position of needles, catheters and endoscopes within the body. AMIGO combines imaging and guidance with the latest therapy and robotic devices. Multidisciplinary, multi-departmental use of AMIGO provides the 'test bed' to prototype, refine and standardize entire gamut of image-guided surgical procedures and interventions. Once perfected, clinically tested procedures would migrate out into the mainstream of the operating rooms and interventional suites. Supported by a medical and technical staff of surgeons and interventional radiologists, imaging physicists, computer scientists and biomedical engineers, AMIGO is a high-technology clinical research environment in which we will explore, develop and refine new approaches to open surgeries, percutaneous and transcutaneous interventions, various thermal ablations and endoscopies.

# Session 1: Prostate Intervention

Session Chair: Clare Tempany, MD

## Invited Speakers

1. Tandem-robot assisted laparoscopic radical prostatectomy (T-RALP).
   Misop Han, MD, JHU

2. Biopsy tracking and MRI fusion to enhance imaging of cancer within the prostate.
   Daniel Margolis, MD, UCLA

3. MR-guided prostate biopsy and brachytherapy.
   Kristy Brock, PhD, PMH, Toronto

## Posters

1. Statistical Learning Algorithm for Segmenting Prostate Tumors from DCE-MRI. J. Jayender, J. Tokuda, Y. Tang, K.G. Vosburgh and C.M. Tempany. Brigham and Women's Hospital, Boston, MA

2. Towards joint MRI-US based tissue typing and guidance for prostate interventions in AMIGO. Mehdi Moradi, PhD; Tina Kapur, PhD; William M. Wells, PhD; Firdaus Janoos, PhD; Andriy Fedorov, PhD; Kemal Tuncali, MD; Paul L Nguyen, MD; Clare M. C. Tempany, MD. Brigham and Women's Hospital.

3. Image-guided Focal Laser Ablation for Prostate Tumors. Anil Shetty, Ashok Gowda, Roger McNichols Visualase Inc. Houston, TX

4. Real-Time Tissue Change Monitoring on the Sonablate® 500 during High Intensity Focused Ultrasound (HIFU) Treatment of Prostate Cancer. Narendra T. Sanghvi, Wo-Hsing Chen, Roy Carlson, Toyoaki Uchida, G. Schatzl and M. Marberger. Focus Surgery, Inc., Tokai University, Medical University, Vienna.

5. Visualization of Patient-specific Model Based on Preoperative MRI for Robot-Assisted Laparoscopic Prostatectomy (RALP). Tokuda J, Hu, JC, Hata N, Fennessy F, Tempany C. Brigham and Women's Hospital, Boston, MA

6. Design Study for a Fully-Actuated MRI-Compatible Robotic Device for MRI-Guided Transrectal Prostate Injections. Jonathan Bohren, Iulian Iordachita, Louis L. Whitcomb. The Johns Hopkins University, MD.

7. Electrical Property Imaging for Enhanced TRUS-Guided Prostate Biopsy. Ryan Halter, Yuqing Wan, Andrea Borsic, Alex Hartov, Haider Syed, John Heaney, Dartmouth, Hanover NH

8. Needle Artifact Localization for Intraprocedural Biopsy Position Confirmation in 3T MRI-guided Robotic Transrectal Prostate Intervention. Sang-Eun Song, Nathan B. Cho, Iulian Iordachita, Peter Guion, Gabor Fichtinger, and Louis L. Whitcomb, JHU, NCI, Queens University.

9. Assessment of Motion and Targeting Accuracy during Transperineal MR-guided Prostate Biopsy. A. Fedorov, K. Tuncali, F. Fennessy, J. Tokuda, N. Hata, W.M. Wells, C. Tempany. Brigham and Women's Hospital, Boston, MA

10. An ultrasonic motor actuated robotic needle guide device for 3T MRI-guided transperineal prostate interventions. Sang-Eun Song, Junich Tokuda, Clare Tempany and Nobuhiko Hata, Brigham and Women's Hospital, Boston, MA

11. Multi-slice-to-volume registration for reducing targeting error during MRIguided transrectal biopsy. Andras Lasso1, Hadi Tadayyon, Aradhana Kaushal, Peter Guion, and Gabor Fichtinger. Queen's University, Laboratory for Percutaneous Surgery, Kingston ON, Canada; University of Toronto, Medical Biophysics; National Institutes of Health, Bethesda, MD.

12. RadVision: An Image-Guided Brachytherapy Planning/Implant Tool with Extensible Image Acquisition/Processing
    Jack Blevins, Junichi Tokuda, Robert Cormack, Junghoon Lee, Nathanael Kuo, Jerry Prince, Gabor Fichtinger, Clare MC Tempany, E Clif Burdette. Acoustic MedSystems, Inc., Brigham & Women's Hospital, Harvard University, Johns Hopkins University, Queen's University

# TANDEM-ROBOT ASSISTED LAPAROSCOPIC RADICAL PROSTATECTOMY (T-RALP)

M. Han, B. Trock, D. Petrisor, C. Kim, D. Stoianovici
Urology, Johns Hopkins Medical Institutions, Baltimore, MD,
United States of America

Introduction and Objective: The preservation of the neurovascular bundle (NVB) during radical prostatectomy improves the postoperative recovery of sexual potency. The accompanying blood vessels in the NVB can serve as a macroscopic landmark to localize the microscopic cavernous nerves in the NVB. We examined the feasibility of image-guided navigation using transrectal ultrasound (TRUS) to visualize NVB during robot assisted laparoscopic radical prostatectomy (RALP).

Methods: A novel, robotic transrectal ultrasound probe manipulator (TRUS Robot) was developed and used concurrently with the daVinci® surgical robot (Intuitive Surgical Inc., Sunnyvale, CA) in a tandem-robot assisted laparoscopic radical prostatectomy (T-RALP). We performed T-RALP on 46 subjects with prostate cancer. TRUS Robot steadily held the TRUS probe and allowed remote manipulation by the surgeon. We utilized the TilePro function of the daVinci system to visualize both the surgical field and the TRUS images simultaneously.

Results: As a part of an ongoing clinical trial, all 46 subjects underwent T-RALP without associated complications. Each T-RALP portion added less than 30 minutes to surgery. With the TRUS Robot, the surgeon was able to remotely control the TRUS probe and utilize the ultrasound images at critical points of the operation.

Conclusions: TRALP is safe and feasible. The use of TRUS imaging during radical prostatectomy can potentially improve the visualization of the NVB and subsequently improve postoperative recovery of potency in men.

**Title:** Biopsy Tracking and MRI Fusion to Enhance Imaging of Cancer Within the Prostate

**Authors:** Daniel J A Margolis MD[1], Dinesh Kumar PhD[2], Maria Luz Macairan RN[3], Ram Narayanan PhD[2], Shyam Natarajan PhD (candidate)[4], Leonard Marks MD[3]

**Affiliations:** UCLA Departments of 1: Radiology, 3: Urology, and 4: Biomedical Engineering; and 2: Eigen, Inc, Grass Valley CA

**Purpose:** Trans-rectal ultrasound (TRUS) guided 12-core sextant biopsy is falsely negative in up to 30% of cases when used for prostate cancer detection. MRI-identified targets and fusion of MRI data with TRUS in real time may improve biopsy targeting.

**Methods:** With IRB approval, 57 men underwent MRI with diffusion weighted imaging/apparent diffusion coefficient (ADC), dynamic contrast enhancement (DCE) and T2-weighted imaging on a 3.0 T magnet with external phased array. Targets were chosen based on decreased T2 signal, abnormally decreased ADC or abnormal DCE. Level of suspicion was scored on a 1-5 scale for each parameter. These men then underwent ultrasound-guided biopsies using MR/ultrasound fusion software (Artemis, Eigen) in addition to standard 12-core sextant biopsies.

**Results:** In 56 patients, 101 suspicious areas were identified by MRI. 28 positive targets were found in 22 men, including 19 Gleason 3+3 (68%), 8 Gleason 3+4 (29%), and one with HGPIN (3%).

A significant correlation was found with biopsy positivity and ADC ($p = 0.007$) and there was a trend to significance for discriminating Gleason 3+4 from combined Gleason 3+3 and negative biopsies ($p=0.08$).

Positive cores were found in 12 patients on targets only, including 6 Gleason 3+4. The Gleason score of systematic and targeted cores was identical in 8 patients, 2 Gleason 3+4 and 6 Gleason 3+3. In 7 patients systematic cores were positive with negative targets, all Gleason 3+3, less than 4 mm and less than 25 percent of the core, which qualifies the patient for active surveillance. In one patient positive for Gleason 4+4 disease, the systematic cores had penetrated the target but the targeted cores missed. In 28 patients, neither targets nor systematic cores were positive.

**Conclusions:** MRI-TRUS fusion for targeted prostate biopsies appears to find additional cancers, and does not appear to miss significant cancers. MRI-TRUS fusion biopsies may be able to replace systematic biopsies avoiding the discomfort and risks associated, improve diagnostic yield, and improve confidence in appropriateness of patients appropriate for active surveillance.

# MR-guided Prostate Biopsy and Brachytherapy

Kristy Brock[1,2], Jenny Lee[1], Jessy Abed[1], Deirdre McGrath[1], Navid Samavati[1], Warren Foltz[1], Peter Chung[1,2], Masoom Haider[3], Michael Jewett[4], Theo van der Kwast[5], Cynthia Ménard[1,2]

[1]Radiation Medicine Program, Princess Margaret Hospital, Toronto, Canada,
[2]Department of Radiation Oncology, University of Toronto, Toronto, Canada
[3]Sunnybrook Health Sciences Center, Toronto, Canada,
[4]Department of Surgical Oncology, Princess Margaret Hospital, Toronto, Canada,
[5]Department of Pathology, University Health Network, Toronto, Canada,

The research platform and results to date of an MR-guided system for prostate biopsy and salvage brachytherapy will be described. An integrated diagnostic MRI and interventional mapping biopsy procedure has been performed on patients under sedation in a 1.5-tesla (T) scanner, using a pelvic coil and an endorectal coil attached to a stereotactic transperineal template assembly (Hologic Inc, MA). The imaging examination included: conventional diagnostic axial T2-weighted (T2w), dynamic contrast-enhanced (DCE) MRI and diffusion-weighted MRI (ADC). The integrated biopsy procedure involved targeted radial biopsy of suspicious regions and random sextant sampling of the normal-appearing peripheral zone. All MR images, and their associated tumor contours, are mapped together to obtain the best estimate of the gross tumor volume. The biopsy results are then obtained to evaluate the accuracy of the MRI in detecting and delineating GTV boundaries for salvage brachytherapy. Results indicate that although MRI is a promising tool to detect regions of tumor recurrence, it is not sufficiently accurate to define boundaries, as the biopsy results changed the subsequent brachytherapy planning in 40% of patients.

Once the tumor boundaries are defined, it must be accurately mapped onto the MR image obtained at the time of brachytherapy, for patients electing this treatment option. Differences in patient position and relative location of the endorectal coil often limit the accuracy of a simple rigid registration between the tumor defined during the biopsy procedure and the image acquired at the time of catheter insertion just prior to high dose rate (HDR) brachytherapy. Deformable registration, using MORFEUS, a biomechanical model-based algorithm, has been employed to map the image/biopsy confirmed tumor onto the image acquired at HDR. The deformable registration is completed in under 5 minutes and does not interfere with the clinical workflow. The mapped tumor, based on MORFEUS, has been evaluated for both spatial accuracy and improvement over an clinician-based estimation of the tumor at HDR. The registration error is smaller than 1.5 mm, which is smaller than the largest voxel dimension. Small, but potentially relevant, dosimetric discrepancies were observed between the estimated and mapped, via deformable registration, tumor.

Alternatively, patients may elect to have a radical prostatectomy. These prostate samples then undergo whole mount histo-pathology, MR elastography for measurements of material properties, and deformable registration of the histo-pathology to the in vivo MR images. This provides validation of the diagnostic MR images for the entire prostate.

## Title: Statistical Learning Algorithm for Segmenting Prostate Tumors from DCE-MRI

**Authors:** J. Jayender[1,2,3], J. Tokuda[1,2], Y. Tang[1,2], K.G. Vosburgh[1,2,3] and C.M. Tempany[1,2]
[1]Department of Radiology, Brigham and Women's Hospital, [2]Harvard Medical School, [3]Clinical Image Guidance Laboratory, Boston, MA 02115, USA

**Purpose:** Model-based evaluation of tumor margins images from DCE-MRI depends on many factors such as MR technique, physiology, arterial input function and tracer delays leading to inaccurate tumor maps. The purpose is to develop a segmentation algorithm which can auto-segment peripheral zone (PZ) prostate tumors from DCE-MRI without requiring a model.

**Methods:** We have developed a new statistical learning algorithm (SLA) based on Hidden Markov Models to auto-segment PZ tumors from DCE-MRI. MRI data on 12 patients with confirmed adenocarcinoma were utilized in this study. DCE-MRI, T2 weighted, ADC images, and biopsy reports were collected. A radiologist (Rad1; 8 years experience) outlined the prostate PZ tumor boundaries based on T2 images, Subtraction images (second arterial phase image minus baseline image) and ADC images using 3D Slicer, with additional knowledge of the biopsy results. To evaluate the SLA approach, the ROI around the prostate was delineated and the Gadolinium concentration time profile at each voxel was logged in Slicer and input to the algorithm. The SLA clustered the concentration-time profile at all voxels into two classes and trained two models corresponding to "healthy" and "tumor" tissue using a few points in the clustered classes. For each remaining voxel, the probability of its concentration curve matching the models was computed, and a scalar color value, defined as the ratio of the log-likelihood of observing the sequence from the tumor model to healthy model, was assigned to the voxel. A second independent radiologist (Rad2;12 years experience) outlined the PZ tumors using only the resultant color map; this was compared to findings of Rad1.

**Results:** The result of Rad2 compared to Rad1 findings was: Accuracy=78.3%, Precision=85.7%, Sensitivity=90.0% and Positive predictive value= 85.71%. The amount of overlap, measured using Dice Similarity Coefficient, was 0.6 ± 0.1. Tumors in the posterior apex and left of the midgland reported in a single whole-mount pathology report were identified correctly by the SLA.

**Conclusion:** In this preliminary study, the SLA, a model free algorithm, appears to demonstrate high accuracy and precision in segmenting prostate tumors from DCE-MRI. This may be a useful tool for delineating tumors for image-guided interventions.

**Acknowledgements:** P41RR019703

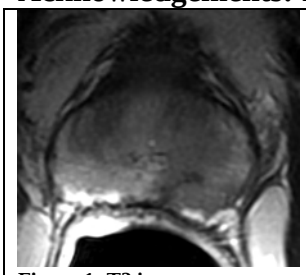

**Figure 1: T2 image**

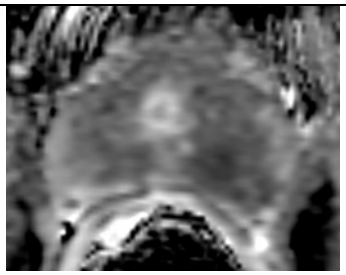

**Figure 2: ADC image**

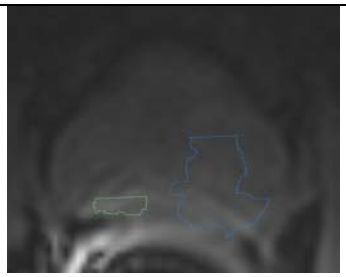

**Figure 3: DCE-MRI with tumor boundaries delineated by radiologist 1**

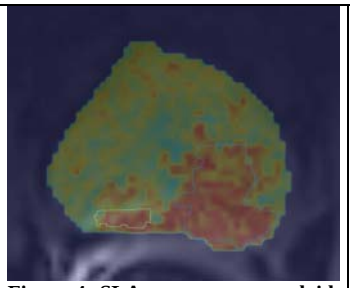

**Figure 4: SLA tumor map overlaid with radiologist finding. Red – tumor, Blue - healthy**

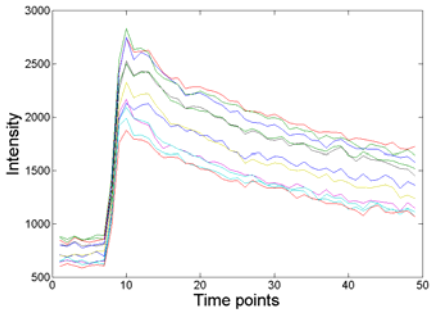


**Figure 5: Time-intensity curves for tumors**

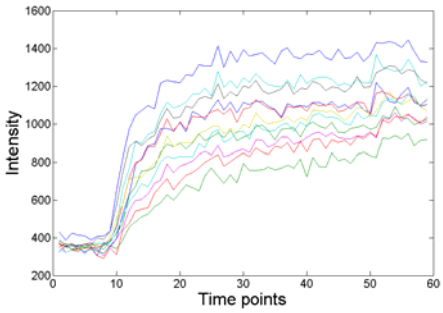


**Figure 6: Time-intensity curves for healthy tissue**

# Towards joint MRI-US based tissue typing and guidance for prostate interventions in AMIGO

Mehdi Moradi, PhD; Tina Kapur, PhD; William M. Wells, PhD; Firdaus Janoos, PhD; Andriy Fedorov, PhD;
Kemal Tuncali, MD; Paul L Nguyen, MD; Clare M. C. Tempany, MD
Department of Radiology, Brigham and Women's Hospital, Harvard Medical School, Boston, MA

**Purpose:** With an estimated 240,890 cases to be diagnosed in 2011, prostate cancer remains the most common malignancy (other than skin) among the men and is projected to cause 33,270 deaths. A non-invasive imaging technique that can reliably characterize and grade prostate cancer has the potential to improve the delivery of prostate interventions such as biopsy, prostatectomy and brachytherapy by providing the local extent of the disease and facilitating focal therapy. This can result in targeted biopsies, more accurate positive margins in prostatectomy, and enhanced dynamic dosimetry in brachytherapy. We have previously developed cancer detection and characterization techniques based on both multiparametric MRI [1] and ultrasound-based methods [2]. The goal of this work is to leverage our previous efforts and experience in the two areas and create the translational technology to perform MR-guided interventions assisted by tissue typing information from registered MRI and ultrasound.

**Methods:** The recent launch of the Advanced Multimodality Image Guided Operating (AMIGO) suite at BWH provides us with a unique opportunity to develop and validate the enabling technology to combine the state of the art methods in ultrasound and MRI based tissue typing techniques. The AMIGO suite features a 3T MRI wide bore (70 cm) Siemens Verio scanner streaming data through an OpenIGT link to 3D Slicer, and a Pro Focus ultrasound system (BK Medical Systems) with the capability of streaming both the B-mode images and raw RF ultrasound signals to an external PC through a camera link and custom software under development.

The access to ultrasound RF data gives us the ability to extract tissue typing features from the spectral analysis of the RF data [2,3], and work towards developing ultrasound elastography to compute tissue elasticity. MRI and ultrasound will be registered in 3D slicer environment and tissue typing features from ultrasound (texture features, RF spectral features, elasticity) and MRI (DCE and DTI features) will be combined for tissue classification. An MR compatible and US transparent adjustable sleeve template assembly is being developed to house the transrectal ultrasound probe and the MRI coil, interchangeably, during the procedures. This will ensure similar configurations of the prostate and the rectal wall during MRI scan and the ultrasound scan performed using a non-MR compatible transducer after the MRI magnet is moved out of the central part of the AMIGO suite.

**Previous experience:** Currently in BWH, brachytherapy procedures are performed with dynamic intraoperative dosimetry and robotic delivery. MRI is acquired pre-operatively in the assessment stage. However, images are not available during the implant procedure. The addition of MR-ultrasound fusion to the procedure will be the first step in the new initiative. Transition to AMIGO will follow and will take advantage of the MRI-compatible robotic technology developed in our group [4]. In the past we have reported on the BWH clinical experience with 3T MRI-guided transperineal prostate biopsy [5], and have now completed the first case of that type in AMIGO.

**Conclusions:** The AMIGO suite affords us the opportunity to develop and quantitatively validate the effects of registered MRI and ultrasound tissue typing. The final product will be translated to the conventional TRUS-guided interventional environment by using 3D ultrasound as the intraoperative modality and registration to pre-operative MRI. This will enable wider accessibility of the developed technology.

Acknowledgment: This work is partially supported by NIH grants R01CA111288 and P41RR019703, and DoD W81XWH-10-1-0201.

References:

[1] Chan I, et al., "Detection of prostate cancer by integration of line-scan diffusion, T2-mapping and T2-weighted magnetic resonance imaging; a multichannel statistical classifier," Medical Physics, 2003: 2390-2398.
[2] M. Moradi, et al., "Augmenting Detection of Prostate Cancer in Transrectal Ultrasound Images Using SVM and RF Time Series," IEEE TBME, 2009: 2214-2224.
[3] Feleppa EJ, et al., "Recent developments in tissue-type imaging (TTI) for planning and monitoring treatment of prostate cancer." *Ultrasonic Imaging*, 2004: 163-712.
[4] Fischer GS, et al., "Development of a Robotic Assistant for Needle-Based Transperineal Prostate Interventions in MRI," Proc. MICCAI 2007: pp 425-433.
[5] K. Tuncali, et al., "3T MRI-guided Transperineal Targeted Prostate Biopsy: Clinical Feasibility, Safety, and Early Results, Proc. ISMRM 2011: 53.

## Image-guided Focal Laser Ablation for Prostate Tumors

**Anil Shetty, Ashok Gowda, Roger McNichols**
**Visualase Inc. Houston, TX**

**Purpose:** Approximately 200,000 men in the US will be diagnosed with prostate cancer this year. MRI-guided focal laser ablation (FLA) of localized prostate cancer tumors may overcome side effects associated with currently standard whole-gland treatments. Recently multi-parametric magnetic resonance imaging (MRI) has been shown to be useful for localization of prostate tumors. The goal of this study was to develop techniques for implementing MR-guided FLA with real-time MR temperature monitoring in patients with low-risk, low-volume disease.

**Methods**: Men with biopsy-confirmed, MR-imageable prostate cancer with Gleason score $\leq$ 7 were offered FLA. Laser delivery was accomplished using either a trans-perineal (n=52) or trans-rectal (n=13) approach. For transperineal treatments, patients were placed supine inside the bore of a clinical high-field MRI, fitted with a perineal needle guide template and axial volume set acquired. Software (Visualase, Inc, Houston, TX) allowed identification of three fiducials on the template and subsequent projection of needle guide trajectories through the prostate volume. For transrectal treatments, a transrectal needle guide designed for MR-guided biopsy (DynaTRIM, Invivo, Peewaukee, WI) was fitted to the patient, similar imaging performed, and software (DynaLOC, Invivo) used to determine trajectory setting for reaching targets. In either case, a 14-cm catheter with titanium stylet was inserted to the targeted lesion. The stylet was replaced with a 15-Watt 980-nm laser applicator (400-micron-core-diameter silica fiber with diffusing tip in a 1.65mm water-cooled sheath). During continuous MR imaging, laser energy was delivered and the therapy workstation transferred MR images in real-time to display temperature changes in the tissue every 5 seconds. Laser doses of 7-12W were delivered for 60-120 seconds. Post-treatment contrast images were used to confirm treatment zones.

**Results:** Both systems enabled reproducible, accurate placement of applicators into desired anatomical targets in the peripheral and central zones and apex of the prostate. Real-time thermal monitoring was useful to ensure target destruction while avoiding heating of structures including rectal wall, neurovascular bundles, and urethra. Procedural time was as low as 75 minutes, with an average of 120 minutes. A laser exposure of 10 W for 75 seconds commonly resulted in an ablation area of 14 by 12 mm.

**Conclusion:** MR-guided FLA of prostate tumors with real-time thermal imaging is technically feasible, safe, and has a low rate of complications or side effects. It is a viable minimally invasive option for treating focal prostate tumors [Gleason 6-7 ], but long term followup studies need to completed before it is widely accepted in clinical practice.

Title: Real-Time Tissue Change Monitoring on the Sonablate® 500 during High Intensity Focused Ultrasound (HIFU) Treatment of Prostate Cancer

Authors: Narendra T. Sanghvi[1], Wo-Hsing Chen[1], Roy Carlson[1], Toyoaki Uchida[2], G. Schatzl[3] and M. Marberger[3]

Affiliation: [1]Focus Surgery, Inc., 3940 Pendleton Way, Indianapolis, Indiana 46226, [2]Department of Urology, Tokai University, Hachioji, Japan, and [3]Department of Urology, Medical University, Vienna, Austria

*Abstract:* Recently HIFU devices are used to treat prostate, kidney and other cancer using B-mode ultrasound guidance known as Visually directed HIFU. These changes are qualitative and operator dependent. There is a monotonic increase in ultrasound attenuation and backscattered ultrasound energy as tissue temperature elevates from 37° to 65°C and thereafter attenuation remains at the peak level. The backscattered Radio Frequency (RF) ultrasound signals contain information related to tissue changes. Therefore new research efforts are pursued in signal processing to analyze RF pulse-echo backscattered signals to estimate tissue alterations caused by HIFU energy. Based on these novel algorithms, Tissue Change Monitoring (TCM) software for the Sonablate® 500 systems has been developed that display quantitative information on tissue status during the HIFU exposure.

*Method:* The RF backscattered signals were acquired for each treatment site pre and post HIFU. These signals are processed by Fast Fourier Transform (FFT) to derive their frequency spectra. These spectra are further divided into sub, center and higher harmonic bands for calculating the changes in the energy levels. During the HIFU treatment green, yellow or orange color is overlaid on each treatment site on the B-mode image that represent low, medium and high levels of tissue change respectively along with a value of energy change (range 0-1). The software validation was conducted *in-vitro* using chicken tissue and tissue temperature was monitored with thermocouples to correlate energy change to measured temperatures at ultrasound energy deposition.

Clinical Validation: TCM *in-vivo* tests were conducted in a clinical study at the Tokai University Hachioji Hospital. Contrast enhanced MR Images of the prostate were taken post HIFU (24-48 hours). These images were compared to TCM data.

*Results: In-vitro* data resulted high degree of cross correlation ($R^2$>0.92) between temperature and RF signal energy level changes. Early clinical studies with TCM were conducted in Japan (n=97). Post HIFU contrast enhanced MRI showed whole gland tissue ablation. Pre and post HIFU treatment nadir PSA (ng/ml) median changed from 6.89 to 0.07.

*Conclusion*: TCM measurements are independent of ultrasound images and independent of the operator and provide essential feedback required to assure that tissues are properly treated. In some cases immediate feedback can allow re-treatment of undertreated sites.

*Acknowledgement*: This research was partially supported by NIH / NCI grant 5R44CA083244-03 and clinical study in Japan was sponsored by Takai Hospital Supply Co., Tokyo, Japan. Authors would like to thank all other TCM users for their input and feedback.

# Visualization of Patient-specific Model Based on Preoperative MRI for Robot-Assisted Laparoscopic Prostatectomy (RALP)

Tokuda J[1], Hu, JC[2], Hata N[1], Fennessy F[1], Tempany C[1]
Department of Radiology[1] and Division of Urologic Surgery[2], Brigham and Women's Hospital, Boston, MA, USA

## Introduction

Prostate cancer is the most common cancer among men in the U.S.; it causes about 28,660 deaths annually. Recently, RALP has supplanted conventional open retropubic radical prostatectomy (RRP), with advantages of less blood loss, pain, and shorter lengths of stay. However, comparisons of cancer control outcomes remain sparse with open RRP surgeon claims that palpation of the prostate during surgery aids in intraoperative decision-making regarding nerve-sparing to preserve sexual function versus a wider excision to prevent positive surgical margins. Prostate MRI imaging may aid in surgical planning and intraoperative decision making.. We present a method for assisting pre-operative planning and subsequent intra-operative guidance with imaging, utilizing '3D-Slicer'.

## Methods

Subjects underwent pre-operative staging MRI scans at 3T, with sequences optimized for tumor detection. The total gland, the tumor, the neurovascular bundles (NVB) and the external urethral sphincter (EUS) were manually segmented on the T2-weighted images using medical image processing and visualization software, 3D Slicer [1]. Apparent diffusion coefficient (ADC) maps generated from diffusion-weighted MRI was also referred to segment the tumor. A 3D patient-specific model was then generated from the label map by using marching-cube algorism available in 3D Slicer. The patient-specific model was reviewed in detail by the surgeon prior to the operation to gain a sense of tumor location within the gland and its proximity to the nerves.

## Results

As of September 8, 2011, a total of 21 patients were scaned were used to generate maps and 3D images. The models were easily accessible and provided a clear demonstration of tumor location and course of NVB for pre-operative planning. This application was noted to be most helpful in cases where a small degree of extracapsular extension was observed, requiring careful dissection of the adjacent NVB.

## Discussion

Current use of MRI enabled by the 3D-Slicer in the pre-operative planning of prostatectomies and its availability as a reference tool during the procedure is feasible and can be easily integrated into the pre-operative workflow. Further work seeks to overlay the 3D prostate MR models onto the visualization display of the *da Vinci* system at the command of the surgeon, to provide further intra-operative guidance. Real time imaging mapped to the pre-op MRI is a desirable future challenge.

**Acknowledgements** This work is supported by R01CA111288, P41RR019703, P01CA067165, U01CA151261, U54EB005149 from NIH, and Center for Integration of Medicine and Innovative Technology (CIMIT 11-325). Its contents are solely the responsibility of the authors and do not necessarily represent the official views of the NIH.

## Refereces

[1] Gering, D.T., A. Nabavi, R. Kikinis, N. Hata, L.J. O'Donnell, W.E. Grimson, F.A. Jolesz, P.M. Black, and W.M. Wells, 3rd, *An integrated visualization system for surgical planning and guidance using image fusion and an open MR.* J Magn Reson Imaging, 2001. **13**(6): p. 967-75.PMID 11382961

# Design Study for a Fully-Actuated MRI-Compatible Robotic Device for MRI-Guided Transrectal Prostate Injections

Jonathan Bohren, Iulian Iordachita, Louis L. Whitcomb

## I. Purpose

We report a design study and preliminary design of the latest in a family of MRI-compatible robotic devices for performing transrectal MRI-guided prostate interventions. This device, named the *Access to the Prostate Tissue Robot, Generation IV, or APT-IV*, is designed to perform MRI-guided transrectal needle interventions of the prostate under clinician control while the patient and device remain within the bore of a closed MRI scanner. This differs from most previously reported MRI-guided prostate needle intervention systems, including our own, in which needle insertion is performed outside the MR bore. Needle insertion within the scanner bore may offer several advantages including reduced procedure time, increased targeting accuracy, and the ability to perform real-time monitoring of needle insertion.

## II. Methods

We reported the design and testing of the unactuated (APT-II) and partially actuated (APT-III) devices with a needle workspace identical to that of the APT-IV. The APT-III provides two degrees-of-freedom (DOF) of actuation to orient a needle guide used for manual needle insertion. The novel feature of the APT-IV design is an actuated needle-insertion stage (3-DOF) suitable for therapeutic injection. The APT-IV design utilizes non-magnetic ultrasonic actuators for needle orientation and insertion, to both minimize the complexity of the power transmission and reduce the footprint of the device.

## III. Results

To date, the APT-I and APT-II systems have been employed to perform injection, fiducial seed insertion, and/or biopsy of the prostate in 58 clinical procedures at National Institutes of Health National Cancer Institute Bethesda, MD, the Radiation Oncology Department at Princess Margaret Hospital, Toronto, Canada, and the Johns Hopkins University Department of Radiology, Baltimore, MD. We have analyzed data from 12 of these procedures in order to better-define the anatomical constraints imposed by the MR bore and patient anatomy. These data validate the feasibility of the APT-IV design, and we show that its footprint is small enough to enable remote-controlled in-bore needle insertions.

## IV. Conclusion

We report a design study and preliminary design for a novel 3-DOF device for MRI-guided transrectal prostate interventions. The APT-IV will enable clinicians to perform MR-guided needle insertions while a patient is inside an active MR bore. This has the potential to make transrectal prostate interventions faster, more accurate, and also permits real-time tracking during needle insertion.

The authors are with the Department of Mechanical Engineering at The Johns Hopkins University, Bethesda, MD, USA

# Electrical Property Imaging for Enhanced TRUS-Guided Prostate Biopsy

Ryan Halter[1,2,4], Yuqing Wan[1], Andrea Borsic[1], Alex Hartov[1,4], Haider Syed[1], John Heaney[1,2,3,4], John Seigne[2,3,4], Alan Schned[2,3,4], Michael Baker[2,3]

[1]Thayer School of Engineering, Dartmouth College, Hanover, NH, [2]Dartmouth Medical School, Hanover, NH, [3]Dartmouth-Hitchcock Medical Center, Lebanon, NH, [4]Norris Cotton Cancer Center, Lebanon, NH

**Purpose**
Currently employed transrectal ultrasound (TRUS)–guided prostate biopsy procedures miss up to 30% of all cancers and are not able to accurately gauge the extent and aggressiveness of the disease. Recent studies by our group have shown that significant electrical property differences existing between malignant and benign prostate tissues provide levels of contrast exceeding those of routinely employed sensing and imaging technologies including TRUS.

**Methods**
We have developed an integrated electrical property imaging and sensing device coupled to a side-fired TRUS-probe to improve biopsy guidance and enhance prostate cancer detection and staging. The imaging device has been used to image a series of 50 men immediately prior to undergoing radical prostatectomy and electrical property images have been compared to histological assessment of the extracted prostate. We have also instrumented an end-fired TRUS probe with electrical property sensors in order to perform electrical property imaging during conventional biopsy approaches (end-fired vs. side-fired).

**Results**
Paired t-tests revealed that electrical property image pixels of prostate cancer were significantly different than those of bengin tissues ($p<0.03$) in the cohort of men imaged during radical prostatectomy. Image reconstruction algorithms developed to incorporate sensors on the biopsy needle demonstrate an obvious improvement in identifying inclusions within a prostate. Augmenting an end-fired probe with electrical property sensors does not impede routine biopsy; multiple clinical biopsies have been performed with the electrical property sensors integrated onto an end-fired probe.

**Conclusions**
We have demonstrated that 1) electrical property imaging is able to discriminate between cancer and non-cancerous prostate, 2) incorporating internal electrical property sensors improves image contrast, resolution, and accuracy, and 3) augmentation of a clinically standard end-fired TRUS probe with electrical property sensors is a feasible approach to multi-modal TRUS and electrical property imaging. Further development and additional pre-clinical trials with an end-fired TRUS probe configuration is necessary to demonstrate clinical efficacy of this dual-modality image-guided prostate biopsy system.

**Needle Artifact Localization for Intraprocedural Biopsy Position Confirmation in 3T MRI-guided Robotic Transrectal Prostate Intervention**

Sang-Eun Song[1, *], Nathan B. Cho[1], Iulian Iordachita[1], Peter Guion[2], Gabor Fichtinger[3], and Louis L. Whitcomb[1]

[1] Laboratory for Computational Sensing and Robotics, The Johns Hopkins University, Baltimore, Maryland, US

[2] Radiation Oncology Branch, National Cancer Institute, National Institutes of Health, Bethesda, Maryland, US

[3] School of Computing, Queen's University, Kingston, Ontario, Canada

[*] Currently with NCIGT, Brigham & Women's Hospital and Harvard Medical School, Boston, MA, US

* Corresponding author: S. Song (sam@bwh.harvard.edu)

**Purpose**

In MRI-guided needle interventions, after a biopsy needle is inserted, the needle position is often confirmed with a volumetric MRI scan. However, commonly used titanium needles are not directly visible in an MR image, but they generate a susceptibility artifact in the immediate neighborhood of the needle. The objective of this phantom study is to map the spatial relationship between observed needle artifact and true needle position in the operational volume of the APT robot that we developed and evaluated in clinical trials for MRI-guided transrectal needle access of the prostate.

**Methods**

We conducted a phantom experiment using a 150 mm 14G MRI-compatible automatic titanium biopsy gun, and a 14 gauge sized glass rod with conical tip to identify the true needle position. A set of 15 needle positions that cover the APT targeting range were selected and the titanium needle and glass rod were inserted at each position. 30 volumetric MR axial volumetric scans of needles were obtained and analyzed.

**Results**

The geometry and position of both titanium needle and glass rod were identified by connecting the center of artifact void from each axial scan. The artifact localization resulted that the titanium needle tip artifact extended approximately 9 mm beyond the actual needle tip location with tendency to bend towards the scanner's $B_0$ magnetic field direction, and axially displaced 0.38 mm and 0.32 mm (mean) in scanner's frequency and phase encoding direction, respectively. This accuracy is significantly smaller than commonly accepted values of clinically significant prostate tumor size.

**Conclusions**

We conducted a quantitative study of the relation between the true position of titanium biopsy needle and the corresponding needle artifact position in MR images to provide a better understanding of the influence of needle artifact on confirmation imaging of MRI-guided transrectal prostate biopsy. The results suggest that clinicians can locate true needle position from confirmation images of needle artifacts with satisfactory accuracy.

**Assessment of Motion and Targeting Accuracy during Transperineal MR-guided Prostate Biopsy**

*A. Fedorov, K. Tuncali, F. Fennessy, J. Tokuda, N. Hata, W.M. Wells, C. Tempany*
*Surgical Planning Laboratory, Brigham and Women's Hospital, Boston, MA, USA*

**Purpose:** (1) To quantify intra-procedural motion of the prostate and evaluate the accuracy of targeting of cancer-suspicious foci in the prostate gland during 3T MRI-guided 18G core needle transperineal prostate biopsy, and (2) to evaluate the utility of image registration for intra-procedural compensation of prostate motion and deformation.
**Methods:** The study was conducted retrospectively using the imaging and biopsy target locations acquired for patients (N=11) undergoing MR-guided targeted prostate biopsy in a wide-bore (70 cm) Siemens Magnetom Verio 3T MRI scanner. The patients were immobilized on the table top with velcro wrap. External imaging coil and intravenous conscious sedation was used. Biopsy targets were prospectively identified on the pre-procedural T2-weighted (T2w) axial scans aided by multi-parametric data that included T1w, diffusion-weighted (DWI), dynamic contrast-enhanced (DCE) MRI and derived pharmacokinetic maps from DCE MRI. Biopsies were performed as described in [1]. Intra-procedural imaging included an initial T2w scan to register pre-procedural planning data, and subsequent T2w scans during the procedure to demonstrate the biopsy needle location before the specimen collection. Intra-procedural motion of the pelvis and prostate gland relative to the initial intra-procedural scan were characterized by rigid transformations recovered by intensity-based image registration [2,3]. Displacements of the planned biopsy targets were characterized using deformable transformations based on registration of the prostate gland region of the image [2,3]. The needle shaft line trajectory was defined in the needle confirmation images by two points placed manually. Targeting error was defined as the distance from the needle to the targets following registration of the needle confirmation scans.
**Results:** Image registration involved manual segmentation of the prostate in selected (at most 2 per case) needle confirmation images, and 1-2 minutes of computation. Registration quality was evaluated qualitatively and was deemed successful in most of the cases. The dominant component for pelvis and prostate motion was in cranio-caudal direction (10 out of 11 cases). The magnitude of prostate motion was larger than the global pelvic motion in 7 out of 11 cases. The time between the initial intra-procedural scan and the final needle confirmation scan varied from 69 to 130 minutes. Magnitude of displacements for pelvis, prostate gland and the largest displacement among planned biopsy targets showed high to very high correlation with the time since the initial intra-procedural scan in 7, 6 and 5 cases, respectively. Maximum displacement of the planned biopsy targets ranged from 8 to 19.7 mm. Average targeting error was 4.3 mm (range 0.6 to 10.9 mm).
**Conclusions:** Based on our preliminary evaluation, there appears to be significant motion of the prostate throughout the procedure that cannot be completely resolved by compensating for pelvic motion. Continuous monitoring of the biopsy locations is therefore recommended during the intervention. Estimation of the target movement and compensation for prostate motion using primarily visual assessment by the interventional radiologist resulted in the average targeting error of 4.3 mm. Image registration to the repeated intra-procedural scans of the prostate gland offers a fast and robust approach which should be evaluated as part of the interventional biopsy workflow.
**Acknowledgments** This work was supported by NIH grants R01 CA111288, P41 RR019703, P41 RR013218, P01 CA067165, and U01 CA151261.

**References**
[1] K. Tuncali et al. 3T MRI-guided Transperineal Targeted Prostate Biopsy: Clinical Feasibility, Safety, and Early Results. 19th ISMRM Annual Meeting, 2011.
[2] A. Fedorov et al. Hierarchical Image Registration for Improved Sampling during 3T MRI-guided Transperineal Targeted Prostate Biopsy. 19th ISMRM Annual Meeting, 2011.
[3] 3D Slicer Software. *http://slicer.org*

# An ultrasonic motor actuated robotic needle guide device for 3T MRI-guided transperineal prostate interventions

Sang-Eun Song, Junich Tokuda, Clare Tempany and Nobuhiko Hata

NCIGT, Radiology Department, Brigham & Women's Hospital and Harvard Medical School, Boston, MA, US

* Corresponding author: S. Song (sam@bwh.harvard.edu)

**Purpose**

Despite emerging MRI and robotic technologies in the recent years, transrectal ultrasound (TRUS) guided procedure remains as the main prostate procedure in clinical practice due to complexity of the MRI-guided robotic interventions. To shorten the gap between widely used TRUS and prototype level MRI-guided robotic interventions, we developed an MRI-compatible motorized needle guide device "Smart Template" that resembles a conventional prostate template to perform MRI-guided prostate interventions.

**Methods**

We designed and developed the Smart Template consisting of vertical and horizontal crossbars that are driven by two ultrasonic motors via timing belt transmission. Navigation software that controls the crossbar position to provide needle insertion positions was developed, which can be operated independently or interactively with an open-source navigation software, 3D Slicer. Hardware and navigation software have been fabricated and successfully integrated. MRI distortion and SNR tests were conducted for preliminary evaluation.

**Results**

Significant MRI distortion was found around the brass components of the template. However, the affected volume is far from clinical region of interest. SNR values were measured and insignificant image degradation was observed except the motor moving configuration, suggesting that real-time imaging during motorized needle insertion can be problematic.

**Conclusions**

In order to bridge the gap between conventional TRUS and complex robotic interventions, we developed a motorized needle guide device, Smart Template, for MRI-guided transperineal prostate interventions. To evaluate the device, MRI distortion and SNR tests were conducted. Insignificant MRI distortion was observed around the clinical region of interest. In real-time imaging during motorized needle insertion, noticeable image degradation was measured.

# Multi-slice-to-volume registration for reducing targeting error during MRI-guided transrectal biopsy

Andras Lasso[1], Hadi Tadayyon[2], Aradhana Kaushal[3], Peter Guion[3], and Gabor Fichtinger[1]
*[1]Queen's University, Laboratory for Percutaneous Surgery, Kingston ON, Canada; [2]University of Toronto, Medical Biophysics; [3]National Institutes of Health, Bethesda, MD, USA*

**Purpose**

MRI has been shown to be a valuable tool for guiding prostate biopsy. Biopsy target points are selected in an image acquired at the beginning of the procedure. Intra-procedural patient motion dislocates the target points, which results in targeting error. Image registration methods can be used to estimate the patient motion. If the patient motion is known then the actual target positions can be computed, which results in reduced targeting error. Most of the existing registration methods require lengthy volumetric image acquisition. A method that can recover the prostate motion from only a few image slices may better fit into the interventional workflow and could be utilized frequently during interventions.

**Methods**

A registration method was developed to align the volumetric image that was used for planning to a set of orthogonal image slices that were acquired right before needle insertion. The registration method is composed of a preprocessing step and two registration stages. The preprocessing step involves intensity inhomogeneity correction using the N4ITK method and construction of a sparse volumetric image from the image slices. The first registration stage is a rigid registration to obtain an initial pose of the target planning volume, which is then non-rigidly registered to the fixed sparse volume in the second stage. Mutual information is used as similarity metric. A grid with 30mm spacing between the control points and B-spline interpolation is used to model the deformation. Simple gradient descent and L-BFGS-B optimizers are used in the first and second stages, respectively.

**Results**

The intra-procedural prostate motion compensation method was tested on simulated and clinical images using three orthogonal intra-procedural slices. Simulation results showed that the slice-to-volume registration reduced the initial (without registration) error of 2.1–5.6 mm to as low as 0.6–0.9 mm. Testing on clinical images taken during 4 different MRI-guided robot-assisted prostate biopsy procedures resulted in a mean registration error of about 1mm. Average computation time of the registration was about 40 seconds.

**Conclusions**

The proposed registration technique is a promising method for reducing the targeting error during MRI-guided prostate biopsy procedure, which provides considerable error reduction, without requiring lengthy volumetric image acquisitions. The next step in this work is extensive testing of the algorithm on image slices acquired during clinical procedures.

# RadVision: An Image-Guided Brachytherapy Planning/Implant Tool with Extensible Image Acquisition/Processing

Jack Blevins[1], Junichi Tokuda[2], Robert Cormack[2], Junghoon Lee[3], Nathanael Kuo[3], Jerry Prince[3], Gabor Fichtinger[4], Clare MC Tempany[2], E Clif Burdette[1]
[1]Acoustic MedSystems, Inc., [2]Brigham & Women's Hospital, Harvard University, [3]Johns Hopkins University, [4]Queen's University

## Purpose:

RadVision is developed to become a commercial product that provides a capability for real-time image guided interventional delivery of radiation sources primarily for treatment of prostate cancer and simultaneous intraoperative dosimetry and rapid implant re-optimization during the procedure. This new system incorporates the results of research performed by teams from Acoustic MedSystems, Brigham & Women's Hospital, John Hopkins University, and Queen's University. A major aspect of this research is the use of higher quality MR imaging to better define the prostate anatomy to facilitate improved implant accuracy. The goal is to apply these results to achieve improved therapeutic and quality of life outcomes for each patient.

## Methods:

The basic design principle of RadVision is to create an environment where both the user interface and data processing facilities are flexible and highly extensible. The result is a non-traditional Windows application that maintains isolation of the user interface and data processing functions to achieve this desired result. One benefit from this design is image acquisition. The program can accept streaming images from multiple sources simultaneously. The image sources include: real time MR (openIGTLink), real time ultrasound (video capture), real time Fluoroscopy (video capture), pushed DICOM images, DICOM files, and Jpeg/Bmp/Tiff ultrasound files. The DICOM files may contain MR, CT, PET/CT or ultrasound images. An image may have any orientation and use any coordinate system. During import, the image coordinate system is converted to an internal coordinate system convenient for Windows based image display. Following image import, all image coordinates are displayed in a user selected coordinate system (LPS, RAS, etc.). RadVision's image import processing results in a custom internal format which permits the application of the same image processing tools regardless of the original modality, and provides image output consistent with the application coordinate system. Dosimetry is updated based on actual implant specific spatial locations of inserted seeds and needles. A rapid iterative dose optimization algorithm incorporating case specific boundary conditions re-optimizes the remaining seeds to be implanted.

## Results:

For brachytherapy, the dose to target, nearby anatomical structures, needle positions, and seeds on 2D images or throughout a 3D volume are requirements for planning. RadVision overlays these items on real time images for monitoring a seed implant. To achieve the best outcome, the resulting seed positions are accurately identified, immediate changes in dose based on actual seed position are determined, and the plan for balance of implant adjusted accordingly. The images acquired using real time MR, pushed DICOM, and real time ultrasound provide visualization for the physician. Intraoperative fluoroscopy (3 images) provides for the use of automated algorithms for seed reconstruction and registration with the target volume. Seed localization and reconstruction accuracy in actual target volume exceeds 99%. Re-optimization of implant requires 30-45 seconds.

## Conclusions:

Developing an application that supports extensible imaging capabilities and meets FDA development guidelines has been realized. The modular design incorporates new algorithms and processes to identify seeds / needles with the objective to provide improved clinical outcomes.

### Acknowledgements:

Special acknowledgement is for important and seminal work on this project performed by the following individuals: Ameet Jain (Philips Research), Anton Deguet (Johns Hopkins), Pascal Fallavollita (Technische Universitat Munchen), Ehsan Dehghan (Queen's & Johns Hopkins), Nobuhiko Hata (Brigham & Women's), Maria Ayad (Johns Hopkins), Randy Stahlhut (Acoustic MedSystems), Paul Neubauer (Acoustic MedSystems).

## Session 2: Optical Imaging

Session Chair: David Boas, PhD

## Invited Speakers

1. Intraoperative optical coherence tomography for assessing tumor margins and lymph node status during breast cancer surgery.
   Stephen Boppart, MD, PhD, University of Illinois Urbana-Champaign

2. Reflectance confocal microscopy of shave biopsy wounds in patients with skin cancer: feasibility of intra-operative mapping of tumor margins.
   Milind Rajadhyaksha, PhD, Sloan-Kettering Inst for Cancer Research

3. 3D optical imaging and digital xray of breast lesions.
   David Boas, PhD, Massachusetts General Hospital

4. In vivo detection of neoplasia in the digestive tract.
   Thomas D. Wang, MD, PhD, University of Michigan

## Posters

1. Rapid mosaicing of large areas of tissue by strip scanning.
   Sanjee Abeytunge, Yongbiao Li, Bjorg Larson, Brian Park, Emily Seltzer, Milind Rajadhyaksha, Ricardo Toledo-Crow. Memorial Sloan Kettering Cancer Center NY, NYU, Livingston High School, Livingston, NJ

2. Improved Diagnosis of Pancreatic Cystic Lesions with EUS-guided Optical Coherence Tomography
   N. Iftimia, D. Hammer, M. Mujat, R.D. Ferguson, M. Pitman, and W. Brugge. Physical Sciences, Inc., Andover, MA, MGH.

3. Real-time Laser Speckle Imaging in the Treatment of Port Wine Stain Birthmarks
   Yang BY, Yang OR, Guzman JG, Young M, Nguyen P, Kelly KM, Nelson JS, Choi B1. University of California, Irvine.

4. Coherent Raman Imaging: The Development of Label Free Intraoperative Microscopy
   Daniel Orringer M.D., Chris Freudiger Ph.D., Sunney Xie Ph.D. Brigham and Women's Hospital, Harvard Medical School, Department of Chemistry and Chemical Biology, Harvard University, Cambridge, MA

5. Construction of a Microendoscope for Vibrational Imaging during Image Guided Lung Cancer Biopsy
   Liang Gao, Fuhai Li, Yaliang Yang, Yongjun Liu, Michael J. Thrall, Jiong Xing, Ahmad A. Hammoudi, Hong Zhao, Philip T. Cagle, Yubo Fan, Kelvin K. Wong, Zhiyong Wang, Stephen T.C. Wong, The Methodist Hospital Research Institute, The Methodist Hospital and Weill Cornell Medical College, Houston TX

# Intraoperative Optical Coherence Tomography for Assessing Tumor Margins and Lymph Node Status during Breast Cancer Surgery

Stephen A. Boppart, M.D., Ph.D.
Beckman Institute for Advanced Science and Technology
Departments of Electrical and Computer Engineering, Bioengineering, and Medicine
University of Illinois at Urbana-Champaign

PURPOSE:
Re-operation rates following breast conserving surgery can be as high as 30-40%, based on current post-operative histological assessment of surgical margins. Current practice also involves resection of lymph nodes for post-operative histological assessment for staging cancer. We have developed and demonstrated an intraoperative optical coherence tomography (OCT) system for the high-resolution, real-time assessment of tumor margins and lymph nodes during breast lumpectomy procedures, with the goal of reducing re-operation rates and enabling intraoperative evaluation of lymph nodes to stage cancer.

METHODS:
Portable OCT systems were constructed for intraoperative imaging. These spectral-domain OCT systems operate at 1310 nm wavelength with a resolution of approximately 10 microns. Real-time acquisition permits 3-D OCT imaging over areas of 10 x 10 $mm^2$, and to depths up to 2 mm in highly-scattering tissues. Resected tumor and lymph node specimens from breast cancer patients were imaged at multiple sites during surgery. Sites were marked and specimens were sent for post-operative histological assessment as per standard of care. Intraoperative OCT images were correlated with post-operative histological findings.

RESULTS:
To date, over 120 patient specimens have been imaged intraoperatively. From a training set involving 17 patients and a study set involving 20 patients, intraoperative OCT determined positive/negative margin status with a sensitivity of 100% and a specificity of 82%. Three-dimensional OCT of intact lymph nodes also exhibited image-based biomarkers indicative of normal, reactive, and metastatic nodes, which correlates with histology.

CONCLUSIONS:
Intraoperative OCT has the potential to determine margin status (positive/negative for tumor) within 2 mm of the cut surface, the depth assessed histologically. Image features from lymph nodes also suggest the use of OCT for determining the presence of metastatic disease, without histological processing. Ongoing efforts are developing a handheld surgical probe to perform OCT imaging *in situ* in the tumor cavity, and in exposed lymph nodes. This portable optical imaging technology has the potential to provide high-resolution real-time image guidance to reduce re-operation rates and to determine the presence of metastatic disease in loco-regional lymph nodes.

## Reflectance confocal microscopy of shave biopsy wounds in patients with skin cancer: feasibility of intra-operative mapping of tumor margins

Alon Scope, M.D.
Umbareen Mahmood, M.D
Kishwer Nehal, M.D.
Milind Rajadhyaksha, Ph.D.
*Dermatology Service, Memorial Sloan-Kettering Cancer Center*

Reflectance confocal microscopy (RCM) images human skin with nuclear-level resolution and detects basal cell carcinomas (BCCs) *in vivo* with sensitivity of 92% and specificity of 97%. We report the feasibility of RCM imaging of residual BCCs in shave biopsy wounds *in vivo*, using aluminium chloride (35% concentration, 1 minute), to brighten nuclear morphology and enhance tumor-to-dermis contrast. RCM imaging in 50 patients detected either the absence of BCCs or the presence with consistent patterns of tumor margins, with excellent comparison to the corresponding pathology. The results demonstrate the future possibility of RCM imaging for intra-operative mapping of tumor margins to potentially guide surgery.

## 3D OPTICAL IMAGING AND DIGITAL XRAY OF BREAST LESIONS

David Boas, Qianqian Fang, Stefan Carp, Mark Martino, Rick Moore, Dan Kopans

The majority of breast cancers are currently diagnosed with X -ray mammography. While mammography offers better than 80% sen sitivity, there is still roo m for sensitivit y improvement, as well as a need to reduce the n umber of false positives from the current 20%-30%. The recent advent of c ombined PET-CT scanners has demonstrated the significant d iagnostic improvements afforded by the fusion of structur al and funct ional images. Breast cancer screening is well serv ed by X -ray mammography but, following the exampl e of PET-CT, can still be si gnificantly enhanced by fusion with tissue functional in formation. We are syn ergistically interfacing o ur tomographic opt ical b reast imaging (TOBI) technology, with X-ray Digital Breast Tomosynthesis (DBT) to produce a multi-modality imaging method that integrates structural (ad ipose and glandular tissues, micro-calcifications) a nd functio nal (angiogenesis, metabolic activity/oxygen consumption) information relevant to the scree ning and dia gnosis of br east cancer. We anticipate t hat this will allow bette r differentiat ion of lesio ns through angiogenic and metabolic markers known to have prognostic value . To date, we have succe ssfully integrated D BT and TOBI and sho wn the registration of t heir respe ctive structural and functional clinical images and obtained evidence of their diagnostic value by discriminating benign and malignant lesions fro m healthy ti ssue. We a re now forming industrial pa rtnerships to develop a commercial TOBI prototype that ca n be interfa ced with DBT systems (or conventional digital mammography) for simultaneous imaging.

David A. Boas, Ph.D., Director, Optics Division, Massachusetts General Hospital, Harvard Medical School, Martinos Center for Biomedical Imaging
Qianqian Fang, Ph.D., Biomedical Engineering, Optics Division, Massachusetts General Hospital, Harvard Medical School, Martinos Center for Biomedical Imaging
Stefan Carp, Ph.D., Chemical Engineering, Optics Division, Massachusetts General Hospital, Harvard Medical School, Martinos Center for Biomedical Imaging
Mark Martino, Optics Division, Massachusetts General Hospital, Harvard Medical School, Martinos Center for Biomedical Imaging
Rick Moore, Ph.D., Director, Breast Imaging Research, Avon Foundation Comprehensive Breast Evaluation Center, Massachusetts General Hospital
Dan Kopans, M.D., Director, Breast Imaging, Avon Foundation Comprehensive Breast Evaluation Center, Massachusetts General Hospital

**Title**: In Vivo Detection of Neoplasia in the Digestive Tract
**Author**: Thomas D. Wang, MD,PhD
**Affiliation**: Depts of Medicine and Biomedical Engineering, University of Michigan

**Purpose**: We aim to develop and validate the use of peptides to target colorectal neoplasia in vivo. This disease is the second leading cause of cancer-related deaths in the US. Currently, surveillance is performed with white light endoscopy by identifying polyps and masses. However, the polyp miss rate can be as high as 22%. Moreover, there is evidence that up to 25% of neoplasia arises from flat or depressed lesions. These lesions frequently contain high-grade dysplasia and progress more rapidly than polypoid adenomas.
**Methods**: Specific-binding peptides are selected with phage display technology. Validation of peptide specificity was performed on flow cytometry and in vivo endoscopy. Peptides can achieve high clonal diversity, nanomolar binding affinity, small size, ease for labeling, scalability to large quantities, and minimal immunogenicity. These probes are well-suited for clinical use because of their rapid binding kinetics, deep tissue penetration, lack of toxicity, capacity for large-scale GMP synthesis, and low cost. They selectively bind to over expressed cell surface targets, and can be labeled optically. Because of their small size (<1 kD), peptides are less likely to elicit an immune reaction. The specificity of peptides can be high, given the large diversity of sequences that are possible, and there is low likelihood for toxicity with use in the colon.
**Results**: We have demonstrated real-time in vivo multi-spectral imaging in the visible regime using a scanning fiber endoscope for wide-field fluorescence detection of colonic dysplasia in a pre-clinical CPC;Apc model. Excitation at 440, 532 and 635 nm was delivered into a spiral scanning fiber, and fluorescence was collected by a ring of objectives placed around the periphery of the instrument. The peptides were selected and labeled with visible dyes, including DEAC, TAMRA, and CF633, respectively. Separate application of the fluorescent-labeled peptides demonstrated specific binding to colonic adenomas. Administration of these two peptides together resulted in distinct patterns binding in the blue and green channels. We have also demonstrated wide-field imaging with near-infrared (NIR) fluorescence using peptides that are labeled with Cy5.5. Imaging is performed at 10 Hz with a 3 mm diameter endoscope that delivers 671 nm excitation, collects fluorescence emission from 696 to 736 nm, and has a resolution of 12 μm. The in vivo NIR fluorescence images collected demonstrate individual dysplastic crypts.
**Conclusions**: We have developed and validated the use of highly-specific peptides to target colorectal neoplasia in vivo using a multi-spectral endoscope visualize 3 peptides in the visable regime and an NIR imaging system that can achieve single crypt resolution.

## Rapid mosaicing of large areas of tissue by strip scanning

Sanjee Abeytunge[1], Yongbiao Li[1], Bjorg Larson[2], Brian Park[3], Emily Seltzer[4], Milind Rajadhyaksha[2], Ricardo Toledo-Crow[1]

[1]Research Engineering Laboratory, Memorial Sloan Kettering Cancer Center, New York, NY
[2]Optical Imaging Laboratory, Dermatology Service, Memorial Sloan Kettering Cancer Center, New York, NY
[3]New York University School of Medicine, New York, NY
[4]Livingston High School, Livingston, NJ

### Purpose

In surgical oncology, the selective excision of tumors with minimal damage to the surrounding normal tissue is guided by examining pathology that is prepared during surgery. Preparation of pathology typically requires hours for frozen pathology during Mohs surgery of skin cancer and days for fixed pathology in head-and-neck, breast and other procedures. Consequently, 20-70% of the patients must return for re-excision, radiotherapy or chemotherapy. Confocal mosaicing microscopy offers an optical imaging means to examine large areas of tissue with nuclear-level resolution directly on fresh excisions without the need for tissue processing.

We previously reported mosaicing of up to 36 x 36 confocal images to display up to 12 x12 $mm^2$ area of Mohs surgical excisions. Basal cell carcinomas were detected with sensitivity of 96.6% and specificity of 89.2%. The time for mosaicing was nine minutes. While this showed initial feasibility, the increased time for large excisions may make this impracticable. To increase speed we employ mosaicing of long “strip” images in one dimension.

### Methods

Instead of standard square images, we scan a line on the tissue and acquire long strip images with aspect ratio 1:27 for a 10 mm strip. Overlap between strips may be varied between 20% and 50% to optimize between scanning time, illumination artifacts and stitching performance. Two algorithms are being developed for stitching strips, one intensity gradient based approach and the second a phase correlation method. A tissue fixture is being designed to mount Mohs surgical excisions for reproducible mosaicing.

### Results

Mosaics of 10 x 10 $mm^2$ with 50% overlap between strips were acquired in 3.8 minutes, with data acquired only in one scan direction. Stitching of 41 strips took 25 seconds using the phase-correlation method with few stitching artifacts. Mosaics of skin excisions from Mohs surgery show nuclear detail and morphology of basal cell carcinomas and normal skin features that visually correlate well to the corresponding pathology.

### Conclusions

Strip mosaicing confocal microscopy may enable rapid pathology at the bedside. Preliminary analysis suggests that up to 2.5 x 2.5 $cm^2$ of excised tissue may be imaged and stitched in three minutes if data are acquired in both scan directions with improved staging and synchronization.

# Improved Diagnosis of Pancreatic Cystic Lesions with EUS-guided Optical Coherence Tomography

N. Iftimia*, D. Hammer*, M. Mujat*, R.D. Ferguson*, M. Pitman**, and W. Brugge**

*Physical Sciences, Inc., Andover, MA-01810

**Massachusetts General Hospital, Boston, MA

## ABSTRACT

**Purpose:** Cystic lesions of the pancreas represent an increasingly common diagnostic and therapeutic challenge for the gastrointestinal surgeon. Currently, endoscopic ultrasound-fine needle aspiration (EUS-FNA) is used as the first line of diagnosis for pancreatic cysts. EUS-guided FNA is frequently being utilized as the diagnostic method of choice due to its increased resolution compared to computed tomography (CT) and due to the ability to provide cystic material (cells and fluid) for cytopathological analysis. However, at least two major problems are still associated with the current EUS-FNA practice: (1) early diagnosis of malignant pancreatic lesions is not possible because of lack of imaging resolution; (2) the diagnostic accuracy of cystic neoplasms varies in a large range (30-80%) because of the difficulty in subclassifying pancreatic cysts with respect to non-neoplastic and neoplastic as well as with respect to the type of neoplastic cyst (serous versus mucinous and benign versus malignant); this leads very often to unnecessary surgery. Here we propose a new diagnostic approach based on EUS-guided optical coherence tomography (EUS-OCT), which has shown some potential for providing improved diagnosis of the cystic lesions of the pancreas.

**Methods:** A common path fiber optic-based catheter, fitting the bore of existing FNA-EUS needles, is launched into the cystic cavity under EUS guidance to reveal the morphology of the cystic wall and the scattering properties of the cystic fluid. Thus, besides the aspirated material, the gastroenerologist and the pathologist will also benefit by the capability of OCT for providing micron-scale images of the cyst. A therapeutic capability could also be provided by sending a laser beam through the same catheter, to thermally coagulate (cause necrosis of) the diseased epithelial tissue layer of the potentially malignant cysts.

**Results:** Preliminary *ex vivo* testing of this approach has been performed at the Massachusetts General Hospital (MGH) on over 40 tissue specimens, which were obtained from patients that undergone pancreatomy. This study has shown over 90% specificity of OCT imaging in differentiating between mucinous and serous cystic lesions. A pilot study is planned at MGH to test this new diagnostic approach *in vivo* on patients identified with cystic lesions that are difficult to differentiate radiologically.

**Conclusion:** High-resolution (micron scale) OCT imaging, has shown great promise in differentiating between serous and mucinous cysts of the pancreas. Therefore, it has the potential of being used in the future to more reliably differentiate between various neoplastic lesions in pancreas, and possibly in other organs, like kidney, liver, and lungs.

**Real-time Laser Speckle Imaging in the Treatment of Port Wine Stain Birthmarks**

Yang BY[1,3]; Yang OR[1,3]; Guzman JG[1,3]; Young M[1,3]; Nguyen P[1,3], Kelly KM[1,2]; Nelson JS[1,2,3]; Choi B[1,3]

1Beckman Laser Institute and Medical Clinic, University of California, Irvine.
2Department of Dermatology, University of California, Irvine.
3Department of Biomedical Engineering, University of California, Irvine.

**Purpose:** Laser Speckle Imaging (LSI) has shown promise in the treatment of Port Wine Stain (PWS) Birthmarks.

PWS birthmarks are vascular malformations seen in approximately 12,000 births a year. Since the majority of cases are found in highly visible regions on the face and neck, PWS can have a profound effect on an individual's psychosocial development. In addition to its obvious cosmetic detriments, facial PWS lesions have also been linked to a higher propensity for glaucoma and seizures, thereby compounding the need for a cure.

LSI is a technique in which imaging of coherent light remitted from an object results in a speckle pattern. The spatio-temporal statistics of this pattern is related to the movement of optical scatterers, such as red blood cells, and image processing algorithms are applied to produce speckle flow index (SFI) maps, which are representative of tissue blood flow. If performed in real time, LSI can play an important role in image-guided surgery.

**Methods:** With real-time LSI, we have imaged 33 patients, 2 to 64 years of age. Imaging at 8 frames per second, we continuously calculate SFI values for both the treated PWS regions as well as the surrounding normal tissue. We look to see if treated regions show a uniform reduction in flow exhibited by decreased SFI values, similar to that of surrounding normal tissue. If the treated region appears to have high or non-uniform SFI values, that area will undergo retreatment.

**Results:** With over 40 qualitative treatment assessments, SFI values within treated regions showed a progressive decrease with each treatment pass, as well as a border of hyperemia surrounding the treated region. At a sample size of 8, measured SFI values before treatment, after first treatment pass, and after second treatment pass were 1591 +/- 110, 1164 +/- 73, and 935 +/- 74 respectively. Since patient protocols vary, not all patients receive multiple treatment passes, thus pre and post treatment values with a sample size of 10 show SFI values of 1402 +/- 200 and 829 +/- 123, respectively, representing an overall 40% decrease in SFI values.

With real-time feedback, the physician was in most cases able to achieve uniform vascular shutdown in the region of interest.

**Conclusion:** Access to real-time blood-flow maps enables direct visualization of the degree of photocoagulation achieved with pulsed-dye laser therapy. In several cases, we have retreated regions with persistent perfusion to achieve complete vascular shutdown, which is the hallmark of a successful PWS treatment session.

Title: Coherent Raman Imaging: The Development of Label Free Intraoperative Microscopy

Authors: Daniel Orringer[1,2] M.D., Chris Freudiger[3] Ph.D., Sunney Xie[3] Ph.D.

Affiliations:

1: Department of Neurosurgery, Brigham and Women's Hospital

2: Harvard Medical School, Boston, MA

3: Department of Chemistry and Chemical Biology, Harvard University, Cambridge, MA

Purpose: Achieving a maximal, safe tumor cytoreduction is the central goal of all brain tumor resections. However, surgeons lack a uniform, objective method for determining when all safely resectable tumor has been removed. Here, we describe the *ex vivo* and *in vivo* application of coherent Raman imaging, a nontoxic, stain- and label-free modality capable of delineating the tumor-brain interface on a microscopic level.

Methods: Coherent anti-Stokes Raman microscopy and stimulated Raman scattering microscopy were employed to evaluate the histologic borders of fresh specimens from the following models: 9L gliomas, MDA-MB-211 implanted breast cancer metastases, and human glioblastoma xenografts. Subsequently, brain tumor window animals were used to image brain tumor margins in vivo. Imaging conditions were tuned to detect CH2 and CH3 molecular vibrations and hemoglobin autoflorescence. Coherent Raman imaging data were compared to corresponding hematoxylin and eosin-stained specimens.

Results: Coherent Raman imaging provides subcellular resolution of brain tumor tissue *ex vivo* and *in vivo.* The difference in cellularity, nuclear to cytoplasmic ratio and vascularity between tumor tissue and normal brain is readily apparent with coherent Raman imaging. Dynamic tumor conditions such as blood flow are readily apparent. Histologic and biochemical differences between tumor and normal brain imaged with coherent Raman imaging mimic those demonstrated by traditional hematoxylin and eosin staining. There was no adverse effect of coherent Raman imaging on tissue histology or the health of the animals imaged.

Conclusions: Coherent Raman Imaging is a safe and effective method for delineating tumor tissue from normal brain on the cellular level in animal brain tumor models. Translational studies designed to integrate coherent Raman imaging into brain tumor surgery are warranted. Coherent Raman imaging may ultimately become the basis of a method to objectively judge the completeness of a brain tumor resection on a cellular level.

This work was supported in part by grants R25CA089017 (DO) and R01EB010244-03 (XSX)

**Title:** Construction of a Microendoscope for Vibrational Imaging during Image Guided Lung Cancer Biopsy

**Authors:** Liang Gao [a], Fuhai Li [a], Yaliang Yang [a], Yongjun Liu [a], Michael J. Thrall [b], Jiong Xing [a], Ahmad A. Hammoudi [a], Hong Zhao [a], Philip T. Cagle [b], Yubo Fan [a], Kelvin K. Wong [a], Zhiyong Wang [a], Stephen T.C. Wong [a, b, *]

**Affiliations:** [a] Department of Systems Medicine and Bioengineering, The Methodist Hospital Research Institute, Houston, Texas 77030; [b] Department of Pathology and Laboratory Medicine, The Methodist Hospital and Weill Cornell Medical College, Houston, Texas 77030; * STWong@tmhs.org

**Purpose:** Lung carcinoma is the most prevalent type of cancer, and it is responsible for more deaths than other types of cancer. Image-guided molecular imaging potentially enables real time diagnosis of early stage lung lesions. Image-guided coherent anti-Stokes Raman scattering (CARS) microscopy offers submicron spatial resolutions and video-rate temporal resolution along with chemical specificity. In this study, we tested the potential use of CARS microscopy as a method of differentiating lung cancer from non-neoplastic lung tissues and classifying lung cancer cell types. The established pathological workup and diagnostic features were used as prior knowledge for establishment of a knowledge-based CARS classification module using a machine learning approach. In addition, a polarization-based scheme was tested for building a CARS microendoscope prototype, miniaturizing this imaging system to a compatible size with intra-operative application.

**Methods:** A total of 1014 CARS images were acquired from 92 fresh frozen lung tissue samples, including 19 normal lung samples, 20 adenocarcinomas, 25 squamous cell carcinomas, 5 small cell carcinomas, 6 organizing pneumonias and 17 examples of interstitial fibrosis. Employing a machine learning approach, normal, non-neoplastic, and lung cancer subtypes were separated based on the extraction of a set of quantitative features describing fibrils and cell morphology. In addition, a raster-scan CARS microendoscope prototype was constructed for further *in vivo* imaging applications. In it, a polarization-based scheme was used to suppress the Four-Wave-Mixing background noise caused by the simultaneous transmission of the pump and Stokes beams in an optical fiber.

**Results:** The CARS method distinguishes lung cancer from normal and non-neoplastic lung tissue with 91% sensitivity and 92% specificity. Small cell carcinomas were distinguished from non-small cell carcinomas with 100% sensitivity and specificity. The microendoscope prototype has been shown to provide micrometer resolution.

**Conclusions:** CARS method with machine learning approach is able to provide real-time differential diagnosis of lung lesions using quantitative measurements taken from the visualized cellular features and patterns. In addition, a microendoscope prototype was further developed for miniaturization of the system for intra-operative applications, potentially enabling identification of different types of lung lesions.

## Session 3: Small Business Innovations in IGT

Session Chair: Keyvan Farahani, PhD

## Invited Speakers

1. MR-guided laser ablation
   Roger McNichols, PhD. Vice President, Visualase, Houston, TX

2. Fast, easy, and accurate 3d ultrasound guidance for surgical needle ablation
   Sharif Razzaque, PhD. Chief Technology Officer, InnerOptic Technology, Inc., Chapel Hill, North Carolina

3. Image guided interventional ultrasound ablation and radiation therapy
   Clif Burdette, PhD. CEO Acoustic MedSystems

## Posters

1. Stereotactic MRI-guided Laser Ablation (SLA) of Epileptogenic Foci
   Anil Shetty, Ashok Gowda, Roger McNichols. Visualase Inc. Houston, TX

2. Image-guided Focal Laser Ablation for Prostate Tumors
   Anil Shetty, Ashok Gowda, Roger McNichols Visualase Inc. Houston, TX

3. Real-Time Tissue Change Monitoring on the Sonablate® 500 during High Intensity Focused Ultrasound (HIFU) Treatment of Prostate Cancer
   Narendra T. Sanghvi, Wo-Hsing Chen, Roy Carlson, Toyoaki Uchida, G. Schatzl and M. Marberger. Focus Surgery, Inc., Tokai University, Medical University, Vienna.

4. RadVision: An Image-Guided Brachytherapy Planning/Implant Tool with Extensible Image Acquisition/Processing
   Jack Blevins, Junichi Tokuda, Robert Cormack, Junghoon Lee, Nathanael Kuo, Jerry Prince, Gabor Fichtinger, Clare MC Tempany, E Clif Burdette. Acoustic MedSystems, Inc., Brigham & Women's Hospital, Harvard University, Johns Hopkins University, Queen's University

5. Improved Diagnosis of Pancreatic Cystic Lesions with EUS-guided Optical Coherence Tomography
   N. Iftimia, D. Hammer, M. Mujat, R.D. Ferguson, M. Pitman, and W. Brugge. Physical Sciences, Inc., Andover, MA, MGH.

# MRI-Guided Laser Ablation

Roger J. McNichols, Ph.D.
Visualase, Inc.
Houston, TX

**Purpose:**
Minimally-invasive, percutaneous methods for delivering energy into the body provide effective means for destroying ("ablating") tissue and often replicate success rates of conventional surgical interventions, especially in the case of focal tumor masses. Imaging methods including CT and ultrasound play a crucial role in directing percutaneous access to target tissues, but are less useful for determining the extent of the effected treatment zone. For this reason "ablation" techniques have not found widespread use in specific applications where highly precise knowledge or control of the extent of the ablation zone is required.

**Methods:**
We have developed a system and software which allows real-time visualization and control of laser interstitial thermal therapy (LITT, laser ablation) based on thermally sensitive magnetic resonance imaging (MRI) data. The system comprises a water-cooled diffusing tip laser applicator, a 980nm diode laser, cooling pump, and computer system for interfacing to a clinical MRI scanner. The system is FDA-cleared, compatible with most clinical MRI installations, and commercially available.

**Results:**
To date, over 200 procedures have been performed using this system in a variety of applications encompassing neurosurgery, gastroenterology, interventional radiology, and urology, including interventions which could not have been accomplished surgically. LITT lesions have demonstrated particularly sharp demarcation borders, and the system has demonstrated an excellent safety profile.

**Conclusions:**
MRI thermal imaging combined with laser interstitial thermal therapy provides an effective means for highly precise control of thermal ablation of soft tissue targets. This precision will enable promulgation of minimally invasive ablation methods to areas previously not amenable, and may enable treatment of conditions not otherwise addressable with other technologies.

**Title**: Fast, easy and accurate 3D ultrasound guidance for surgical needle ablation.

Authors:
Sharif Razzaque[1], Caroline Green[1], Brian Heaney[1], Kurtis Keller[1], Andrei State[1,]
David Sindram[2], Iain H. McKillop[2], David A. Iannitti[2], and John B. Martinie[2]

Affiliations:
[1]InnerOptic Technology, Hillsborough, NC, USA
[2]Division of Hepatobiliary Surgery, Carolinas Medical Center, Charlotte, NC, USA

Abstract:

InnerOptic AIM™ is a novel, FDA-approved guidance system for needle ablation during open and laparoscopic surgery. Surgical ablation involves coordinating multiple complex spatial relationships between ablation tool, ablation zone, ultrasound image, camera and the surgeon's own viewpoint. AIM's stereoscopic user interface makes these relationships intuitive and obvious, thereby improving the effectiveness of ablation by increasing needle placement accuracy, decreasing procedure time, reducing injury, and reducing the rate of incomplete ablation.

In this talk, I will discuss the technology and design decisions behind AIM, and present results from recent phantom, animal and human patient studies. I will also discuss the many surprises, changes in direction, lessons learned and insights gained, as our team evolved a university research project into an FDA-approved and commercially viable medical device.

# IMAGE GUIDED INTERVENTIONAL ULTRASOUND ABLATION AND RADIATION THERAPY

E Clif Burdette
Acoustic MedSystems, Inc., Champaign, IL

**Purpose:**

Needle-based procedures are pervasive in medicine, because needles are among the least invasive vehicles for accessing the interior of the human body. Needles can be used for diagnoses (e.g. biopsy), as well as interventions (e.g. drugs or biologics, radioactive seed implantation, thermal ablation). Accuracy in targeting the desired location is essential in nearly all needle-based procedures to ensure therapeutic or diagnostic efficacy and safety. However, even perfect initial alignment of the needle toward its target can never eliminate tip placement error, because it cannot compensate for registration error (which can never be completely eliminated) or perturbations that occur during insertion, including tissue deformation, patient motion, deflection of the needle at membranes, etc. We have developed new approaches and technology that addresses each of the present limitations of current brachytherapy and minimally invasive surgical interventions that use ablative energy. Current interventional ablation technologies yield highly variable results, including under-treatment of diseased tissue, damage to healthy tissue, long treatment times, limited treatment volume. A novel solution is developed using real time 3D image-based targeting, real-time non-invasive treatment monitoring, precise control over energy direction, shape and volume, and patient-customized therapy. This provides for the first time: 3D tracked image guided targeting of precisely controlled conformal energy direction, shape and size. Initial implementation has been developed and animal tissue studies are in progress.

**Methods:**

The developed ablation technology is needle or catheter based and consists primarily of small ultrasound transducers with high power capacity, excellent tissue penetration, and high directivity, located at the tip of a disposable applicator (needle or catheter), designed for direct insertion to the treatment site with a simple and minimally invasive approach. A steerable delivery tool provides controlled targeting. Angular or rotational heating patterns are achieved by sectoring the transducer surface. Active zones can be selected (i.e., focused, 90°, 180°, 360°) to produce angularly selective patterns. Ultrasound energy is emitted and absorbed locally in the target tissue, producing high temperatures (50-90$^{o}$C) that rapidly thermally destroy the target volume within only a few minutes. Power output, target temperature, and thermal dose are controlled and monitored with a portable dedicated generator/monitoring/control module with an internal PC workstation. All of the real time and streaming image import, manipulation, and processing functions of RadVision are incorporated in the ablation system. Methods for non-invasive ultrasound image-based monitoring of thermal therapy under development will permit real time dynamic control and optimization of delivered thermal dose. Treatment can be performed percutaneously. Thermal lesions were produced with single ablator placement having three transducer devices on a single device. A steerable introducer, with three sequential applicator placements at 120° apart was used. The test apparatus included linear and rotational manipulators to precisely position and rotate the introducer in 120° increments. The ablator was inserted within liver tissue along the planned trajectory and ablation performed. The introducer was partially withdrawn, rotated 120°, re-inserted, and ablation performed.

**Results:**

We have completed development of an ablation system, interstitial HIFU applicators, active steerable delivery device, 3D tracked ultrasound. Experiments have been performed in prostate, liver, and kidney. Treatment planning & modeling system and control strategies, as will the real-time monitoring and active robotic optimization are underway. We demonstrated greater than 40 mm diameter lesions with single device placements and 75 mm with multiple placements using the active nitinol steerable introducer. For 3 placements, the average ablation diameter was 7.0-7.5cm for 10min treatment. Conformal focal prostate therapy was also demonstrated with 1-2mm targeting accuracy. Results for multiple clinical treatment sites will be presented.

**Conclusions:**

Developing an application that supports extensible imaging capabilities and meets FDA development guidelines has been realized. The modular design incorporates new algorithms and processes for both ablative or radiation therapy with the objective to provide improved clinical outcomes. The above results demonstrate two novel breakthroughs (1) steerable needle with an integrated interventional ablator, and (2) able to treat a large liver tumor ablatively through a single percutaneous insertion. Studies will be conducted to support indications for treatment of spine tumors, liver, kidney, and prostate.

# Stereotactic MRI-guided Laser Ablation (SLA) of Epileptogenic Foci

**Anil Shetty, Ashok Gowda, Roger McNichols**

**Visualase Inc. Houston, TX**

**PURPOSE:**

An estimated 200,000 patients are eligible for epilepsy surgery in the United States, yet less than 5000 procedures are performed annually due to a number of factors including surgery related morbidity. We evaluate the feasibility of this stereotactic technique for thermal ablation of epileptogenic foci, and examine its safety profile in patients with intractable localization-related epilepsy.

**METHODS:**

10 patients (5 pediatric cases and 5 adults) with varied etiologies like tuberous sclerosis (TS), mesial temporal sclerosis (MTS) and deep seated foci like hypothalamic hamartoma (HH) were consented for MRI-guided laser ablation . Under general anesthesia, laser applicator was placed via a 3.2mm twist drill hole with aid of a stereotactic frame or a frameless navigation system. An MR-compatible 980nm diode laser applicator (1.6mm diameter) housing a 1cm diffusing tipped optical fiber was placed into MRI visible target lesions , secured with a plastic bone anchor and thermal ablation doses (6W-12W for 45-120 seconds) was delivered. Real-time magnetic resonance thermal imaging (MRTI) was monitored on the FDA-cleared Visualase workstation. MRTI was accomplished using PRF phase difference imaging techniques using a fast field echo or gradient echo (FFE, 256x128 acquisition matrix, TE=20ms, TR=38ms, flipangle = 30 deg) sequence. The software used Arrhenuis damage model to predict tissue damage based on temperature history. Safety limits (50$^{o}$C) were placed to protect critical structures such as the optic tract, and cerebral arteries. Post ablation T1-weighted plus gadolinium contrast (T1 + Gd) images were acquired post-ablation to confirm areas of thermal ablation.

**RESULTS:**

SLA was successful in all cases without any procedure related complications. MRTI was an effective monitoring tool for the surgeon to control the ablation volumes and limit damage to critical structures. The twist drill hole required a single stitch for closure, and in most cases, patients were discharged within 24 hours. Post-contrast MRI exhibited a non-enhancing central coagulated region surrounded by a rim of enhancement typical of acute thermal injury that encompassed the targeted foci.

**CONCLUSIONS:**

MR-guided stereotactic laser ablation may offer advantages over conventional resective surgical approaches for removal of epileptic foci. The small diameter of the laser applicator provides a minimally invasive approach to reaching target foci including deep seated lesions. Additionally, the use of real-time MRTI feedback control and online estimates of thermal damage, allow excellent visualization of target and protection of critical structures during ablation process. Short term follow-up outcomes after SLA are encouraging and justify further studies.

## Image-guided Focal Laser Ablation for Prostate Tumors

**Anil Shetty, Ashok Gowda, Roger McNichols**
**Visualase Inc. Houston, TX**

**Purpose:** Approximately 200,000 men in the US will be diagnosed with prostate cancer this year. MRI-guided focal laser ablation (FLA) of localized prostate cancer tumors may overcome side effects associated with currently standard whole-gland treatments. Recently multi-parametric magnetic resonance imaging (MRI) has been shown to be useful for localization of prostate tumors. The goal of this study was to develop techniques for implementing MR-guided FLA with real-time MR temperature monitoring in patients with low-risk, low-volume disease.

**Methods**: Men with biopsy-confirmed, MR-imageable prostate cancer with Gleason score $\leq$ 7 were offered FLA. Laser delivery was accomplished using either a trans-perineal (n=52) or trans-rectal (n=13) approach. For transperineal treatments, patients were placed supine inside the bore of a clinical high-field MRI, fitted with a perineal needle guide template and axial volume set acquired. Software (Visualase, Inc, Houston, TX) allowed identification of three fiducials on the template and subsequent projection of needle guide trajectories through the prostate volume. For transrectal treatments, a transrectal needle guide designed for MR-guided biopsy (DynaTRIM, Invivo, Peewaukee, WI) was fitted to the patient, similar imaging performed, and software (DynaLOC, Invivo) used to determine trajectory setting for reaching targets. In either case, a 14-cm catheter with titanium stylet was inserted to the targeted lesion. The stylet was replaced with a 15-Watt 980-nm laser applicator (400-micron-core-diameter silica fiber with diffusing tip in a 1.65mm water-cooled sheath). During continuous MR imaging, laser energy was delivered and the therapy workstation transferred MR images in real-time to display temperature changes in the tissue every 5 seconds. Laser doses of 7-12W were delivered for 60-120 seconds. Post-treatment contrast images were used to confirm treatment zones.

**Results:** Both systems enabled reproducible, accurate placement of applicators into desired anatomical targets in the peripheral and central zones and apex of the prostate. Real-time thermal monitoring was useful to ensure target destruction while avoiding heating of structures including rectal wall, neurovascular bundles, and urethra. Procedural time was as low as 75 minutes, with an average of 120 minutes. A laser exposure of 10 W for 75 seconds commonly resulted in an ablation area of 14 by 12 mm.

**Conclusion:** MR-guided FLA of prostate tumors with real-time thermal imaging is technically feasible, safe, and has a low rate of complications or side effects. It is a viable minimally invasive option for treating focal prostate tumors [Gleason 6-7 ], but long term followup studies need to completed before it is widely accepted in clinical practice.

Title: Real-Time Tissue Change Monitoring on the Sonablate® 500 during High Intensity Focused Ultrasound (HIFU) Treatment of Prostate Cancer

Authors: Narendra T. Sanghvi[1], Wo-Hsing Chen[1], Roy Carlson[1], Toyoaki Uchida[2], G. Schatzl[3] and M. Marberger[3]

Affiliation: [1]Focus Surgery, Inc., 3940 Pendleton Way, Indianapolis, Indiana 46226, [2]Department of Urology, Tokai University, Hachioji, Japan, and [3]Department of Urology, Medical University, Vienna, Austria

*Abstract:* Recently HIFU devices are used to treat prostate, kidney and other cancer using B-mode ultrasound guidance known as Visually directed HIFU. These changes are qualitative and operator dependent. There is a monotonic increase in ultrasound attenuation and backscattered ultrasound energy as tissue temperature elevates from 37° to 65°C and thereafter attenuation remains at the peak level. The backscattered Radio Frequency (RF) ultrasound signals contain information related to tissue changes. Therefore new research efforts are pursued in signal processing to analyze RF pulse-echo backscattered signals to estimate tissue alterations caused by HIFU energy. Based on these novel algorithms, Tissue Change Monitoring (TCM) software for the Sonablate® 500 systems has been developed that display quantitative information on tissue status during the HIFU exposure.

*Method:* The RF backscattered signals were acquired for each treatment site pre and post HIFU. These signals are processed by Fast Fourier Transform (FFT) to derive their frequency spectra. These spectra are further divided into sub, center and higher harmonic bands for calculating the changes in the energy levels. During the HIFU treatment green, yellow or orange color is overlaid on each treatment site on the B-mode image that represent low, medium and high levels of tissue change respectively along with a value of energy change (range 0-1). The software validation was conducted *in-vitro* using chicken tissue and tissue temperature was monitored with thermocouples to correlate energy change to measured temperatures at ultrasound energy deposition.

Clinical Validation: TCM *in-vivo* tests were conducted in a clinical study at the Tokai University Hachioji Hospital. Contrast enhanced MR Images of the prostate were taken post HIFU (24-48 hours). These images were compared to TCM data.

*Results: In-vitro* data resulted high degree of cross correlation ($R^2$>0.92) between temperature and RF signal energy level changes. Early clinical studies with TCM were conducted in Japan (n=97). Post HIFU contrast enhanced MRI showed whole gland tissue ablation. Pre and post HIFU treatment nadir PSA (ng/ml) median changed from 6.89 to 0.07.

*Conclusion*: TCM measurements are independent of ultrasound images and independent of the operator and provide essential feedback required to assure that tissues are properly treated. In some cases immediate feedback can allow re-treatment of undertreated sites.

*Acknowledgement*: This research was partially supported by NIH / NCI grant 5R44CA083244-03 and clinical study in Japan was sponsored by Takai Hospital Supply Co., Tokyo, Japan. Authors would like to thank all other TCM users for their input and feedback.

# RadVision: An Image-Guided Brachytherapy Planning/Implant Tool with Extensible Image Acquisition/Processing

Jack Blevins[1], Junichi Tokuda[2], Robert Cormack[2], Junghoon Lee[3], Nathanael Kuo[3], Jerry Prince[3], Gabor Fichtinger[4], Clare MC Tempany[2], E Clif Burdette[1]
[1]Acoustic MedSystems, Inc., [2]Brigham & Women's Hospital, Harvard University, [3]Johns Hopkins University, [4]Queen's University

## Purpose:

RadVision is developed to become a commercial product that provides a capability for real-time image guided interventional delivery of radiation sources primarily for treatment of prostate cancer and simultaneous intraoperative dosimetry and rapid implant re-optimization during the procedure. This new system incorporates the results of research performed by teams from Acoustic MedSystems, Brigham & Women's Hospital, John Hopkins University, and Queen's University. A major aspect of this research is the use of higher quality MR imaging to better define the prostate anatomy to facilitate improved implant accuracy. The goal is to apply these results to achieve improved therapeutic and quality of life outcomes for each patient.

## Methods:

The basic design principle of RadVision is to create an environment where both the user interface and data processing facilities are flexible and highly extensible. The result is a non-traditional Windows application that maintains isolation of the user interface and data processing functions to achieve this desired result. One benefit from this design is image acquisition. The program can accept streaming images from multiple sources simultaneously. The image sources include: real time MR (openIGTLink), real time ultrasound (video capture), real time Fluoroscopy (video capture), pushed DICOM images, DICOM files, and Jpeg/Bmp/Tiff ultrasound files. The DICOM files may contain MR, CT, PET/CT or ultrasound images. An image may have any orientation and use any coordinate system. During import, the image coordinate system is converted to an internal coordinate system convenient for Windows based image display. Following image import, all image coordinates are displayed in a user selected coordinate system (LPS, RAS, etc.). RadVision's image import processing results in a custom internal format which permits the application of the same image processing tools regardless of the original modality, and provides image output consistent with the application coordinate system. Dosimetry is updated based on actual implant specific spatial locations of inserted seeds and needles. A rapid iterative dose optimization algorithm incorporating case specific boundary conditions re-optimizes the remaining seeds to be implanted.

## Results:

For brachytherapy, the dose to target, nearby anatomical structures, needle positions, and seeds on 2D images or throughout a 3D volume are requirements for planning. RadVision overlays these items on real time images for monitoring a seed implant. To achieve the best outcome, the resulting seed positions are accurately identified, immediate changes in dose based on actual seed position are determined, and the plan for balance of implant adjusted accordingly. The images acquired using real time MR, pushed DICOM, and real time ultrasound provide visualization for the physician. Intraoperative fluoroscopy (3 images) provides for the use of automated algorithms for seed reconstruction and registration with the target volume. Seed localization and reconstruction accuracy in actual target volume exceeds 99%. Re-optimization of implant requires 30-45 seconds.

## Conclusions:

Developing an application that supports extensible imaging capabilities and meets FDA development guidelines has been realized. The modular design incorporates new algorithms and processes to identify seeds / needles with the objective to provide improved clinical outcomes.

### Acknowledgements:

Special acknowledgement is for important and seminal work on this project performed by the following individuals: Ameet Jain (Philips Research), Anton Deguet (Johns Hopkins), Pascal Fallavollita (Technische Universitat Munchen), Ehsan Dehghan (Queen's & Johns Hopkins), Nobuhiko Hata (Brigham & Women's), Maria Ayad (Johns Hopkins), Randy Stahlhut (Acoustic MedSystems), Paul Neubauer (Acoustic MedSystems).

# Improved Diagnosis of Pancreatic Cystic Lesions with EUS-guided Optical Coherence Tomography

N. Iftimia*, D. Hammer*, M. Mujat*, R.D. Ferguson*, M. Pitman**, and W. Brugge**

*Physical Sciences, Inc., Andover, MA-01810

**Massachusetts General Hospital, Boston, MA

## ABSTRACT

**Purpose:** Cystic lesions of the pancreas represent an increasingly common diagnostic and therapeutic challenge for the gastrointestinal surgeon. Currently, endoscopic ultrasound-fine needle aspiration (EUS-FNA) is used as the first line of diagnosis for pancreatic cysts. EUS-guided FNA is frequently being utilized as the diagnostic method of choice due to its increased resolution compared to computed tomography (CT) and due to the ability to provide cystic material (cells and fluid) for cytopathological analysis. However, at least two major problems are still associated with the current EUS-FNA practice: (1) early diagnosis of malignant pancreatic lesions is not possible because of lack of imaging resolution; (2) the diagnostic accuracy of cystic neoplasms varies in a large range (30-80%) because of the difficulty in subclassifying pancreatic cysts with respect to non-neoplastic and neoplastic as well as with respect to the type of neoplastic cyst (serous versus mucinous and benign versus malignant); this leads very often to unnecessary surgery. Here we propose a new diagnostic approach based on EUS-guided optical coherence tomography (EUS-OCT), which has shown some potential for providing improved diagnosis of the cystic lesions of the pancreas.

**Methods:** A common path fiber optic-based catheter, fitting the bore of existing FNA-EUS needles, is launched into the cystic cavity under EUS guidance to reveal the morphology of the cystic wall and the scattering properties of the cystic fluid. Thus, besides the aspirated material, the gastroenerologist and the pathologist will also benefit by the capability of OCT for providing micron-scale images of the cyst. A therapeutic capability could also be provided by sending a laser beam through the same catheter, to thermally coagulate (cause necrosis of) the diseased epithelial tissue layer of the potentially malignant cysts.

**Results:** Preliminary *ex vivo* testing of this approach has been performed at the Massachusetts General Hospital (MGH) on over 40 tissue specimens, which were obtained from patients that undergone pancreatomy. This study has shown over 90% specificity of OCT imaging in differentiating between mucinous and serous cystic lesions. A pilot study is planned at MGH to test this new diagnostic approach *in vivo* on patients identified with cystic lesions that are difficult to differentiate radiologically.

**Conclusion:** High-resolution (micron scale) OCT imaging, has shown great promise in differentiating between serous and mucinous cysts of the pancreas. Therefore, it has the potential of being used in the future to more reliably differentiate between various neoplastic lesions in pancreas, and possibly in other organs, like kidney, liver, and lungs.

# Session 4: Thermal Imaging and Therapy

Session Chair: Nathan McDannold, PhD

## Invited Speakers

1. Prospective 3-D treatment planning for MR-guided laser induced thermal therapy
   Jason Stafford, PhD, University of Texas MS, Anderson Cancer Center

2. Improved MRI temperature imaging using a subject-specific biophysical model
   Dennis Parker, PhD, University of Utah

3. Noninvasive estimation of temperature change using pulse-echo ultrasound: in vivo results
   Emad Ebbini, PhD

4. Focused ultrasound of the liver during free breathing
   Kim Butts-Pauly, PhD, Stanford

## Posters

1. Stereotactic MRI-guided Laser Ablation (SLA) of Epileptogenic Foci
   Anil Shetty, Ashok Gowda, Roger McNichols. Visualase Inc. Houston, TX

2. Image-guided Focal Laser Ablation for Prostate Tumors
   Anil Shetty, Ashok Gowda, Roger McNichols Visualase Inc. Houston, TX

3. Real-Time Tissue Change Monitoring on the Sonablate® 500 during High Intensity Focused Ultrasound (HIFU) Treatment of Prostate Cancer
   Narendra T. Sanghvi, Wo-Hsing Chen, Roy Carlson, Toyoaki Uchida, G. Schatzl and M. Marberger. Focus Surgery, Inc., Tokai University, Medical University, Vienna.

4. Design and characterization of a laterally mounted phased array transducer breast specific MRgHIFU device with integrated 11 channel receiver array
   Allison Payne, Robb Merrill, Emilee Minalga, Joshua de Bever, Nick Todd, Rock Hadley, Erik Dumont, Leigh Neumayer, Doug Christensen, Robert Roemer, Dennis Parker. University of Utah, Salt Lake City, Image Guided Therapy, Pessac, France, Huntsman Cancer Institute, Salt Lake City, UT.

5. Tumor therapy by ultrasound-triggered drug release from microbubble-liposome complex
   A.L. Klibanov, T. Shevchenko, W. Shi, S. Sethuraman, Z. Du, M. Campa, R. Seip, E. Leyvi, B. Raju. Cardiovascular Division, University of Virginia School of Medicine Charlottesville VA, Philips Research North America, Briarcliff Manor NY.

# PROSPECTIVE 3-D TREATMENT PLANNING FOR MR-GUIDED LASER INDUCED THERMAL THERAPY

Jason Stafford, PhD, The University of Texas M. D. Anderson Cancer Center

MR-guided laser induced thermal therapy (MRgLITT) for treatment of cancerous lesions in the brain presents a minimally invasive alternative to conventional surgery, gaining use worldwide with multiple on-going clinical trials currently. These therapies incorporate real-time MR temperature imaging (MRTI) to provide feedback which makes these procedures safe and feasible. However, as these therapies translate into clinical studies, there are two deficiencies worth addressing. Firstly, laser heating in the presence of tissue interfaces and convective heat transfer (e.g., ventricles, vessels and tissue perfusion) may render planning of treatments by assuming symmetric ellipsoidal lesion generation difficult, particularly when multiple applicators with arbitrary placement are used. Second, MRTI information may become corrupt in some regions (e.g., from temperature dependent signal losses, blood, or susceptibility effects at interfaces) and the temperature information may be lost or become extremely uncertain, making decisions about treatment outcome difficult. Therefore, in order to enhance the safety, efficacy and conformality of treatment delivery, there exists a critical need for prospective 3D treatment planning of MRgLITT procedures as well as more robust real-time monitoring to complement MRTI. Here we report on our progress toward our goal to develop and validate algorithms to provide both prospective 3D treatment planning and real-time model driven treatment monitoring for MRgLITT procedures in the brain. Treatment planning software is being designed to incorporate the use of 3D MRI acquisitions currently used for neurosurgical and stereotactic treatment planning and allow the user to interactively navigate the tissue and simulate the effects of various applicator trajectories and laser exposures, update these plans once the laser is positioned, as well as provide real-time 3D estimation of damage based on the acquired multi-slice MR temperature imaging input. Reduced order models which rely on image feedback are being designed to assist in the real-time monitoring aspect of MRgLITT. In each case, the goal is to create a framework in which the uncertainty in the predicted temperatures and damage can also be estimated.

# IMPROVED MRI TEMPERATURE IMAGING USING A SUBJECT-SPECIFIC BIOPHYSICAL MODEL

Nick Todd, Allison Payne, Douglas A. Christensen, Henrik Odeen, Dennis L. Parker
Utah Center for Advanced Imaging Research, University of Utah

## Purpose

There are applications of MRI guided high intensity focused ultrasound (MRgHIFU), such as transcranial MRgHIFU of the brain, where current MR temperature imaging (MRTI) methods do not achieve sufficient spatial resolution, temporal resolution or coverage. Even with parallel imaging, it is not possible to acquire all of the data fast enough to satisfy resolution and volume coverage needs. We have demonstrated that temporally constrained reconstruction (TCR) of subsampled MRTI measurements can achieve the require resolution/volume coverage requirements, but the temperatures are only obtained retrospectively. The purpose of the current work is to develop a method to predict volumetric temperatures in real time, using tissue physical properties and knowledge of the current temperature distribution.

## Methods

Subsampled MRTI measurements obtained during low levels of heating and subsequent cooling are reconstructed retrospectively using TCR. Tissues, including bone, fat, muscle and other aqueous tissues are segmented from high resolution images of the volume of interest. Tissue properties are inferred from the TCR temperature measurements in corresponding tissues during heating and cooling. 3D model predictive filtering, similar to the 2D approach that we have already presented, will use tissue properties, the known ultrasound power distribution, and the current distribution to predict temperature over the full volume of interest.

## Results

This work forms part of a major 4-year NIH grant to develop fully volumetric temperature measurements for transcranial MRgHIFU and also builds on work performed in the development of a system for MRgHIFU of the breast. The TCR method has been used for large FOV MRTI measurements in phantoms and stability measurements in brain. After volumetric tissue segmentation, tissue property estimates have been made based upon dynamic TCR temperature measurements. Development of the fully 3D model predictive filtering using the subject-specific biophysical model is ongoing.

## Conclusions

There is excellent evidence that the MRTI measurements can be obtained rapidly, with high spatial resolution, over a large FOV using a model-based forward prediction technique based on knowledge of a subject-specific biophysical model.

## NONINVASIVE ESTIMATION OF TEMPERATURE CHANGE USING PULSE-ECHO ULTRASOUND: IN VIVO RESULTS

Emad S. Ebbini, Department of Electrical and Computer Engineering, College of Science and Engineering, University of Minnesota Twin Cities

**Purpose:** Modern therapeutic ultrasound applicators increasingly utilize phased array transducers capable of synthesizing complex multiple-focus patterns in a variety of thermal therapies. The use of high intensity focused ultrasound (HIFU) in thermal therapy mode (both high temperature and low temperature) currently prevalent and is likely to continue to play a major role for the foreseeable future. Modern phased array drivers are capable of dynamic control of pulsed HIFU (pHIFU) patterns with millimeter accuracy and millisecond time resolution. Realtime temperature control algorithms with spatial and temporal resolutions matching those of the drivers are needed to realize the full potential of phased array technology in thermal therapy. Furthermore, to preserve the noninvasive nature of the treatment, the algorithm must utilize a noninvasive method for measuring temperature change within the treatment volume.

**Methods:** We have developed a noninvasive method for imaging temperature change using diagnostic ultrasound. A realtime implementation of the method was recently completed on a Sonix RP scanner (Ultrasonix, Vancouver, BC, Canada). The method is employs speckle tracking to estimate echo strains due to temperature change from diagnostic ultrasound echo data. The realtime system has been tested in tissue mimicking phantoms with known thermal and acoustic properties, freshly excised ex vivo tissues, and *in vivo* small-animal (mouse and rat models). In addition, we have developed a spatio-temporal filter based on the transient bioheat transfer equation (tBHTE) to remove strain artifacts from breathing, pulsation, and other natural tissue motion.

**Results:** Temperature profiles measured in phantoms using our noninvasive 2D imaging method were in agreement with direct measurements performed using thermocouples. Ex vivo experiments in liver and kidney tissue samples were also in agreement with phantom experiments. Muscle tissue exhibited some discrepancies around tissue layers, fatty and connective tissues, as expected. Temperature imaging results from subtherapeutic heating experiments in the hind limb of Copenhagen rat will also be shown.

**Conclusions:** Our results demonstrate the validity of our temperature measurement model as well as the feasibility of imaging localized temperature-change patterns in vivo in the presence of pulsation and breathing. They also demonstrate the effectiveness of the tBHTE-inspired filter in removing tissue strain artifacts from echo strain data necessary for temperature estimation, even in the vicinity of pulsating blood vessels.

**Focused Ultrasound of the Liver During Free Breathing**

Kim Butts Pauly[1], Andrew Holbrook[1], Pejman Ghanouni[1], Juan Santos[2]

[1] Department of Radiology, Stanford University
[2] HeartVista, Palo Alto, CA

**Purpose**: Focused ultrasound ablation of liver and renal cancer could be a desirable treatment option for many patients. FUS of the liver and kidney can be done in either multiple breathholds or during free breathing. The purpose of this work was to develop a system capable of treating during free breathing and perform initial studies to test the capabilities of the system.

**Methods**: The system was designed to include a) real-time imaging and thermometry, b) transducer tracking with MR tracking coils on the transducer, c) liver tracking by vessel tracking and respiratory monitoring, and d) slewing of the beam to maintain a constant position of the focal spot in the liver during free breathing. The system also includes a) near-real time MR-thermometry, b) MR-ARFI imaging to calibrate the focal spot position, and c) rapid display of ultrasound reflection data.

Experiments were performed in a moving tissue phantom and *in vivo* porcine liver and kidney with the InSightec ExAblate 2000 Conformal Bone System operating at 0.55 MHz. For liver access, the transducer was placed on the ventral surface of the animal, below the ribs. For renal access, the transducer was placed in the lateral decubitus position and the transducer was placed inferior to the lateral costal margin. Gated, dual single shot MR-ARFI acquisitions demonstrated the focus for calibration. Real time MR thermometry used a multishot RS-EPI sequence (TE/TR = 15.9 ms/117 ms and a frame rate of 2.85 frames/s) reconstructed with RTHawk. Temperature processing was done with a hybrid multibaseline and L2 referenceless processing. Both breathheld and free breathing ablations were made for comparison. Typical operating transducer power was 150 acoustic W for both ablation and ARFI. Ablation durations were approximately 60 seconds, while for each ARFI image, the ultrasound was on for a duration of approximately 20 ms.

**Results**: Rapid display of the reflection data was critical for positioning the transducer. Rapid MR-ARFI images provided an easy means of calibrating the focal position in seconds across the entire range of respiration. Real-time thermometry provided sufficient frame rate and temporal resolution to accurately image the focal spot.

In a moving tissue phantom, beam steering method required only 13% more energy to reach 15°C above baseline temperature over a stationary ablation, while simulated breathing required 712% more energy. *In vivo* real-time beam steering similarly reduces the energy requirements, although there is considerable variability in the improvement, presumably due to the complex motion of the liver and variability in perfusion.

**Conclusions:** Focused ultrasound ablation of the liver during free breathing is a realistic goal. MR-ARFI plays a key role in the rapid calibration of the system.

Acknowledgements: NIH R01 CA121163

# Stereotactic MRI-guided Laser Ablation (SLA) of Epileptogenic Foci

**Anil Shetty, Ashok Gowda, Roger McNichols**

**Visualase Inc. Houston, TX**

**PURPOSE:**

An estimated 200,000 patients are eligible for epilepsy surgery in the United States, yet less than 5000 procedures are performed annually due to a number of factors including surgery related morbidity. We evaluate the feasibility of this stereotactic technique for thermal ablation of epileptogenic foci, and examine its safety profile in patients with intractable localization-related epilepsy.

**METHODS:**

10 patients (5 pediatric cases and 5 adults) with varied etiologies like tuberous sclerosis (TS), mesial temporal sclerosis (MTS) and deep seated foci like hypothalamic hamartoma (HH) were consented for MRI-guided laser ablation . Under general anesthesia, laser applicator was placed via a 3.2mm twist drill hole with aid of a stereotactic frame or a frameless navigation system. An MR-compatible 980nm diode laser applicator (1.6mm diameter) housing a 1cm diffusing tipped optical fiber was placed into MRI visible target lesions , secured with a plastic bone anchor and thermal ablation doses (6W-12W for 45-120 seconds) was delivered. Real-time magnetic resonance thermal imaging (MRTI) was monitored on the FDA-cleared Visualase workstation. MRTI was accomplished using PRF phase difference imaging techniques using a fast field echo or gradient echo (FFE, 256x128 acquisition matrix, TE=20ms, TR=38ms, flipangle = 30 deg) sequence. The software used Arrhenuis damage model to predict tissue damage based on temperature history. Safety limits (50$^{o}$C) were placed to protect critical structures such as the optic tract, and cerebral arteries. Post ablation T1-weighted plus gadolinium contrast (T1 + Gd) images were acquired post-ablation to confirm areas of thermal ablation.

**RESULTS:**

SLA was successful in all cases without any procedure related complications. MRTI was an effective monitoring tool for the surgeon to control the ablation volumes and limit damage to critical structures. The twist drill hole required a single stitch for closure, and in most cases, patients were discharged within 24 hours. Post-contrast MRI exhibited a non-enhancing central coagulated region surrounded by a rim of enhancement typical of acute thermal injury that encompassed the targeted foci.

**CONCLUSIONS:**

MR-guided stereotactic laser ablation may offer advantages over conventional resective surgical approaches for removal of epileptic foci. The small diameter of the laser applicator provides a minimally invasive approach to reaching target foci including deep seated lesions. Additionally, the use of real-time MRTI feedback control and online estimates of thermal damage, allow excellent visualization of target and protection of critical structures during ablation process. Short term follow-up outcomes after SLA are encouraging and justify further studies.

## Image-guided Focal Laser Ablation for Prostate Tumors

**Anil Shetty, Ashok Gowda, Roger McNichols**
**Visualase Inc. Houston, TX**

**Purpose:** Approximately 200,000 men in the US will be diagnosed with prostate cancer this year. MRI-guided focal laser ablation (FLA) of localized prostate cancer tumors may overcome side effects associated with currently standard whole-gland treatments. Recently multi-parametric magnetic resonance imaging (MRI) has been shown to be useful for localization of prostate tumors. The goal of this study was to develop techniques for implementing MR-guided FLA with real-time MR temperature monitoring in patients with low-risk, low-volume disease.

**Methods**: Men with biopsy-confirmed, MR-imageable prostate cancer with Gleason score $\leq$ 7 were offered FLA. Laser delivery was accomplished using either a trans-perineal (n=52) or trans-rectal (n=13) approach. For transperineal treatments, patients were placed supine inside the bore of a clinical high-field MRI, fitted with a perineal needle guide template and axial volume set acquired. Software (Visualase, Inc, Houston, TX) allowed identification of three fiducials on the template and subsequent projection of needle guide trajectories through the prostate volume. For transrectal treatments, a transrectal needle guide designed for MR-guided biopsy (DynaTRIM, Invivo, Peewaukee, WI) was fitted to the patient, similar imaging performed, and software (DynaLOC, Invivo) used to determine trajectory setting for reaching targets. In either case, a 14-cm catheter with titanium stylet was inserted to the targeted lesion. The stylet was replaced with a 15-Watt 980-nm laser applicator (400-micron-core-diameter silica fiber with diffusing tip in a 1.65mm water-cooled sheath). During continuous MR imaging, laser energy was delivered and the therapy workstation transferred MR images in real-time to display temperature changes in the tissue every 5 seconds. Laser doses of 7-12W were delivered for 60-120 seconds. Post-treatment contrast images were used to confirm treatment zones.

**Results:** Both systems enabled reproducible, accurate placement of applicators into desired anatomical targets in the peripheral and central zones and apex of the prostate. Real-time thermal monitoring was useful to ensure target destruction while avoiding heating of structures including rectal wall, neurovascular bundles, and urethra. Procedural time was as low as 75 minutes, with an average of 120 minutes. A laser exposure of 10 W for 75 seconds commonly resulted in an ablation area of 14 by 12 mm.

**Conclusion:** MR-guided FLA of prostate tumors with real-time thermal imaging is technically feasible, safe, and has a low rate of complications or side effects. It is a viable minimally invasive option for treating focal prostate tumors [Gleason 6-7 ], but long term followup studies need to completed before it is widely accepted in clinical practice.

Title: Real-Time Tissue Change Monitoring on the Sonablate® 500 during High Intensity Focused Ultrasound (HIFU) Treatment of Prostate Cancer

Authors: Narendra T. Sanghvi[1], Wo-Hsing Chen[1], Roy Carlson[1], Toyoaki Uchida[2], G. Schatzl[3] and M. Marberger[3]

Affiliation: [1]Focus Surgery, Inc., 3940 Pendleton Way, Indianapolis, Indiana 46226, [2]Department of Urology, Tokai University, Hachioji, Japan, and [3]Department of Urology, Medical University, Vienna, Austria

*Abstract:* Recently HIFU devices are used to treat prostate, kidney and other cancer using B-mode ultrasound guidance known as Visually directed HIFU. These changes are qualitative and operator dependent. There is a monotonic increase in ultrasound attenuation and backscattered ultrasound energy as tissue temperature elevates from 37° to 65°C and thereafter attenuation remains at the peak level. The backscattered Radio Frequency (RF) ultrasound signals contain information related to tissue changes. Therefore new research efforts are pursued in signal processing to analyze RF pulse-echo backscattered signals to estimate tissue alterations caused by HIFU energy. Based on these novel algorithms, Tissue Change Monitoring (TCM) software for the Sonablate® 500 systems has been developed that display quantitative information on tissue status during the HIFU exposure.

*Method:* The RF backscattered signals were acquired for each treatment site pre and post HIFU. These signals are processed by Fast Fourier Transform (FFT) to derive their frequency spectra. These spectra are further divided into sub, center and higher harmonic bands for calculating the changes in the energy levels. During the HIFU treatment green, yellow or orange color is overlaid on each treatment site on the B-mode image that represent low, medium and high levels of tissue change respectively along with a value of energy change (range 0-1). The software validation was conducted *in-vitro* using chicken tissue and tissue temperature was monitored with thermocouples to correlate energy change to measured temperatures at ultrasound energy deposition.

Clinical Validation: TCM *in-vivo* tests were conducted in a clinical study at the Tokai University Hachioji Hospital. Contrast enhanced MR Images of the prostate were taken post HIFU (24-48 hours). These images were compared to TCM data.

*Results: In-vitro* data resulted high degree of cross correlation ($R^2$>0.92) between temperature and RF signal energy level changes. Early clinical studies with TCM were conducted in Japan (n=97). Post HIFU contrast enhanced MRI showed whole gland tissue ablation. Pre and post HIFU treatment nadir PSA (ng/ml) median changed from 6.89 to 0.07.

*Conclusion*: TCM measurements are independent of ultrasound images and independent of the operator and provide essential feedback required to assure that tissues are properly treated. In some cases immediate feedback can allow re-treatment of undertreated sites.

*Acknowledgement*: This research was partially supported by NIH / NCI grant 5R44CA083244-03 and clinical study in Japan was sponsored by Takai Hospital Supply Co., Tokyo, Japan. Authors would like to thank all other TCM users for their input and feedback.

**Design and characterization of a laterally mounted phased-array transducer breast-specific MRgHIFU device with integrated 11-channel receiver array**

Allison Payne[1], Robb Merrill[1], Emilee Minalga[1], Joshua de Bever[1], Nick Todd[1], Rock Hadley[1], Erik Dumont[2], Leigh Neumayer[3], Doug Christensen[1], Robert Roemer[1], Dennis Parker[1]

[1]University of Utah, Salt Lake City, Utah, 84112
[2]Image Guided Therapy, Pessac, France
[3]Huntsman Cancer Institute, Salt Lake City, UT, 84112

**Purpose:** This work presents the design and characterization of a new laterally mounted phased-array MRI-guided high-intensity focused ultrasound (MRgHIFU) system intended for breast cancer treatment. The design goals for the system included the ability to treat the majority of tumor locations, to increase the signal-to-noise ratio (SNR) throughout the treatment volume and to provide adequate comfort for the patient.

**Methods:** In order to treat the majority of the breast volume, the device was designed such that the treated breast is suspended in a 17-cm diameter treatment cylinder. A laterally shooting 1-MHz, 256-element phased-array ultrasound transducer with adjustable positioning is mounted outside the treatment cylinder. This configuration enables a reduced water volume to minimize RF coil loading effects, to position the coils closer to the breast for increased signal sensitivity, and to reduce the MR image noise associated with using water as the coupling fluid. This design uses an integrated 11-channel phased-array radio frequency (RF) coil that is placed on the outer surface of the cylinder surrounding the breast. Mechanical positioning of the transducer and electronic steering of the focal spot enable placement of the ultrasound focus at arbitrary locations throughout the suspended breast. The treatment platform allows the patient to lie prone on the treatment platform. The system was tested for comfort with 18 normal volunteers and SNR capabilities in one normal volunteer and for heating accuracy and stability in *ex vivo* porcine tissue.

**Results:** The SNR achieved in a normal volunteer's breast was significantly improved to that seen using only a single loop coil around the chest wall, particularly in regions towards the nipple. The repeatability of the system's energy delivery in a single location was excellent, with less than 3% variability between repeated temperature measurements at the same location in *ex vivo* tissue. The execution of a pre-defined 48-point, 8-minute trajectory path resulted in a mean ablation volume of 8.17 $cm^3$, with one standard deviation of 0.35 $cm^3$ between tissue samples. Comfort testing resulted in negligible side effects for all volunteers.

**Conclusions:** This new design holds the promise of both safe and efficacious MRgHIFU treatments on breast tumors in a wide range of breast sizes and tumor locations.

# Tumor therapy by ultrasound-triggered drug release from microbubble-liposome complex.

A.L. Klibanov[1], T. Shevchenko[1], W. Shi[2] S. Sethuraman[2], Z. Du[1], M. Campa[1], R. Seip[2], E. Leyvi[2], B. Raju[2].

[1]Cardiovascular Division, University of Virginia School of Medicine Charlottesville VA 22908, [2]Philips Research North America, Briarcliff Manor NY 10510.

**Purpose.** Ultrasound-guided tumor therapy may improve drug therapeutic index via a localized personalized intervention strategy. In addition to providing inexpensive real-time imaging guidance, ultrasound presents means of drug activation, e.g., release of the drug sequestered in the carrier particle. In this study, we formulate doxorubicin-liposome-microbubble particles and destroy them in the tumor vasculature by focused ultrasound in a murine tumor model.

**Methods.** Microbubbles were prepared from decafluorobutane gas coated with phosphatidylcholine shell containing biotin-lipid. Liposomes (phosphatidylcholine, cholesterol, biotin-phosphatidylethanolamine) were attached to microbubbles via streptavidin. Doxorubicin (~0.6 pg/particle) was incorporated in liposomes by remote loading. MC38 murine colon adenocarcinoma cells (J. Schlom, NIH) were injected subcutaneously in the hind leg of C57BL/6 mice (>6 months of age). After tumor size reached ~5mm, therapy was initiated. Therapy study arm (n=6) received intravenous bolus injection of doxorubicin-liposome-microbubble complex (3 mg doxorubicin per kg animal body mass) under control of ultrasound contrast imaging (Philips iE33, L15-7 probe) and immediately followed by ultrasound treatment (TIPS system, Philips Research). Ultrasound was generated by a focused transducer array attached to an X-Y positioner operated for 6 min in a spiral pattern, set to cover tumor area fully. Ultrasound parameters were: 1.2 MHz, 2 MPa, 10 Hz PRF, 10,000 cycles, 15 s/10 s on/off regimen. A week later the treatment was repeated (1 mg/kg doxorubicin dose). Control groups received the complex but lacked ultrasound treatment, or received saline.

**Results.** Formation of microbubble-liposome complexes entrapping doxorubicin was confirmed by flotation, fluorescence microscopy and spectroscopy quantification. Circulating particles were observed in the tumor vasculature by ultrasound imaging. Focused ultrasound treatment of the tumor mass, under ultrasound imaging guidance confirmed microbubble destruction in the bloodstream. On days 4-8 of the study, statistically significant ($p<0.05$) delay of tumor growth was observed in comparison with control groups. Treatment was tolerated well; animals retained body mass.

**Conclusions** Ultrasound activation of doxorubicin-carrying microbubble-liposome complexes in the tumor vasculature following intravenous administration resulted in a statistically significant but transient hindrance of tumor growth in comparison with control groups.

# Session 5: Cardiac Imaging for Intervention

Session Chair: Ehud Schmidt, PhD

## Invited Speakers

1. Real-time MRI guided cardiovascular intervention
   Robert Lederman, PhD, NHLBI/NIH

2. Clinical evaluation of an ultrasound based imaging system for Guiding cardiac ablation
   P. D. Wolf, Ph.D., S. A. Eyerly M.S., D. M. Dumont, Ph.D., G. E. Trahey, Ph.D., and T. D. Bahnson, M.D. Departments of Biomedical Engineering and Medicine, Duke University and Duke University Medical Center, Durham NC.

3. MRI guided EP ablation
   Henry Halperin M.D. MA, Saman Nazarian MD, Aravandan Kolandaivelu MD, Albert Lardo PhD, Menekhem Zviman PhD., Ronald Berger MD PhD. Johns Hopkins Medical Insititutions

4. 5D Image Guided Cardiac Ablation Therapy
   Richard Robb, Ph.D., David Holmes, III Ph.D., Maryam Rettman Ph.D. Mayo Clinic

## Posters

1. Intracardiac Ultrasound Imaging with CMUT-based Catheters
   Azadeh Moini, Amin Nikoozadeh, Ömer Oralkan, Jung Woo Choe, Fatih Sarioglu, Douglas N. Stephens, Alan de la Rama, Peter Chen, Carl Chalek, Aaron Dentinger, Douglas Wildes, Lowell S.Smith, Kai Thomenius, Kalyanam Shivkumar, Aman Mahajan, Matthew O'Donnell, David J. Sahn and Pierre T. Khuri-Yakub. Stanford University, University of California, Davis, St. Jude Medical, General Electric Global Research, University of California, Los Angeles, University of Washington, Oregon Health and Science University.

2. Augmented Image-Guidance for Transcatheter Aortic Valve Implantation
   Pencilla Lang, Michael W.A. Chu, and Terry M. Peters, University of Western Ontario, London, Canada

3. Electroanatomical Mapping Guided Acoustic Radiation Force Impulse Imaging for Lesion Assessment during Cardiac Ablation Procedures
   Stephanie Eyerly, MS, Tristram Bahnson, MD, Jason Koontz, MD, PhD, Joshua Hirsch, BS, David Bradway, BS, Douglas Dumont, BS, Gregg Trahey, PhD, Patrick Wolf, PhD. Duke University, Duke University Medical Center

# Interventional cardiovascular MRI

Robert Lederman, NHLBI/NIH

Interventional cardiovascular MRI (iCMR) represents an attempt to harness the tissue imaging capabilities of MRI to guide therapeutic catheter procedures. By making small compromises in spatial or temporal resolution, and with minor modifications to commercial high performance MRI systems, images can be acquired and displayed almost instantaneously to physicians manipulating catheter devices. This may be useful to avoid ionizing radiation during conventional catheter-based procedures, especially in children. More important, iCMR may enable more advanced procedures not otherwise possible without open surgical exposure. The key barrier to wider testing of cardiovascular interventional MRI is the unavailability of commercial-grade conspicuous and safe catheter devices including guidewires and catheters. In this presentation we shall review attractive applications of iCMR, novel accomplishments in preclinical systems, and investigational clinical work to date.

## CLINICAL EVALUATION OF AN ULTRASOUND BASED IMAGING SYSTEM FOR GUIDING CARDIAC ABLATION

P. D. Wolf, Ph.D., S. A. Eyerly M.S., D. M. Dumont, Ph.D., G. E. Trahey, Ph.D., and T. D. Bahnson, M.D.
Departments of Biomedical Engineering and Medicine, Duke University and Duke University Medical Center, Durham NC.

Thousands of cardiac ablation procedures are performed daily yet no method is commonly used to visually guide ablation procedures in the heart. We have developed a method of evaluating thermal ablation lesions using Acoustic Radiation Impulse imaging(ARFIi). Thermal ablation causes a coagulation of proteins, locally increasing tissue stiffness. ARFIi measures and displays the relative elastic property of tissue by measuring the tissue displacement caused by a high-energy acoustic pulse delivered from an ICE transducer.

The most difficult component of the evaluation process is knowing the location of lesions in the same frame of reference as the imaging system thus allowing the ultrasound imaging plane to transect the lesions. Our method uses intracardiac echo (ICE) catheter based transducers to perform the imaging and a magnetic catheter tracking system to record ablation lesion locations and to guide the imaging plane of the ICE catheter to the lesion locations for interrogation. The method was prototyped in animals and shown in vitro to correlate with lesion size and in animals to correlate with electrical block. The method is now ready for clinical proof of concept.

Clinically, we seek to understand 1) the elasticity contrast in senescent and diseased hearts 2) the ability to access all lesions in both the right and left atria with a limited field of view, 3) the effect of atrial fibrillation on ARFIi contrast, and 4) the correlation of ARFIi evaluation with electrical outcome in atrial flutter and atrial fibrillation ablation procedures. With the assistance of Siemens Medical Imaging and Biosense Webster, we have developed a tool to answer these important clinical questions and to move the promise of ARFI image guided cardiac ablation towards the goal of clinical acceptance.

## MRI GUIDED EP ABLATION

**Henry Halperin M.D. MA, Saman Nazarian MD, Aravandan Kolandaivelu MD, Albert Lardo PhD, Menekhem Zviman PhD., Ronald Berger MD PhD.**

**Johns Hopkins Medical Insititutions**

Atrial fibrillation (AF) and ventricular tachycardia (VT) affect millions of patients in the United States. These arrhythmias can be cured with catheter ablation, but the arrhythmias often recur. The inability to confirm the presence of ablated lesions in the desired locations is the major factor in the greater than 30 % recurrence of AF after ablation. Additional limitations of current ablation technology include: (1) difficulty in navigating catheters to exact locations, making it difficult to accurately place ablations, and (2) the lack of ability to adequately predict the pathways of VT through scar, which are the targets for ablation. We are developing ways of combining the anatomic information from magnetic resonance imaging (MRI) with catheter ablation, for performing advanced real-time image guided interventions.

We hypothesize that high resolution imaging with MRI with compatible electrode catheters, catheter-tip location sensors, remote-controlled catheter manipulators, real-time scanner control, thermal imaging, and 4-dimensional (3 spatial dimensions plus time) imaging software can (1) provide for accurate navigation of catheters, (2) provide the ability to titrate and confirm the presence of ablated lesions in the desired locations, (3) aid in producing more accurate electrical maps, and (4) aid in predicting the extent of ablation needed to eliminate the target arrhythmia. We have previously demonstrated the feasibility of (1) real-time MRI guidance of catheters, (2) lesion visualization using MRI, (3) high resolution imaging of preserved myocardial tissue in scar, and (4) using computational modeling to predict the location of VT circuits.

We are currently developing (1) improved catheter tip location sensors, (2) improved real-time scanner control, (3) dynamic 3-dimensional image reconstruction, with superimposed catheter tip location information, (4) improved high resolution imaging of myocardium so that details of preserved myocardium within scar can be adequately visualized, (5) a computational model that can predict the VT circuits in individual patients based on the detailed scar morphology, (6) improved methods for predicting individual patient's response to ablation, (7) methods for real-time registration of multimodal information, including electrical maps, and multiple images, (8) MRI thermography to aid in real-time titrating and assessing of ablation lesion formation, and (9) remote controlled catheter manipulators to improve the accuracy of catheter placement. We will apply this technology to real-time advanced image guided therapy in patients with atrial and ventricular arrhythmias, and potentially broaden its use to interventional procedures in general.

# 5D Image Guided Cardiac Ablation Therapy

**Richard Robb, Ph.D.**
**David Holmes, III Ph.D.**
**Maryam Rettman Ph.D.**

**Mayo Clinic**

Cardiac arrhythmias are a major clinical health problem. We have developed a significant and unique solution with grant funding from NIBIB/NIH. We have designed, constructed and extensively tested a novel prototype system, (which we refer to as the "5DEP" system) which is designed and engineered to integrate in real time multiple image and associated physiological variables, device signals and computer generated data required for accurate navigation and precise targeting in catheter based ablative treatment of cardiac arrhythmias. We are initially focusing on atrial fibrillation, but other cardiac arrhythmias will also be addressed. This advanced system, when fully completed and validated, has the potential to set a new standard of care in cardiac arrhythmia ablation therapy. Our system design and engineered prototype is technologically advanced, open and flexible, permitting ready integration of new imaging modalities, interventional devices and physiologic signals as they become available. This system has demonstrated potential for real time performance in fusing dynamic cardiac anatomy with physiologic signals (specifically electrophysiological signals). Based on this promising but preliminary progress we are now able to specify and complete the requirements for seamless clinical implementation and application of this system. These requirements include further enhancement, optimization and addition of novel algorithms and technology. Our continuing specific aims include achieving real time segmentation of pre and intra operative image data including Dyna-CT and 3D ultrasound. This segmented multi-modality image data will be registered and fused with electrophysiological signals in real time during the ablative procedure. Using catheter tracking and tissue characterization, we will develop and validate an innovative approach to physiologic visualization of intra operative ablation sites ("burns"). This capability will provide accurate visualization of burn targets on myocardial anatomy to guide and verify the desired ablation patterns. These high performance segmentation, fusion and quantitative visualization capabilities will be the basis for our final real time platform for 5D image guided cardiac ablation. This system is being validated in detailed phantom and animal experiments as well as preliminary clinical evaluations. We plan to demonstrate this system as efficacious both in a standard clinical setup using catheter tracking and x-ray fluoroscopy and/or pre-operative CT, and in an advanced instrumentation clinical setup using dynamic CT or 3D ultrasound, including a robotic manipulator for precise and stable catheter control. This system will be fully documented to facilitate ready reproduction and utilization. In summary, this project is poised to deliver a new generation of technology for effective treatment of cardiac arrhythmias that will result in significant clinical benefits, including dramatically improved outcomes with reduced morbidity, mortality, procedure time, x-ray exposure and cost.

# Intracardiac Ultrasound Imaging with CMUT-based Catheters

Azadeh Moini[1], Amin Nikoozadeh[1], Ömer Oralkan[1], Jung Woo Choe[1], Fatih Sarioglu[1], Douglas N. Stephens[2], Alan de la Rama[3], Peter Chen[3], Carl Chalek[4], Aaron Dentinger[4], Douglas Wildes[4], Lowell S. Smith[4], Kai Thomenius[4], Kalyanam Shivkumar[5], Aman Mahajan[5], Matthew O'Donnell[6], David J. Sahn[7] and Pierre T. Khuri-Yakub[1],

**1** Stanford University, **2** University of California, Davis, **3** St. Jude Medical, **4** General Electric Global Research, **5** University of California, Los Angeles, **6** University of Washington, **7** Oregon Health and Science University.

Corresponding Email: amoini@stanford.edu

## PURPOSE

Currently, over 2.2 million adults in the United States alone suffer from atrial fibrillation, the most common type of cardiac arrhythmia. Clinical electrophysiology (EP) is commonly performed under fluoroscopy guidance, a potentially harmful procedure. Intracardiac echocardiography (ICE) catheters reduce fluoroscopy exposure and provide high-resolution, real-time guidance in clinical EP.

## METHODS

Using capacitive micromachined ultrasonic transducer (CMUT) technology, we developed two types of ICE catheters, providing 2-D and 3-D, real-time, forward-looking ultrasound imaging capability. Custom-designed ICs are integrated at the catheter tip in both designs.
The 2-D imaging catheter uses a 24-element MicroLinear (ML) CMUT array. This catheter measures 9F in size.
The 3-D imaging catheter is equipped with a 64-element ring CMUT array. The second generation of the ring catheter prototype has a reduced number of cables, improving its steerability. Additionally, the ring catheter has a continuous inner lumen, allowing convenient delivery of other devices for a variety of applications, such as RF ablation catheters, HIFU transducers, and optical fibers for photoacoustic imaging. Furthermore, the top CMUT electrode can be grounded in the latest prototype through bias level-shifting without additional circuitry. This clinically significant advancement improves both the safety of the device and its noise susceptibility.

## RESULTS

We have previously demonstrated the *in vivo* images of the heart in a porcine animal model using the ML catheters. In a recent animal study, we also demonstrated the *in vivo*, real-time, volumetric imaging capability of the ring catheters. Furthermore, we used the ML catheters for thermal strain imaging to deduce the *in vivo* tissue temperature during the RF ablation procedure.

## CONCLUSIONS

Several improvements to the first generation forward-looking CMUT catheters have been successfully prototyped. These recent advances improve the functionality of the devices and enhance their use in a clinical environment.

# Augmented Image-Guidance for Transcatheter Aortic Valve Implantation

Pencilla Lang[a], Michael W.A. Chu[b], and Terry M. Peters[a]
[a]Robarts Research Institute, [b] Division of Cardiac Surgery,
University of Western Ontario, London, Canada

## 1. PURPOSE

Transcatheter aortic valve implantation (TAVI) is a minimally invasive procedure in which a bioprosthetic valve is delivered on a catheter through the femoral artery or left ventricular apex, displacing the native valve and functionally replacing it. Significant complications, including valve malposition, embolism, and coronary obstruction, result from inadequate image guidance, with single plane fluoroscopy providing only gross anatomical features. Recent work has focused on using additional intra-operative 3D imaging, including cone-beam CT and intra-operative MRI,[1,2] but these approaches are limited by availability and cost. The objective of this study is to provide real-time augmented visualization for TAVI by registering together existing clinical images: pre-operative CT, intra-operative transeophageal echo (TEE) and fluoroscopy.

## 2. METHODS

The three images are registered into a common coordinate frame in two steps:

1. **Fluoroscopy to TEE:** Fiducial-based single-perspective pose estimation is used to track the spatial position of the TEE probe. Target registration error (TRE) was assessed on a point target phantom, and aortic root targets in *ex vivo* porcine and *in vivo* porcine subjects.
2. **CT to TEE:** TEE points are automatically identified using a graph-cut based segmentation. Segmentation was assessed on 10 patient datasets by comparing algorithm performance against expert gold standards, using the dice coefficient and RMSE as performance metrics. Iterative closest point (ICP) registration is used to register segmented points to an aortic root model generated from CT. Registration performance was assessed by measuring the TRE using the left and right coronary ostia, and the virtual basal plane as targets.

## 3. RESULTS

1. **Fluoroscopy to TEE:** 2D TRE results had RMS errors of 0.75, 1.40 and 1.53mm for the point target, *ex vivo* and *in vivo* subjects respectively (Figure 1a). Registration of each frame took approximately 50ms.
2. **CT to TEE:** Automatic TEE short axis segmentation had a dice coefficient of 0.9 $\pm$ 0.02 and an RMSE of 1.5 $\pm$ 0.45mm(Figure 1b). The RMS TRE was 4.60mm (Figure 1c). Segmentation and registration of each frame took approximately 90ms.

Initial clinical experience suggests that these errors and processing speeds are acceptable for guidance of TAVI.

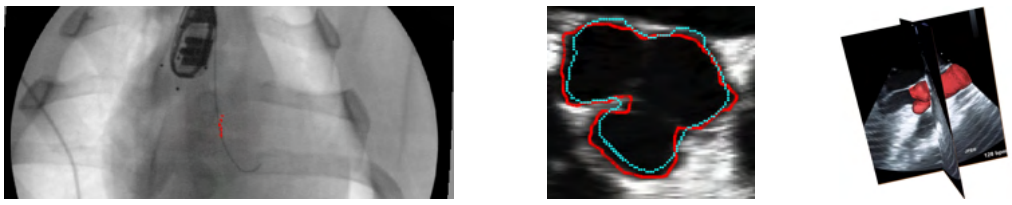

(a) (b) (c)

Figure 1. (a) Wire target points from TEE reprojected onto fluoroscopy (b)Aortic root segmentation: red - gold standard, cyan - algorithm (c) Registration of TEE to CT

## 4. CONCLUSIONS

In this study TEE, fluoroscopy and preoperative CT images were registered together in the development of an augmented image guidance system for TAVI with the potential to significantly reduce patient morbidity and mortality. In addition to real-time capabilities these registration methods provide several advantages: they are fully automatic, require no additional operating room hardware, do not change procedure or imaging workflow and are accessible to all cardiac centres at extremely low cost. Next steps focus on implementation of a clinically suitable visualization environment and clinical testing.

## REFERENCES

[1] Kempfert, J., Rastan, A., Noettling, A., Blumenstein, J., Linke, A., Schule, r G. Mohr, F., and Walther, T., "Perioperative dynact for improved imaging during transapical aortic valve implantation [ aha meeting abstract ]," *Circulation* **122** (Nov 2010).

[2] Horvath, K., Mazilu, D., Kocaturk, O., and Li, M., "Transapical aortic valve replacement under real-time magnetic resonance imaging guidance: Experimental results with balloon-expandable and self-expanding stents," *European Journal of Cardio-thoracic Surgery* **39**(6), 822–828 (2011).

# Electroanatomical Mapping Guided Acoustic Radiation Force Impulse Imaging for Lesion Assessment during Cardiac Ablation Procedures

Stephanie Eyerly, MS,[1] Tristram Bahnson, MD,[2,3] Jason Koontz, MD, PhD,[2]
Joshua Hirsch, BS,[1] David Bradway, BS,[1] Douglas Dumont, BS,[1]
Gregg Trahey, PhD,[1,4] Patrick Wolf, PhD[1]

[1]Deptartment of Biomedical Engineering, Duke University, [2]Duke University Medical Center, [3]Clinical Cardiac Electrophysiology, Division of Cardiovascular Medicine, Duke University Medical Center, [4]Radiology, Duke University Medical Center

**Purpose:** Atrial fibrillation patients undergoing transcatheter ablation (TCA) treatment may require multiple procedures due to reconnection across gaps in lesion lines. Direct visualization of lesion lines could guide the re-ablation of discontinuities during the initial procedure. We have previously shown that intracardiac echo (ICE) based 2D acoustic radiation force impulse (ARFI) imaging can visualize the elasticity contrast between healthy and radiofrequency ablated (RFA) myocardium. Unfortunately, it is time consuming to scan the chamber for RFA lesions with a 2D ICE imaging plane exclusively. Electroanatomical maps (EAM) can plot RFA delivery locations and display the orientation of an ICE imaging plane. ICE-based ARFI imaging was integrated with an EAM system to: 1) steer the imaging plane to RFA delivery locations, 2) construct local activation time (LAT) maps of the chamber, and 3) determine if ARFI imaging based lesion assessments match the presence/absence of conduction block at the imaging location.

**Methods:** A software modified S2000 ultrasound scanner (Siemens Medical) capable of acquiring ICE based (SoundStar™; Biosense Webster) ARFI images was integrated with a software modified CARTO XP system (Biosense Webster). A LAT map was constructed of an *in vivo* canine right atrium using point-mapping. Using the LAT map, the ICE imaging plane was positioned to acquire B-mode and ARFI images transecting an RFA line after two stages of RFA: the first left a conductive gap (~1cm) and the second closed the gap. New LAT maps were constructed after each stage of ablation. The ARFI images and LAT maps for each imaging location were read for discontinuous/continuous lesion and no block/block, respectively. Each image-map pair was counted in a 2x2 contingency table and correlated with a Pearson Chi-square Test and Phi coefficient.

**Results:** In eight canines, 150 ARFI images were counted for statistical analysis. The ARFI imaging lesion assessments were statistically consistent with the conduction block assessments from the LAT maps ($p<0.0001$, $\varphi = -0.72$).

**Conclusions:** The ARFI imaging plane was successfully guided to RFA lesion locations using EAM. Locating and eliminating lesion line discontinuities with ARFI imaging guidance could increase the success rate of initial TCA procedures.

| | | ARFI Image Lesion Assessment | | |
|---|---|---|---|---|
| | | Discontinuous | Continuous | Total |
| LAT Map Assessment | No Block | 84 | 7 | 91 |
| | Block | 13 | 46 | 59 |
| | Total | 97 | 53 | 150 |

Chi-Square Test: $p<0.0001$, $\varphi = -0.72$ (VassarStat)

## Session 6: Abdominal Intervention

Session Chair: Kemal Tuncali, MD

## Invited Speakers

1. 3T MRI for abdominal interventions and computerized monitoring of cryoablation.
   Kemal Tuncali, MD, Brigham & Women's Hospital & Harvard Medial School

2. US-guided liver surgery, Michael Choti, MD FACS, Johns Hopkins Surgery

3. Development of an Intrabiliary MRI-Monitored Local Agent Delivery Technique: Toward MR/RF-Enhanced Chemotherapy of Malignant Biliary Obstructions
   Feng Zhang, MD, PhD, Yanfeng Meng, MD, PhD, Xiaoming Yang, MD, PhD. Image-Guided Bio-Molecular Intervention Research, Department of Radiology, University of Washington School of Medicine, Seattle

## Posters

1. Improved Diagnosis of Pancreatic Cystic Lesions with EUS-guided Optical Coherence Tomography
   N. Iftimia, D. Hammer, M. Mujat, R.D. Ferguson, M. Pitman, and W. Brugge. Physical Sciences, Inc., Andover, MA, MGH.

2. Liver Imaging: Multiparametric Quantitative MRI for Tissue Characterization.
   Stephan W Anderson MD, Hernan J Jara PhD, Al Ozonoff PhD, Michael O'Brien MD, Jonathan Scalera MD, Jorge A Soto. Boston University Medical Center, Children's Hospital, Boston University School

3. Endovascular Catheter-Based Thermal Ablation in the MRI Environment.
   Mark Wilson, MD, K. Pallav Kolli, MD, Rishi Kant, PhD, Maythem Saeed, PhD, DVM, Jeremy Durack, MD, Shuvo Roy, PhD, Steven Hetts, MD. The University of California, San Francisco

4. Methods and Techniques for Intraoperative Image Fusion in Laparoscopic Surgery.
   Mahdi Azizian, PhD, Kevin Cleary, PhD, Timothy Kane, MD, Craig Peters, MD, Raj Shekhar, PhD, Sheikh Zayed. Children's National Medical Center, Washington DC,

5. Aiding Intra-procedural Monitoring and Post-procedural Assessment of CT-guided Liver Tumor Ablation using Non-rigid Image Registration of Pre-procedural MRI with both Intra-procedural CT and Post-procedural MRI.
   A. Yamada PhD, S. Tatli MD, P. R. Morrison MS, S. G. Silverman MD, and N. Hata PhD. Brigham and Women's Hospital, Boston, MA

# 3T MRI FOR ABDOMINAL INTERVENTIONS AND COMPUTERIZED MONITORING OF CRYOABLATION

Kemal Tuncali, MD

At the Brigham and Women's Hospital we have a busy tumor ablation practice. To date, we have performed over 1000 image-guided tumor ablations using CT, ultrasound and MRI guidance, and utilizing cryo, radiofrequency and microwave. Unlike other modalities, MRI-guided cryoablation provides superior visualization of the tumor, adjacent critical structures and the iceball, providing better monitoring of the ablative procedure. Our initial experience had been with an open configuration 0.5 Tesla system. More recently, after needle and cryoprobe testing for heating and artifact, we have started performing abdominal biopsy (n=13) and tumor ablations (n=30) in a wide-bore (70 cm) 3 Tesla MRI (Verio, Seimens Medical Systems, Erlangen, Germany), taking advantage of fast, high resolution sequences with higher signal-to-noise ratio. We have used body matrix or loop coil in combination with spine coil elements incorporated in the scanner table.

High field MRI provides sequences suitable for segmentation and 3D modeling of the iceball, tumor, and adjacent structures. We have preliminary data of a computerized monitoring tool for MRI-guided cryoablation. This tool uses 3D models to provide real-time quantitative assessment of the ablation as it is being done, displaying tumor ablation metrics during the procedure. It helps determine if the tumor is treated appropriately while keeping adjacent structures safe.

In conclusion, we will present our early experience with 3T MRI-guided abdominal biopsy and cryoablations, focusing on advantages and disadvantages of this method, and present the concept and preliminary data of a computerized monitoring tool for MRI-guided cryoablations.

# Ultrasound-Guided Liver Surgery

Michael A. Choti, MD FACS
Jacob C. Handelsman Professor of Surgery
Johns Hopkins University School of Medicine
Baltimore, MD

Advances in preoperative and intraoperative imaging capabilities have significantly improved the safety and effectiveness of abdominal operations. In particular, outcomes from hepatic surgery have markedly improved largely due to the use of intraoperative ultrasonography (IOUS). Even in the era of high-quality preoperative imaging, IOUS remains is the most sensitive modality currently available for detecting otherwise occult liver tumors. In addition, IOUS allows real-time identification of intrahepatic vascular anatomy, assist in characterizing indeterminate lesions, and provide guidance for needle biopsy and ablation.

Several limitations currently exist in clinical ultrasound technology which are being addressed with ongoing research. These include (1) the imprecision of free-hand and laparoscopic approaches, (2) limitations of 2D acquisition and free-hand techniques for limit off-plane needle/probe targeting, (3) the inability to reconcile IOUS with preoperative cross-sectional imaging, and (4) the variable echogenicity and conspicuity of targets on B-mode ultrasound. Our ongoing collaborative research initiatives attempt to provide solutions addressing some of these limitations. These include: (1) development and validation of robotic minimally invasive IOUS using the DaVinci platform; (2) 3D rendering, tool-tracking, and probe guidance systems; (3) CT-IOUS image registration; and (4) US elasticity imaging for thermal ablation monitoring.

References:


- van Vledder M, Pawlik T, Munireddy S, Hamper U, de Jong M, Choti MA. Factors determining the sensitivity of intraoperative ultrasonography in detecting colorectal liver metastases in the modern era. *Ann Surg Oncol* 2010 17(10); 2756-63.
- Schneider CM, Peng PD, Taylor RH, Dachs GW, Hasser CJ, DiMaio SP, Choti MA. Robot-Assisted Laparoscopic Ultrasonography for Hepatic Surgery. Surgery (in press).
- Rivaz H, Boctor EM, Choti MA, Hager GD. Ultrasound elastography using multiple images. Proc MICCAI 2011 (in press).
- Rivaz H, Boctor EM, Choti MA, Hager GD. Real-time regularized ultrasound elastography. IEEE Trans Med Imaging. 2011 Apr;30(4):928-45.
- Stolka P, Kang H, Choti M, Boctor E. Multi-DoF Probe Trajectory Reconstruction with Local Sensors for 2D-to-3D Ultrasound. IEEE (ISBI). 2010.
- van Vledder MG, Boctor EM, Assumpcao LR, Rivaz H, Foroughi P, Hager GD, Hamper UM, Pawlik TM, Choti MA. Intra-operative ultrasound elasticity imaging for monitoring of hepatic tumour thermal ablation. HBP (Oxford). 2010 Dec;12(10):717-23.
- Boctor EM, Choti MA, Burdette EC, Webster III RJ. Three-dimensional ultrasound-guided robotic needle placement: an experimental evaluation. Int J Med Robot. 2008 June;4(2):180-91.
- Rivaz H, Fleming I, Assumpcao L, Fichtinger G, Hamper U, Choti MA, Hager G, Boctor E. Ablation monitoring with elastography: 2D in-vivo and 3D ex-vivo studies. Med Image Comput Comput Assist Interv. 2008;11(Pt 2):458-66.

**Development of an Intrabiliary MRI-Monitored Local Agent Delivery Technique: Toward MR/RF-Enhanced Chemotherapy of Malignant Biliary Obstructions**

Feng Zhang, MD, PhD, Yanfeng Meng, MD, PhD, Xiaoming Yang, MD, PhD*

Image-Guided Bio-Molecular Intervention Research, Department of Radiology, University of Washington School of Medicine, Seattle

**Purpose:** Management of obstructive pancreatobiliary malignancies is a challenging task. The aim of this study was to investigate the feasibility of using magnetic resonance imaging (MRI) to monitor intrabiliary local delivery of motexafin gadolinium (MGd) into pig common bile duct (CBD) walls.

**Methods:** This study was divided into three portions. The first portion with serial in vitro experiments was designed to confirm intracellular MGd uptake by cholangiocarcinoma cells. Human cholangiocarcinoma cells were treated with various concentrations of MGd (a compound serving as MR T1 contrast agent, chemodrug and cell marker), and then examined by 3T MR T1-weighted imaging (T1WI) and confocal microscopy. The second portion with serial ex vivo experiments was to evaluate the capability of locally delivering MGd into CBD walls. MGd/trypan-blue mixture was locally infused into six CBD walls of cadaveric pigs by using a microporous balloon catheter, while additional six pig CBDs served as controls and were infused with saline. Ex vivo MR T1WI of these CBDs was performed. The third portion was designed to validate, in vivo, the feasibility of this new technique. Via a transcholecystic approach, the microporous balloon catheter was placed to locally deliver MGd/blue mixture into CBD walls of six living pigs. T1WIs with both a surface coil and an intrabiliary MR imaging-guidewire (MRIG) were obtained, contrast-to-noise ratios (CNR) of CBD walls pre- and post-MGd/blue infusions were statistically compared, followed by subsequent histologic analysis to confirm the penetration and distribution of MGd/blue into CBD walls.

**Results:** The in vitro experiments confirmed uptake of MGd by human cholangiocarcinoma cells. The ex vivo experiments displayed the penetration of MGd/blue into the CBD walls. The in vivo experiments demonstrated the uptake of the MGd/blue agent, showing increased CNR for the CBD post MGd/blue administration comparing to pre MGd/blue administration (11.6±4.2 vs 5.7±2.8, p=0.04). Correspondingly, histology depicted the blue dye stains and red fluorescence of MGd in CBD walls.

**Conclusions:** It is feasible to use MRI in monitoring the penetration of locally delivered MGd into pig CBD walls, which establishes the groundwork to develop a new technology, intrabiliary MR/radiofrequency-enhanced chemotherapy of malignant biliary obstructions.

# Improved Diagnosis of Pancreatic Cystic Lesions with EUS-guided Optical Coherence Tomography

N. Iftimia*, D. Hammer*, M. Mujat*, R.D. Ferguson*, M. Pitman**, and W. Brugge**

*Physical Sciences, Inc., Andover, MA-01810

**Massachusetts General Hospital, Boston, MA

## ABSTRACT

**Purpose:** Cystic lesions of the pancreas represent an increasingly common diagnostic and therapeutic challenge for the gastrointestinal surgeon. Currently, endoscopic ultrasound-fine needle aspiration (EUS-FNA) is used as the first line of diagnosis for pancreatic cysts. EUS-guided FNA is frequently being utilized as the diagnostic method of choice due to its increased resolution compared to computed tomography (CT) and due to the ability to provide cystic material (cells and fluid) for cytopathological analysis. However, at least two major problems are still associated with the current EUS-FNA practice: (1) early diagnosis of malignant pancreatic lesions is not possible because of lack of imaging resolution; (2) the diagnostic accuracy of cystic neoplasms varies in a large range (30-80%) because of the difficulty in subclassifying pancreatic cysts with respect to non-neoplastic and neoplastic as well as with respect to the type of neoplastic cyst (serous versus mucinous and benign versus malignant); this leads very often to unnecessary surgery. Here we propose a new diagnostic approach based on EUS-guided optical coherence tomography (EUS-OCT), which has shown some potential for providing improved diagnosis of the cystic lesions of the pancreas.

**Methods:** A common path fiber optic-based catheter, fitting the bore of existing FNA-EUS needles, is launched into the cystic cavity under EUS guidance to reveal the morphology of the cystic wall and the scattering properties of the cystic fluid. Thus, besides the aspirated material, the gastroenerologist and the pathologist will also benefit by the capability of OCT for providing micron-scale images of the cyst. A therapeutic capability could also be provided by sending a laser beam through the same catheter, to thermally coagulate (cause necrosis of) the diseased epithelial tissue layer of the potentially malignant cysts.

**Results:** Preliminary *ex vivo* testing of this approach has been performed at the Massachusetts General Hospital (MGH) on over 40 tissue specimens, which were obtained from patients that undergone pancreatomy. This study has shown over 90% specificity of OCT imaging in differentiating between mucinous and serous cystic lesions. A pilot study is planned at MGH to test this new diagnostic approach *in vivo* on patients identified with cystic lesions that are difficult to differentiate radiologically.

**Conclusion:** High-resolution (micron scale) OCT imaging, has shown great promise in differentiating between serous and mucinous cysts of the pancreas. Therefore, it has the potential of being used in the future to more reliably differentiate between various neoplastic lesions in pancreas, and possibly in other organs, like kidney, liver, and lungs.

# Liver Imaging: Multiparametric Quantitative MRI for Tissue Characterization

Stephan W Anderson MD[1], Hernan J Jara PhD[1], Al Ozonoff PhD[2], Michael O'Brien MD[3], Jonathan Scalera MD[1], Jorge A Soto[1]

[1]Boston University Medical Center, Department of Radiology FGH Building, 3rd Floor 820 Harrison Avenue Boston, MA 02218

[2]Biostatistics Core Clinical Research Program Children's Hospital Boston Boston, MA 02115

[3]Department of Pathology and Laboratory Medicine Boston University School of Medicine 715 Albany Street Boston, MA 02218

### Purpose

To describe the use of quantitative MRI techniques, including relaxometric and diffusion weighted imaging based approaches, for deriving hepatic tissue characteristics.

### Methods

Using several murine models of diffuse liver disease as illustrative examples, the derivation of a host of quantitative MRI parameters, as applied to liver imaging, will be detailed. This will include both a discussion of the fundamental physical principles of the MRI techniques, technical considerations in applying the appropriate pulse sequences as well as in the subsequent image-processing, and the utility of these techniques in liver imaging.

### Results

The quantitative MRI techniques to be discussed include $T_1$ and $T_2$ relaxometry, including multi-exponential $T_2$ analyses, and diffusion weighted imaging, including alternative approaches such as bi-exponential and stretched exponential models as well as a relaxometry-derived correlation time diffusion technique. When appropriate, the biological models underpinning these techniques will be detailed, in addition to the physical principles and technical considerations in their acquisition and the derivation of the quantitative parameters. Histopathological correlation with these parameters in diffuse liver disease (steatohepatitis, fibrosis) will be demonstrated, including a discussion of potential utility in image guided therapy, such as monitoring of the liver parenchyma in areas surrounding focal sites of ablation or therapy. In addition, the current and potential future use of these techniques in tissue characterization, including the prediction and monitoring of therapeutic efficacy, in cases of hepatic malignancy, will be discussed. As well as the aforementioned techniques, a literature review and discussion of several other quantitative MRI techniques for liver characterization, including MR elastography (MRE), perfusion imaging, and functional MRI (fMRI) approaches will be undertaken.

### Conclusion

A multiparametric MRI approach to liver imaging offers the potential for quantifying several histopathological features in the hepatic parenchyma. These histopathologic features are of significant clinical importance in diffuse liver disease and may find application in the monitoring of liver parenchyma surrounding sites of focal therapy as well as hepatic tumor evaluation.

## Endovascular Catheter-Based Thermal Ablation in the MRI Environment

Mark Wilson, MD*, K. Pallav Kolli, MD*, Rishi Kant, PhD*, Maythem Saeed, PhD, DVM*, Jeremy Durack, MD*, Shuvo Roy, PhD*, Steven Hetts, MD*
**The University of California, San Francisco*

**Purpose:** We have previously described the construction of magnetically steerable endovascular catheters for interventional procedures performed in clinical MRI scanners. In this project we seek to harness the resistive heating that develops in the coil-tipped, steerable endovascular catheters for thermal tissue ablation under MRI visualization.

**Methods:** 5 French angiographic catheters were modified by winding solenoidal copper coils around the catheter tips. The copper wires leading to and from the coils were wound around the catheter to allow passage of a thermocouple through the catheter lumen (Fig. 1).

Figure 1. Solenoidal coil-tipped catheter, 30 AWG copper wire

*In vitro* testing was performed in a phantom comprised of bovine serum albumin (BSA) in polyacrylamide gel, which is similar in thermoconductivity to liver tissue. The coil-tipped catheters were suspended in the phantoms along with adjacent thermocouples at distances of 5 mm, 10 mm, and 20 mm from the coil-bearing portion of the catheter. Direct current in the range of 3.5-3.9 amperes was applied to the copper coils, with local hyperthermia ensuing as a result of direct thermal conduction. The coil-tipped ablation catheter was also tested in *ex vivo* specimens of porcine liver.

**Results:** BSA coagulation was visible to the naked eye at 50-95°C (Fig. 2). MR images at 1.5 T of the BSA gel phantoms demonstrated a “cold spot” related to T2 shortening when compared with the homogeneous controls (Fig. 3). In the treated *ex vivo* liver specimens, visible regions of tissue necrosis were observed grossly (Fig. 4) and on histology.

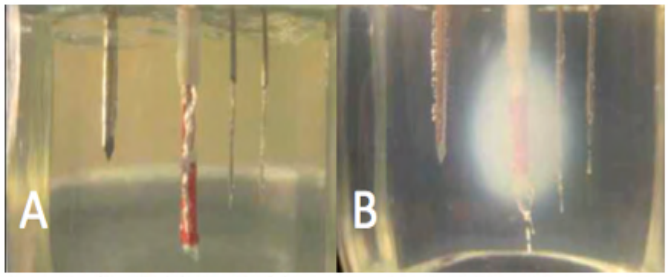


Figure 2. BSA gels (A) pre- and (B) post-current application to coil-tipped catheter to achieve temperature of 50-60°C. Note thermocouple positioning.

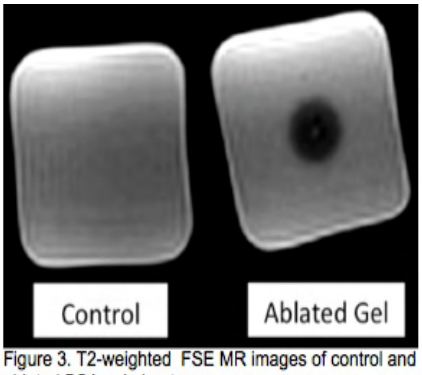


Figure 3. T2-weighted FSE MR images of control and ablated BSA gel phantoms.


Figure 4. Ablated region (arrow) of ex vivo liver specimen

**Conclusion:** The resistive heating properties of the coil-tipped ablation catheters can effectively produce temperatures within BSA gel phantoms and *ex vivo* liver tissue sufficient to induce cellular damage and necrosis. Resistive heating changes are demonstrable on MR imaging.

# *Methods and Techniques for Intraoperative Image Fusion in Laparoscopic Surgery*

*Mahdi Azizian, PhD, Kevin Cleary, PhD, Timothy Kane, MD, Craig Peters, MD, Raj Shekhar, PhD*
Sheikh Zayed Institute for Pediatric Surgical Innovation
Children's National Medical Center, Washington DC, USA

**Purpose:** The goal of this abstract is to review the state of the art of intraoperative image fusion for laparoscopic surgery and present our plans to develop an image fusion system for pediatric laparoscopic surgery. Digital laparoscopic cameras are widely used to provide intraoperative imaging feedback during minimally invasive surgery. However, these cameras only show visible organ surfaces. It is desirable to see beyond the surface to avoid inadvertent injuries to critical structures and to operate more effectively. Preoperative CT and MR images are often used to address this need, but correlating these images with what is seen through the laparoscopic camera is difficult. Intraoperative registration of preoperative images to live laparoscopic images is also challenging because organs may undergo large deformations during the surgery. In current practice, laparoscopic ultrasound is used occasionally to see beyond the visible surface of an organ during surgery, but the use of laparoscopic ultrasound imaging remains limited because it is difficult to interpret the resulting images and correlate them with the laparoscopic images. Overlay of ultrasound images on laparoscopic images may provide an intuitive intraoperative feedback for minimally invasive surgery.

**Methods:** Ultrasound and laparoscopic images can be captured in real time and optical/ magnetic tracking information can be used for registration. Projection of the ultrasound image plane onto the laparoscope image plane and blending of these images can provide a geometrically correct intraoperative image fusion. This technique can be extended to stereo laparoscopic images and/or 3D ultrasound images. Endoscopic laser range scanners or surface reconstruction using laparoscopic images (e.g. by projecting structured light) can also be used to provide tools for deformable registration and overlay of preoperative images.

**Results:** A comparative study of methods and techniques for intraoperative laparoscopic image fusion was performed where the comparison criteria included: software and hardware requirements, real-time performance (latency, synchronization issues, etc.), clinical use, and expected impact. We also present an overall system architecture for an intraoperative image fusion system focused on pediatric laparoscopic surgery.

**Conclusions:** Different techniques for intraoperative laparoscopic image fusion have been compared in terms of system architecture, design requirements, real-time performance, the overall impact and other criteria. Future systems for image fusion in laparoscopic surgery can be expected to benefit from the rapid growth in technology components. Collaborative relationships between scientists and clinicians can help enable the development of these clinically relevant systems.

**Aiding Intra-procedural Monitoring and Post-procedural Assessment of CT-guided Liver Tumor Ablation using Non-rigid Image Registration of Pre-procedural MRI with both Intra-procedural CT and Post-procedural MRI**

*A. Yamada PhD, S. Tatli MD, P. R. Morrison MS, S. G. Silverman MD, and N. Hata PhD*
*Surgical Planning Laboratory, Brigham and Women's Hospital, Boston, MA, USA*

**Rationale and Objectives** During percutaneous image-guided tumor ablations using cryoablation and radiofrequency (RF) ablation, the most common method to assess technical success is based solely on visual inspection of contrast-enhanced CT or MR images obtained at the end of the procedure or at 24 hours. If no residual tumor is detected, patients are typically imaged at 3- to 6-month intervals [1]. Clear identification of the ablation and tumor boundaries allow assess the coverage of tumor and ablation margin and avoid letting a recurrence of the tumor pass. While residual tumor may prompt repeat ablation, narrow ablation margin requires more close follow up this patients to detect recurrence before it reaches the size that cannot be treatable. In our previous study [2], we were able to visualize tumor boundaries after cryoablation and assess tumor coverage using 24-hour post-ablation contrast enhanced (CE) MR images. However, in some patients, tumor visualization was not clear after cryoablation. Furthermore, tumor boundaries are often not visible 24 hours after RF ablation. We therefore built further on our work using non-rigid image registrations to obtain the ablation and tumor boundaries after both cryoablation and RF ablations [3][4][5]. In this study, we investigated whether non-rigid registration of pre-procedural CEMRI with intra-procedural CT and post-procedural CEMRI could be used to 1) improve monitoring of CT-guided ablations of liver cancers, and 2) improve assessment. We also assessed the practicality of these aids by measuring computation time needed to perform the non-rigid image registrations.
**Methods** Non-rigid registration techniques were applied in five patients (48-72 years old) undergoing CT-guided cryoablation and RFA of liver cancers. Both intra-procedural CT and post-procedural MR images were registered to post-procedural MR images. An image dataset from the 24-hour follow-up scan (MRI or CT showing ablation volume) for each treated tumor was set as the "fixed" image and the "moving" image was an image dataset from the pre-procedural diagnostic exam (MRI or CT showing tumor). Non-rigid registration was performed with a B-spline transformation (BRAINSFitIGT Module, 3D Slicer [6]). The B-spline transformation was parameterized by a lattice of 5x5x5 control points. In each dataset, digital contours of the liver were drawn (the 3D Slicer software) and stored as a binary mask of this region of interest. This mask was used to restrict the modeling field to the surrounded area of the liver region. Non-uniform signal intensities in the images were normalized prior to applying the non-rigid registration (N4ITK Bias Correction Module, the 3D Slicer software).
**Results** During the procedure, registered images demonstrated tumor margins more clearly, allowing the precise planning and placement of the ablation probes resulting in better monitoring. The registered images exhibited the index tumor location within the volume of ablation demonstrating the feasibility of intra-procedural image registration. The 24-hour MR images registered to pre-ablation CEMR images allowed visualization of the tumor boundaries within the ablation zone resulting in better determination of the ablation margins. Mean computation time for registrations was 6 minutes.
**Conclusions** Non-rigid image registration between pre-procedural CEMR and intra-procedural CT and post-procedural CEMR images were feasible in a suitable timeframe and provided a practical way of monitoring and assessing CT-guided thermal ablation of liver cancers with improved visualization of the spatial relationship of the ablated volume to the targeted tumor. We plan to quantitate these improvements by comparing percent tumor coverage and dice similarity coefficient metrics with patient outcomes.

**Acknowledgments** This work was supported by NIH grants R01 CA124377, R01 CA138586, and P41 RR019703.

**References**
[1] Goldberg SN, Charboneau JW, Dodd III, GD, Dupuy D, Gervais D, Gilliams AR, Kane RA, Lee Jr FT, Livraghi T, McGahan J, Rhim H, Silverman SG, Solbiati L, Vogl TJ, Wood BJ. Image-guided tumor ablation: proposal for standardization of terminology and reporting criteria. Radiology 2005;235:728-739.
[2] S. Silverman et al. Three-Dimentional Assessment of MRI-Guided Percutaneous Cryotherapy of Liver Metastases. American Roentgen Ray Society; 183:707-712, 2004.
[3] H. Elhawary, S. Oguro, K. Tuncali, P. R. Morisson, S. Tatli, P. B. Shyn, S. G. Silverman, and N. Hata. Multimodality Non-rigid Image Registration for Planning, Targeting and Monitoring During CT-Guided Percutaneous Liver Tumor Cryoablation. Acad Radiol; 17:1334-1344, 2010.
[4] A. Fedorov, K. Tuncali, F. Fennessy, J. Tokuda, N. Hata, S.W. Wells, R. kikins, and C. M. Tempany. Hierarchical Image Registration for Improved Sampling during 3T MRI-guided Transperineal Targeted Prostate Biopsy. 19th ISMRM Annual Meeting, 2011.
[5] Giesel FL, Mehndiratta A, Locklin J, McAuliffe MJ, White S, Choyke PL, Knopp MV, Wood BJ, Haberkorn U, von Tengg-Kobiligk H. Image fusion using CT, MRI and PET for treatment planning, navigation and follow up in percutaneous RFA. Exp Oncol: 31 (2): 106-14, 2009.
[6] 3D Slicer Software. http://slicer.org

## WORKSHOP KEYNOTE: Molecular Medicine and Imaging Science: Focus on Image-Guided Interventions

Belinda Seto, PhD, Deputy Director NIBIB

## Stimulated Raman Scattering Microscopy: Label Free Molecular Imaging for Medicine

Sunney Xie, PhD, Harvard University

## NCI Programs in Image-Guided Interventions

Keyvan Farahani, PhD, NCI

**Molecular Medicine and Imaging Science: Focus on Image-Guided Interventions**

**Belinda Seto, Ph.D.**
**National Institute of Biomedical Imaging and Bioengineering**
**National Institutes of Health**

Molecular biology and imaging science provide powerful tools to the understanding of signatures or biomarkers for healthy state versus disease state at the cellular and molecular levels. Imaging science allows us to "peer" into the individual cell states and a collection of cell data represents a measure of the overall tissue state (dys)function. Thus, by measuring the cellular and molecular markers, we are in effect measuring tissue function. These fields open an exciting possibility for investigating, at the individual cell and tissue levels, the dynamic biological processes and cellular interactions*, in situ*, with temporal and ultra-spatial resolution. For example, it is possible to detect one circulating tumor cell (CTC) in a billion normal blood cells by taking advantage of the over-expressed cell surface tumor markers, e.g., epithelial cell adhesion molecules, epidermal growth factor receptor, etc. These cells can be visualized and characterized with specific fluorescent labels for cell surface, nuclear stain, and proliferating markers. But imagine what we might learn if we could capture in images the *in vivo* life cycle of these CTC's? What might we learn about metastatic processes? What innovative treatment modalities might we develop for cancers that reflect the deep understanding of metastasis? In addition to visualizing and characterizing CTC's, molecular imaging allows us to assess the heterogeneity of cells that make up the primary tumor itself and determine the optimal treatment. The possibility of using imaging to guide the delivery of therapies to target sites and monitor response and adapt treatment exists as micelles, liposomes and dendrimers with multi-functional blocking groups, fluorescent dyes or radionuclides, and drug payloads such as doxorubicin, paclitaxel, etc have been designed for specific tumor targets. This targeted, image-guided drug delivery is molecular therapeutics that requires knowledge in chemistry, physics, biology and clinical sciences. Image guided therapies exist at the cellular, tissue and organ levels. At the level of tissues and organs, we are familiar with the Da Vinci robots and MRI-guided treatments. An expansive view of image guided therapies opens many exciting research and clinical application opportunities.

A central theme for research supported by the National Institute of Biomedical Imaging and Bioengineering (NIBIB) is the convergence of the scientific disciplines: biology, engineering, physical sciences and mathematics. The challenges in solving biological or biomedical problems are not confined to the life sciences. Solutions to these complex problems will require interdisciplinary approaches. Development of image guided interventions has clearly capitalized on the scientific opportunities presented by the convergence of disciplines. Research, development and applications in this arena will no doubt advance medicine such that diagnosis and treatment are targeted at the molecular and cellular levels by pinpointing health and disease states.

## Stimulated Raman Scattering Microscopy: Label Free Molecular Imaging for Medicine

Christian Freudiger[1], Brian Saar[1], Xu Zhang[1], Daniel A. Orringer[2], Geoff Young[2], and X. Sunney Xie[1]

[1]*Harvard University, Department of Chemistry and Chemical Biology, Cambridge (MA)*

[2]Department of Radiology, Brigham and Women's Hospital, Boston (MA)

We recently developed a 3D multiphoton imaging technique, stimulated Raman scattering (SRS) microscopy, which allows imaging based on vibrational spectroscopy without the need for staining or fluorescent labeling. Chemical specificity of the technique for lipids, proteins and water is achieved by probing intrinsic vibrational properties of the molecules. Superb detection sensitivity is achieved by implementation of a high-frequency detection scheme and surpasses that of other label-free imaging techniques. SRS has the advantage in that it does not suffer from unwanted background signals that distort vibrational spectra and is linear with respect to molecular concentrations. We demonstrated video-rate SRS imaging of humans and present applications in drug delivery, medical diagnostics of brain pathologies.

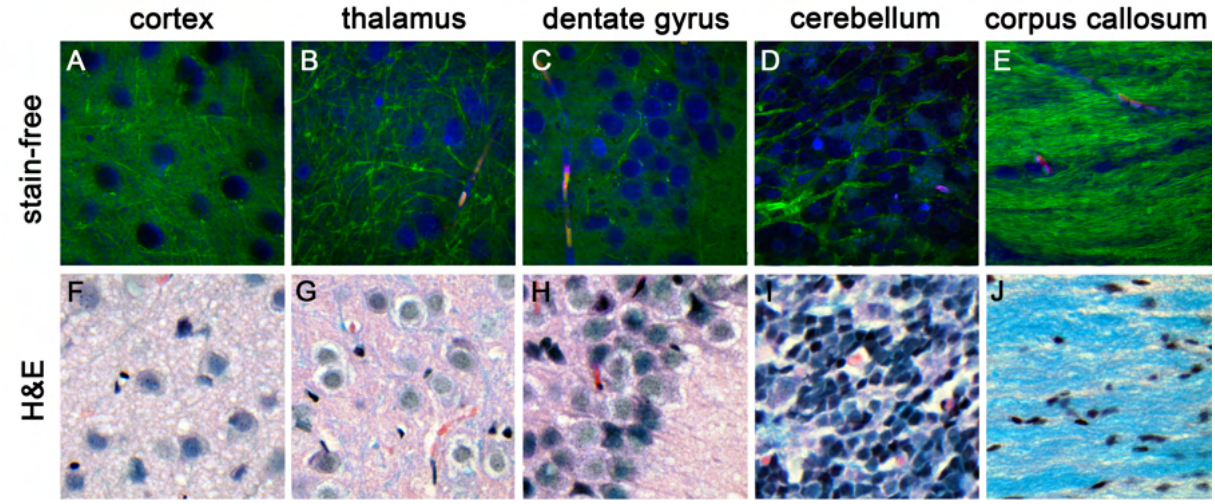


**Multicolor stain-free images of various brain regions in a wild-type mouse in comparison with paraffin-embeded, H&E and Luxol-stained sections.** (green: $CH_2$ image; blue: $CH_3$-$CH_2$ difference image; red: hemoglobin image) of (**A**) cortex, (**B**) thalamus, (**C**) dentate gyrus, (**D**) cerebellum, and (**E**) corpus callosum. (**F**-**J**) show H&E / luxol stained section of corresponding regions.

**References**

[1] Freudiger, C. W., Min, W., Saar, B. G. *et al.* Label-Free Biomedical Imaging with High Sensitivity by Stimulated Raman Scattering Microscopy. *Science* **322**, 1857-1861 (2008).

[2] Saar, B. G., Freudiger, C. W., Reichman, J. *et al.* Video-Rate Molecular Imaging In Vivo with Stimulated Raman Scattering. *Science* **330**, 1368-1370 (2010).

# NCI Programs in Image-Guided Interventions

Keyvan Farahani, PhD
Cancer Imaging Program
National Cancer Institute
Bethesda, MD 20852

The following funding initiatives by the National Cancer Institute (NCI) support research in image-guided interventions (IGI) in cancer:

**PA-09-253: Image-guided Drug Delivery in Cancer (R01)**
http://grants.nih.gov/grants/guide/pa-files/PA-09-253.html
This initiative encourages innovative translational research in the development of quantitative in vivo imaging characterization of image-guided drug delivery (IGDD) in cancer, including characterizations of the target, delivery validation, and therapy response. It will support research in development of integrated imaging-based platforms for multifunctional and multiplexed drug delivery systems in cancer.

**PAR-11-216: Early Phase Clinical Trials in Imaging and Image-Guided Interventions: Exploratory Grants (R21)**
http://grants.nih.gov/grants/guide/pa-files/PAR-11-216.html
The goal of this initiative is to support clinical trials conducting preliminary evaluation of the safety and efficacy of imaging agents, as well as an assessment of imaging systems, image processing, image-guided therapy, contrast kinetic modeling, and 3-D reconstruction and other quantitative tools. It will provide investigators with support for either pilot (Phase I and II) cancer clinical trials, or patient monitoring and laboratory studies.

**Academic-Industrial Partnerships for Development and Validation of In Vivo Imaging Systems and Methods for Cancer Investigations (R01) (PAR-10-169)** http://grants.nih.gov/grants/guide/pa-files/PAR-10-169.html
This funding initiative encourages applications from research partnerships formed by academic and industrial investigators to accelerate the translation of either animal or human in vivo imaging, image guided, and/or spectroscopic systems and methods designed to solve targeted cancer problems for cancer research, clinical trials, and/or clinical practice.

**PAR-11-150: Quantitative Imaging for Evaluation of Responses to Cancer Therapies (U01)**
http://grants.nih.gov/grants/guide/pa-files/PAR-11-150.html
Quantitative imaging of tumor response to cancer therapies, including IGI, in clinical trial settings, with the overall goal of facilitating clinical decision making, is the main thrust of this funding initiative. Proposed projects should include the appropriate development and adaptation/implementation of quantitative imaging methods, protocols and software solutions/tools and their application in current and planned Phase I/II clinical therapy trials. Awardees form a Quantitative Imaging Network (QIN) to share ideas and approaches to validate and standardize imaging data and related imaging meta-data for quantitative measurements of responses to cancer therapies.

**PA-10-080 and PA-10-079: Image-Guided Cancer Interventions**
STTR [R41/R42] http://grants.nih.gov/grants/guide/pa-files/PA-10-080.html
SBIR [R43/R44] http://grants.nih.gov/grants/guide/pa-files/PA-10-079.html
These small business-related funding initiatives support the development and clinical validation of systems for image-guided interventions for cancer. Specifically, the goals of this program are to provide support for: the development and optimization of fully integrated cancer imaging, monitoring, and therapy systems; the validation of integrated IGI systems through clinical evaluations; and partnerships among small business, large business, and academic clinical centers, as well as small business joint ventures, in order to reach the research goals.

For further information on any of the above initiatives please contact Dr. Keyvan Farahani (email: farahani@nih.gov)

# Session 7: Imaging for Gynecologic Cancer Radiation Therapy

Session Chair: Akila Viswanathan, MD, MPH

## Invited Speakers

1. Image Guided Gynecologic Brachytherapy
   Akila Viswanathan, MD, MPH. Brigham and Women's Hospital and Dana Farber Cancer Center, Harvard Medical School, Boston, MA

2. Intra-tumoral metabolic heterogeneity of cervical cancer
   Perry Grigsby. Mallinckrodt Institute of Radiology

3. IGT for cervix cancer using diffusion weighted and dynamic Contrast enhanced magnetic resonance imaging
   Nina A. Mayr, M.D. Arthur G. James Cancer Hospital and Solove Research Institute, Ohio State University

4. Utility of preoperative ferumoxtran-10 MRI to evaluate retroperitoneal lymph node metastasis in advanced cervical cancer: results of ACRIN 6671/GOG 0233
   Atri M, Zhang Z, Marques H, Gorelick J, Harisinghani M, Sohaib A, Koh DM, Raman S, Gee M, Choi H, Landrum L, Mannel R, Chuang L, Yu J, McCourt C, Gold M

## Posters

1. Predictive Power of At-Risk Tumor Voxels during Radiation Therapy for Cervical Cancer
   Zhibin Huang, Ph.D., Nina A. Mayr, M.D., Simon S. Lo, M.D., Guang Jia, Ph.D., John C. Grecula, M.D, Jian Z. Wang, Ph.D., William T. C. Yuh, M.D., M.S.E.E., East Carolina University, Greenville, NC, The Ohio State University, Columbus, OH, Case Western Reserve University, Cleveland, OH

2. Utility of a Novel MRI Technique for the Adaptive Planning of Intracavitary Brachytherapy Treatment for Cervix Cancer Patients
   J. Esthappan, Y. Hu, and P. Grigsby, Washington University School of Medicine, St. Louis, MO

3. Dosimetric Evaluation of Three Dimensional MRI-based Adaptive Treatment Planning for Cervix Cancer Intracavitary Brachytherapy
   A. Apicelli, P. Dyk, C. Bertelsman, B. Sun, S. Richardson, J. Garcia, J. Schwarz, P. Grigsby Washington University School of Medicine, St. Louis, MO

4. Proton density weighted MRI: a sequence to improve the definition of titanium applicators in MR-guided high dose rate brachytherapy for cervical cancer
   Yanle Hu, Ph.D., Esthappan Jacqueline, Ph.D., Sasa Mutic, Ph.D., Susan Richardson, Ph.D., Hiram Gay, M.D., Julie K. Schwarz, M.D., Ph.D., Perry W. Grigsby, M.D., Washington University School of Medicine, Saint Louis, MO

5. Assessment of Advantage of Dosimetric Guidance in Gynecological HDR Interstitial Brachytherapy
   Antonio Damato, Robert Cormack, Tina Kapur, Clare Tempany, Akila Viswanathan, Brigham and Women's Hospital and Dana-Farber Cancer Institute, Boston, Harvard Medical School, Boston

6. Concept Development and Feasibility Study of Image-based Needle Guidance for MR-Guided Interstitial Gynecologic Brachytherapy in AMIGO
   Radhika Tibrewal, BS, Akila Viswanathan, MD, MPH, Kanokpis Townamchai, MD, Janice Fairhurst, BS, RT, Maximilian Baust,MS, Jan Egger, PhD, Antonio Damato, PhD, Sang-Eun Song, PhD, Steve Pieper, PhD, Clare Tempany, MD, William M. Wells, PhD, Tina Kapur, PhD Brigham and Women's Hospital, Dana Farber Cancer Center, Harvard Medical School, Boston, MA

7. Predictive Outcome of Cervical Cancer Treatment Using Tumor Volume and Tumor Regression Rate during Radiation Therapy on Sequential Magnetic Resonance Imaging
   Kanokpis Townamchai MD, Tina Kapur PhD, Radhika Tibrewal BS, Akila Viswanathan MD, MPH, Brigham and Women's Hospital, Dana Farber Cancer Center, Harvard Medical School, Boston, MA

8. The use of Interactive, Real-time, Three-dimensional (3D) Volumetric Visualization for Image Guided assistance in the Brachytherapy Needle Placement for Advanced Gynecological Malignancies
   E. Brian Butler, M.D., Paul E. Sovelius, Jr., Nancy Huynh, Tri Dinh, M.D., Alan Kaplan, M.D. The Methodist Hospital, 1Department of Radiation Oncology and 2Department of Obstetrics and Gynecology

9. Bladder Segmentation for Interstitial Gynecologic Brachytherapy with the Nugget-Cut Approach
   Jan Egger, Ph.D, Akila Viswanathan MD, MPH, Tina Kapur, Ph.D. Brigham and Women's Hospital and Harvard Medical School, Boston, Dept. of Math. and Computer Science, University of Marburg, Dept. of Neurosurgery, University of Marburg, Marburg, Germany

# Image-Guided Gynecologic Brachytherapy

Akila Viswanathan MD, MPH
Brigham and Women's Hospital, Dana Farber Cancer Center, Harvard Medical School, Boston, MA, USA

In 2011, approximately 15,000 women will die of cervical, vaginal, vulvar or recurrent uterine cancer in the U.S.[1]. Most locally advanced gynecologic cancers affecting young women may be highly curable due to the relative sensitivity of these tumors to radiation. The survival rate of these women significantly increases with the addition of brachytherapy. Worldwide, most institutions use plain film x-rays (Figure 1) for gynecologic brachytherapy planning, with radiation dose calculated at a point, rather than to a volume. Over the past 10 years, a surge of interest in 3D imaging for assistance with brachytherapy insertion and planning has occurred, resulting in an appreciation of individual patient and tumor image-detected characteristics. 3D imaging of brachytherapy applicator placement, when used to aid treatment planning, increases the precision of radiation dose delivery by defining the tumor, resulting in maximum sparing of the normal tissues and a reduction in toxicity [2]. In the U.S., research comparing available (CT) and cutting-edge (MR and PET) technology for gynecologic brachytherapy treatment planning to determine appropriate utilization of imaging and its ultimate benefit to patients remains in its infancy.

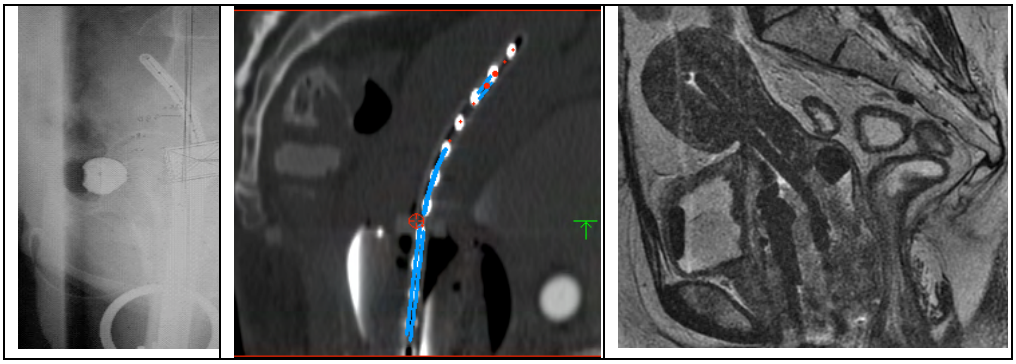

Figure 1. A comparison of plain film x-ray, CT and 3T MRI imaging for brachytherapy demonstrates the ability of plain films to show the applicator but not soft tissue, of CT to show the OAR but not the tumor, and of MRI to show the tumor and OAR.

One of the shared goals of the research programs in the departments of radiation oncology and radiology at BWH/DFCI is to address questions such as: How do the available imaging modalities, including MRI and FLT-PET/CT, quantitatively differ from one another in determining tumor dimensions? How does 3T MRI differ from 0.5 T MRI in terms of patient outcome? And how can 3T MRI best be used to individualize treatment? We performed the first MR-guided brachytherapy needle placement in the newly constructed multimodal imaging suite AMIGO at BWH/DFCI on September 9, 2011 and plan to use the imaging modalities in there to more precisely compare the tumor volumes and resultant dosimetry and to report clinical outcomes.

The long term goal of our work is to devise imaging-based protocols to determine which patients may benefit the most from which specific type of imaging, and to use this information to conduct a trial of dose escalation in patients with residual disease based on imaging-identified residual tumor and de-escalation with a complete response. Should such a trial demonstrate a clearly defined tumor from various imaging modalities that results in a reduced dose to the normal tissues compared to historical controls, this will result in multi-modality image-guided brachytherapy becoming the standard at the BWH/DFCI, and in the U.S.

## References

1. ACS. *Facts and Figures 2011*. 2011; Available from: http://www.cancer.org/acs/groups/content/@epidemiologysurveilance/documents/document/acspc-029771.pdf.
2. Viswanathan, A.N., et al., *Gynecologic Radiation Therapy: Novel Approaches to Image-Guidance and Management* 2011, Berlin Heidelberg: Springer. 308.

# INTRA-TUMORAL METABOLIC HETEROGENEITY OF CERVICAL CANCER

Perry Grigsby

Mallinckrodt Institute of Radiology

**Purpose:** The overall goal of this research is to test the hypothesis that novel PET-based metrics that determine intra-tumoral heterogeneity will predict specific areas within tumors that will fail to respond to standard treatment with chemoradiation.

**Methods:** First-order and higher order metrics were utilized to describe intra-tumoral metabolic heterogeneity. These heterogeneity metrics were obtained from the individual patient's pre-treatment whole body routine clinical FDG-PET/CT. We obtained pre-treatment Cu-ATSM PET/CT images to determine tumor heterogeneity. These pre-treatment images were fused and concordance with the patient's routine pre-treatment FDG-PET/CT was evaluated. Two FDG-PET scans were obtained during treatment and 3 months after treatment.

**Results:** 15 patients diagnosed with squamous cell carcinoma underwent $^{64}$Cu-ATSM-PET/CT and FDG PET/CT before definitive chemoRT $^{64}$Cu-ATSM and FDG PET/CT image were co registered and tumor volumes were autocontoured with thresholding using values in 10% intervals ranging from 40% to 80% of the $SUV_{max}$ for each image set. The hypoxic fraction defined by the volume of $^{64}$Cu-ATSM uptake was determined. No association between $^{64}$Cu-ATSM heterogeneity and $^{64}$Cu-ATSM $SUV_{max}$ ($R^2$= 0.02) was observed, but a relationship between $^{64}$Cu-ATSM heterogeneity and FDG heterogeneity ($R^2$=0.70) was seen. Elevated $^{64}$Cu-ATSM heterogeneity was associated with increased risk of persistent disease after therapy. Regions of highest $^{64}$Cu-ATSM and FDG uptake were discordant indicating that intratumoral regions of elevated hypoxia have low levels of glucose metabolism and may play a role in intratumoral heterogeneity. 25 patients in which FDG-PET/CT was performed pre-treatment, during treatment, and 3 months post-therapy. Mean MTV for patients that were NED was 43.9, 31.9, 25.0, and 0.0 cm3 at pre-therapy, week 2, week 4, and 3 months post-therapy, respectively. Mean heterogeneity was -0.99, -0.73, -0.59, and 0.0 for patients that were NED, and was -2.17, -2.23, -1.48, and -0.99 for patients with progression or death.

**Conclusions:** The findings of these studies indicate that intratumoral heterogeneity is a complex issue with the tumor consisting of areas of differing biologic activity, tumor volumes, and response to therapy. Identification of these areas of heterogeneity and the interplay with tumor volume regarding response to therapy will help researchers develop therapeutic strategies to improve survival outcomes in patients with cervical cancer. We will continue to accrue patients to clinical protocols to evaluate PET-based metrics of intratumoral heterogeneity and how these metrics affect response to therapy.

## IGT FOR CERVIX CANCER USING DIFFUSION WEIGHTED AND DYNAMIC CONTRAST ENHANCED MAGNETIC RESONANCE IMAGING (MRI)

Nina A. Mayr, M.D.
Arthur G. James Cancer Hospital and Solove Research Institute Ohio State University

This presentation will review the role of the clinical functional MR imaging, including the dynamic contrast enhanced (DCE) MRI and diffusion weighted imaging (DWI), for the assessment of the functional/biological properties of cervical cancer. With the new ability to quantify early subtle morphologic and functional/biological changes, prediction of ultimate treatment outcomes, local recurrence and survival, to the ongoing therapy can be made early, within the treatment course, as soon as 2-5 weeks into the radiation/chemotherapy course. MRI-based early response and predictive parameters can be significantly enhanced by synergizing information from morphologic and functional/biological MRI parameters, and further increased by augmenting these with readily available established clinical prognostic factors, including FIGO stage and lymph node status. Because such information is available much earlier than with conventional methods of pre-therapy imaging and post-therapy response assessment, a window of opportunity for adaptive therapy is provided.

Title: Utility of preoperative ferumoxtran-10 MRI to evaluate retroperitoneal lymph node metastasis in advanced cervical cancer: results of ACRIN 6671/GOG 0233

**Authors:**
**Atri M, Zhang Z, Marques H, Gorelick J, Harisinghani M, Sohaib A, Koh DM, Raman S, Gee M, Choi H, Landrum L, Mannel R, Chuang L, Yu J, McCourt C, Gold M**

Background:

Ferumoxtran -10 MRI has been evaluated for lymph node (LN) metastasis. Objective of the study was to determine utility of ferumoxtran -10 MRI in detection of LN metastasis in advanced cervical cancer

Methods:

This is an NCI funded phase II multicenter clinical trial conducted by ACRIN/GOG. Patients with locally advanced cervical cancer undergoing pelvic and abdominal lymphadenectomy prior to chemoradiation were accrued. Preoperative MRI including T2W, T1W, and T2*GRE were obtained following IV administration of ferumoxtran -10 that was provided by AMAG Pharmaceutical Inc. Results of a blinded review by 7 imagers were correlated with pathology findings. Readers reviewed ferumoxtran -10 insensitive sequences (standard MRI) followed by all sequences including ferumoxtran -10 sensitive (T2*GRE) sequence. Correlation was made per region for 8 regions, left and right (para-aortic, common iliac, external iliac, and obturator) LNs. Ferumoxtran -10 MRI was considered positive when there was a defect in LN on T2*GRE. Standard MRI was considered positive when LN short axis was > 8mm

Results:

Thirty three women (mean age 49 ± 11) were included. Mean cervical tumor size was 5.4±1.5cm. Prevalence of LN metastasis was 36% (12/33) in abdomen and 64% (21/33) in pelvis. Median size of largest focus of cancer was 18mm (range 2-50, Q1 11mm)

Average sensitivity/specificity for seven readers on ferumoxtran -10 MRI were 0.60 (95% CI:0.49-0.70)/0.75 (95% CI: 0.67-0.82) in abdomen, and 0.83 (95% CI:0.76-0.88)/0.48 (95% CI: 0.35-0.61) in pelvis. Corresponding numbers for standard MRI were 0.54 (95% CI:0.43-0.64)/0.83 (95% CI: 0.75-0.88) and 0.78 (95% CI:0.78-0.81)/0.75 (95% CI: 0.62-0.84). Use of ferumoxtran -10 showed no significant difference in the diagnostic accuracy of MRI with the exception of specificities in pelvis (p=0.003). Performances of the seven readers were comparable (p>0.32)

Conclusions:

In this cohort, ferumoxtran -10 MRI showed modest accuracy that was not significantly different from standard MRI

**ACRIN/GOG receive funding from the National Cancer Institute through grants U01 CA079778 and U01 CA080098/ CA 27469 and CA 37517**

## Predictive Power of At-Risk Tumor Voxels during Radiation Therapy for Cervical Cancer

Zhibin Huang, Ph.D.[a], Nina A. Mayr, M.D.[b], Simon S. Lo, M.D.[c], Guang Jia, Ph.D.[d], John C. Grecula, M.D[b], Jian Z. Wang, Ph.D.[b], William T. C. Yuh, M.D., M.S.E.E.[d]

*[a]Department of Radiation Oncology, East Carolina University, Greenville, NC 27834*
*[b]Department of Radiation Oncology, [d]Department of Radiology, The Ohio State University, Columbus, OH 43210*
*[c]Department of Radiation Oncology, Case Western Reserve University, Cleveland, OH 44106*

**Purpose:** A threshold value of signal intensity (SI=2.1) was used to characterize the number of low DCE voxels, which is potentially related to treatment failure. The purpose of this study was to investigate the predictive power of at-risk voxels in predicting treatment outcome during radiation therapy for cervical cancer.

**Methods and Materials:** Clinical data including 3D volumetric tumor regression and tumor perfusion from dynamic contrast enhanced MRI (DCE-MRI) from 104 patients with Stage IB2–IVB cervical cancer were collected during radiation therapy (RT). Three sequential MRI scans were performed pre-RT, every 2–2.5 weeks during RT. Based on the signal intensity (SI) curves of the DCE-MRI, the parameter of the number of the low-DCE tumor voxels was obtained for individual patients. Using the ROC analysis on this parameter, subsequentially the threshold values of the number of low DCE voxels were determined. Kaplan-Meier survival curves were performed to evaluate the predictive power of this parameter in predicting the treatment outcome.

**Results:** It has been found that the 6-year actuarial local control rate and survival rate in the patient group with a low number of low DCE voxels (<304) were 90.9% and 79.5%, compared with 75% and 59.6% in the patient group with a high number of low DCE voxels (≥304) for the MRI study #1. The 6-year actuarial local control rate and survival rate in the patient group with a low number of low DCE voxels (<224) were 94.9% and 83.1% compared with 59.5% and 46.5% in the patient group with a high number of low DCE voxels (≥224) for the MRI study #2. The 6-year actuarial local control rate and survival rate in the patient group with a low number of low DCE voxels (<123) were 95.9% and 79.6% compared with 59.5% and 48.8% in the patient group with a high number of low DCE voxels (≥123) for the MRI study #3.

**Conclusion:** It turns out that the number of at-risk voxels can be used as an important prognostic factor for clinical outcomes and helps understand tumor heterogeneity of response to radiation therapy. DCE-MRI technique would be very useful as a tool in selecting patients and designing fields for adaptive radiation therapy.

## Utility of a Novel MRI Technique for the Adaptive Planning of Intracavitary Brachytherapy Treatment for Cervix Cancer Patients

**J. Esthappan, Y. Hu, and P. Grigsby**

**Washington University School of Medicine, Siteman Cancer Center, St. Louis, MO**

**Purpose**: Published guidelines for image-guided brachytherapy (IGBT) of cervix cancer recommend the use of T2-weighted (T2W) magnetic resonance imaging (MRI). Here, we introduce a novel method for MRI-guided IGBT that incorporates the use of multiple MRI sequences: T2W imaging, proton density weighted (PDW) imaging, and diffusion-weighted apparent diffusion coefficient (DW-ADC) mapping. We demonstrate how use of this multi-sequence MRI technique can facilitate adaptive planning over the course of treatment.

**Methods**: Patients were prescribed to receive high dose rate brachytherapy in 6 weekly fractions concurrently with 50.4 Gy external beam dose to the pelvis using intensity-modulated radiation therapy. Brachytherapy dose was based on stage and tumor size at time of diagnosis. Patients were implanted with Fletcher-style titanium tandem and colpostats without shielding. MRI was performed on a 1.5-T Philips scanner using T2W, PDW, and DW imaging sequences. ADC maps were generated from the DW images. Images were imported into a brachytherapy treatment planning system and fused. T2W images were used for the definition of organs at risk (OARs) and dose points. ADC maps in conjunction with T2W images were used for target delineation. PDW images were used for applicator definition. Forward treatment planning was performed using standard source distribution rules normalized to point A. Point doses and dose-volume parameters for the tumor and OAR were entered into a spreadsheet for the individual fractions. Delivered doses were adapted for tumor shrinkage and OAR variations during the 6-week course of therapy.

**Results**: The MRI-based imaging methodology for IGBT described here has been clinically implemented. MR scanning sequences included T2W turbo spin echo (TSE) (TR=[3200-6500] ms, TE=100 ms), single-shot DW echo-planar (TR=1300 ms, TE=75 ms) at *b*-values of 0 and 800 s/mm$^2$, and PDW TSE (TR=[3000-6000] ms, TE=5.5 ms), in-plane resolution $\leq$ 0.2 cm, section thickness $\leq$ 0.5 cm, parasagittal acquisition planes, 3-6 minutes per sequence. Point A dose, target doses (dose to 100% of the volume [D100], D90, equivalent dose in 2 Gy fractions [EQD2]), and OAR doses (D2cc, EQD2) are automatically exported to a spreadsheet in which cumulative doses are recorded. Total procedure time from patient preparation to delivery of treatment is usually about 2 hours per patient.

**Conclusions**: Multiple MRI sequences allow for improved visualization of the target, critical structures, and applicator for the treatment planning of cervix cancer patients using intracavitary brachytherapy. Dose adaptation relative to these structures can be readily performed.

## Dosimetric Evaluation of Three Dimensional MRI-based Adaptive Treatment Planning for Cervix Cancer Intracavitary Brachytherapy

**A. Apicelli, P. Dyk, C. Bertelsman, B. Sun, S. Richardson, J. Garcia, J. Schwarz and P. Grigsby**

**Washington University School of Medicine, Siteman Cancer Center, St. Louis, MO**

**Purpose**: Although CT-based three-dimensional (3D) planning for the external beam component of radiation therapy in the treatment of cervical cancer is well established, the use of 3D imaging in planning intracavitary brachytherapy (ICBT) treatment is not well defined. Since 2008 we have utilized MRI-based image-guided ICBT planning, and in 2011 we developed a novel method of extracting and storing specific dosimetric parameters from each delivered ICBT fraction. We now report our initial results.

**Methods**: Patients are treated with concurrent high-dose rate ICBT and external beam radiation therapy (EBRT), with prescribed dose dependent on tumor size and stage at time of diagnosis. A total of 6 ICBT fractions are delivered with implanted Fletcher-style titanium tandem and colpostats without shielding. After each implant, MRI images are acquired using a 1.5-T Philips scanner. The images are imported into the brachytherapy treatment planning system, and the position of the implant is verified. Organs at risk (OARs) are contoured, including the bladder, rectum, and sigmoid colon, as well as the gross tumor volume (GTV) using T2-weighted images (T2W) in multiple planes. Forward treatment planning is employed using standard source distribution rules normalized to point A. After the plan is finalized and exported in DICOM format, a custom software program (Matlab r2008a) retrieves specific dosimetric parameters based on the volumes of the GTV and OARs. The program automatically populates the information into spreadsheet format, and saves it into a separate easily retrievable database.

**Results:** GEC-ESTRO dosimetric parameters from a total of 20 patients with FIGO stage IB-IIIB cancer of the cervix treated with ICBT and EBRT have been captured using the above methods. The mean biologically equivalent dose to point A in 2 Gy fractions (EQD2) was 69.4 Gy ± 4.4, the mean dose to 100% of the GTV (D100) EQD2 was 64.4 Gy ± 20.8, and the D90 EQD2 was 92.8 Gy ± 37.7. The D2cc EQD2 were also recorded for the bladder and the rectum and were found to be 76.1 Gy ± 18.7 and 61.5 Gy ± 8.8, respectively.

**Conclusions:** Adaptive treatment planning utilizing three dimensional MRI guidance is feasible for ICBT for cancer of the cervix. Further study is required to determine which dosimetric parameters correlate best with patient outcome to allow for appropriate optimization of the treatment plan.

# Proton density weighted MRI: a sequence to improve the definition of titanium applicators in MR-guided high dose rate brachytherapy for cervical cancer

Yanle Hu, Ph.D., Esthappan Jacqueline, Ph.D., Sasa Mutic, Ph.D., Susan Richardson, Ph.D., Hiram Gay, M.D., Julie K. Schwarz, M.D., Ph.D., Perry W. Grigsby, M.D.

Department of Radiation Oncology, Washington University School of Medicine, Saint Louis, Missouri, USA

## ABSTRACT

**Purpose:** For cervical cancer patients treated by MR-guided high dose rate brachytherapy, the accuracy of radiation delivery depends on accurate localization of both tumors and the applicator, e.g. tandem and ovoid. Standard T2-weighted (T2W) MRI has good tumor/tissue contrast. However, it suffers from signal dropout and geometric distortion around titanium tandems. In this study, we evaluated the possibility of using proton density weighted (PDW) MRI to improve the definition of titanium tandems.

**Methods:** After the insertion of the applicator, cervical cancer patients were scanned on a 1.5T MRI scanner. Both T2W and PDW images were obtained from each patient. Imaging parameters were kept the same between the T2W and PDW sequences for each patient except the echo time (90ms for T2W and 5.5ms for PDW) and the slice thickness (0.5cm for T2W and 0.25cm for PDW). The tissue/tandem contrast and the diameter of the tandem were measured for both sets of images. We also segmented the tandem using the histogram thresholding technique.

**Results:** Images from 10 patients were retrospectively reviewed. PDW MRI had a better definition of the tandem in all cases. Compared to T2W MRI, PDW MRI significantly improved the tissue/tandem contrast. It was 0.42±0.24 for PDW MRI and 0.77±0.14 for T2W MRI. This result was found to be statistically significant with a paired t-test value of $p=0.0002$. The average difference between the measured and physical diameters of the tandem 1.5cm away from the tip was reduced from 0.20±0.15cm by using T2W MRI to 0.10±0.10cm by using PDW MRI ($p=0.0003$). The tandem segmented from the PDW image looked more uniform and complete compared to that from the T2W image.

**Conclusions:** We showed both qualitatively and quantitatively that PDW MRI can provide a better definition of the titanium tandem. Standard T2W MRI, however, has good tumor/tissue contrast. The information provided by PDW MRI is complementary to those provided by T2W MRI. By combining T2W and PDW MRI, both the tumor and the applicator can be accurately located, which contributes to improved dose delivery accuracy and more conformal treatments. Therefore, we recommend adding PDW MRI in the MR-guided HDR brachytherapy for cervical cancer.

# Assessment of Advantage of Dosimetric Guidance in Gynecological HDR Interstitial MR guided Brachytherapy

Antonio Damato[1], Robert Cormack[1,3], Tina Kapur[2,3], Clare Tempany[2,3], Akila Viswanathan[1,3]
[1]Department of Radiation Oncology, Division of Medical Physics and Biophysics, Brigham and Women's Hospital and Dana-Farber Cancer Institute, Boston, MA
[2]Department of Radiology, Brigham and Women's Hospital and Dana-Farber Cancer Institute, Boston, MA
[3]Harvard Medical School, Boston, MA

**Purpose:** Intra-procedure assessment of the dosimetric quality of an HDR gynecological interstitial brachytherapy insertion (ISB) is complicated by the difficulty of accurate and time-efficient identification of tumor (CTV) and normal structures (OARs) on a CT or ultrasound, and by the difficulty of providing real-time optimization of dwell loading. MRI guidance during ISB removes ambiguity in the delineation of CTV and OARs, and it has been successfully used to provide superior ISB through geometrical assessment of catheter placement and adaptive repositioning or addition of catheters. In order to evaluate the benefit of providing real time dosimetric guidance during ISB, we studied in this retrospective work the clinical difference between geometric and dosimetric assessment of catheter implantation.

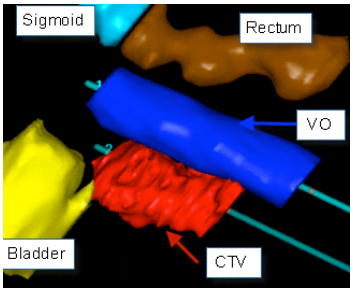


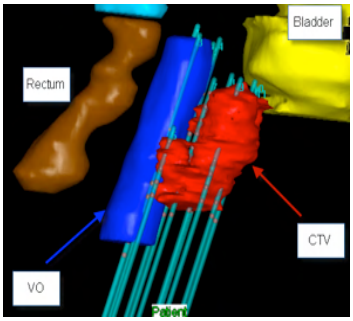


**Methods:** We simulated intra-procedure dosimetric guidance by generating 10 plans (P_2 to P_11) for a recent ISB patient enrolled in a clinical trial. CTV and OARs were contoured on the T2 W MR Images (pelvic coil) obtained at the time of the procedure in an intra-operative wide bore 3T Verio MR (Siemens medical systems) Advanced Multi-modality Image Guided Operating (AMIGO) suite. For the purpose of this study, we disregarded actual needle placement and assumed that all needles are straight and parallel to the vaginal obturator (VO). Hard constraints for all plans are more than 99.7% of CTV covered by 100% of prescription dose (RxD) and 100% of VO covered by 70% of RxD. The succession of plans simulates the progressive addition of catheters, starting from the center of CTV and moving towards the periphery. Number of catheters varies from 1 in CTV + 1 in VO (P_2) to 10 in CTV + 1 in VO (P_11), as shown. 10 is the maximum number of straight catheters that can be inserted in CTV through the template holes, and P_11 represents perfect geometrical coverage. For each of the plans we analyzed the volume outside the CTV receiving RxD or more (Norm_V100), the V2cc for rectum (R_2c), bladder (B_2c) and sigmoid (S_2c), and the total dwell loading (TL). Clinical acceptability of each plan is assessed based on metrics obtained in the clinical plan, that is R_2cc = 220cGy, B_2cc = 255cGy, S_2cc = 120cGy.

**Results:** All metrics are optimal when 9 (8 in CTV, 1 in VO) catheters are used. Additional catheters result in worsening of the metrics. 7 (6 in CTV, 1 in VO) catheters produce a plan meeting the OARs clinical constraints.

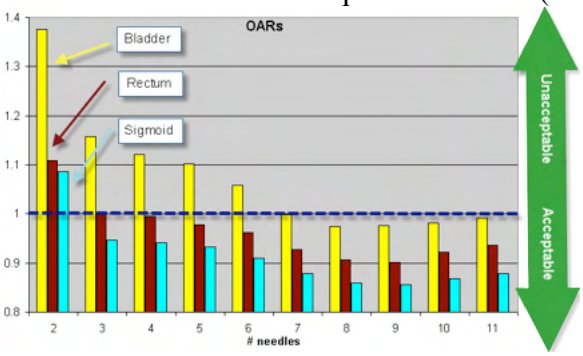


| # Needles | 2 | 3 | 4 | 5 | 6 | 7 | 8 | 9 | 10 | 11 |
|---|---|---|---|---|---|---|---|---|---|---|
| Norm V100 (cc) | 66 | 60 | 58 | 57 | 54 | 52 | 50 | 46 | 48 | 50 |
| R_2c (cGy) | 244 | 220 | 219 | 215 | 212 | 204 | 199 | 198 | 203 | 206 |
| S_2c (cGy) | 130 | 114 | 113 | 112 | 109 | 105 | 103 | 103 | 104 | 105 |
| B_2c (cGy) | 351 | 295 | 286 | 281 | 270 | 255 | 249 | 249 | 250 | 253 |
| TL (Ci*s) | 2824 | 2665 | 2560 | 2498 | 2436 | 2356 | 2280 | 2204 | 2244 | 2283 |

**Conclusions:** We show that in this case study geometric assessment of catheter implantation would have overestimated by 36% the number of catheter needed to achieve dosimetric objectives, and by 18% the number of catheters needed for best planning. We therefore speculate that an insertion technique consisting of MRI guided incremental insertion of catheters from the center of CTV to the periphery, coupled with real time dosimetric analysis, has the potential to significantly reduce the total number of catheters and the time of the procedure.

# Concept Development and Feasibility Study of Image-based Needle Guidance for MR-Guided Interstitial Gynecologic Brachytherapy in AMIGO

Radhika Tibrewal, BS, Akila Viswanathan, MD, MPH, Kanokpis Townamchai, MD, Janice Fairhurst, BS, RT, Maximilian Baust, MS, Jan Egger, PhD, Antonio Damato, PhD, Sang-Eun Song, PhD, Steve Pieper, PhD, Clare Tempany, MD, William M. Wells, PhD, Tina Kapur, PhD
Brigham and Women's Hospital, Dana Farber Cancer Center, Harvard Medical School, Boston, MA, USA
Corresponding author: tkapur@bwh.harvard.edu

## Purpose

Interstitial gynecologic brachytherapy, the placement of radioactive isotopes directly into a cancer of the uterine cervix or vagina in order to eradicate the cancer, requires insertion of hollow catheters with introducers into the tumor. The catheters are guided into place through holes in a template sutured to the patient's perineum. Current clinical practice at BWH/DFCI uses Computed Tomography (CT) and ultrasound images to guide the advancement of these catheters [1]. In the newly constructed ***A****dvanced* ***M****ultimodality* ***I****mage-****G****uided* ***O****perating* (*AMIGO*) suite at BWH/DFCI, intraprocedural Magnetic Resonance (MR) images are acquired to visualize the catheters in relationship to the tumor. The goal of this project is to develop computational algorithms and a visualization workflow to aid catheter placement during MR guided interstitial gynecologic brachytherapy in AMIGO.

## Methods

Imaging: All imaging is performed in the Siemens Verio 3T MR scanner (70cm) in the AMIGO suite. At the start of the procedure, an MR Imaging (MRI) series consisting of T2 Ax, Sag, and Cor slices is acquired (TR 4000, TE 101, Flip Angle 150, Slice Thickness 4mm, Slice Gap 20). At the end of the procedure, a similar T2 weighted MRI series is obtained for final confirmation. During the procedure, alternating T2 and GRE images (plane orthogonal to obturator) are acquired to show the advancing needle and surrounding anatomy.

Image Processing and Visualization Workflow: The free and open source software platform 3D Slicer [2] is used to implement the following workflow. 1) On the initial MRI, the tumor, the organ of interest (OAR), the obturator and the template are segmented. 2) Each subsequent MRI is registered to the initial MRI, the catheters are marked, and rendered in relationship to the previous segmentations, as illustrated in the figure on the right.

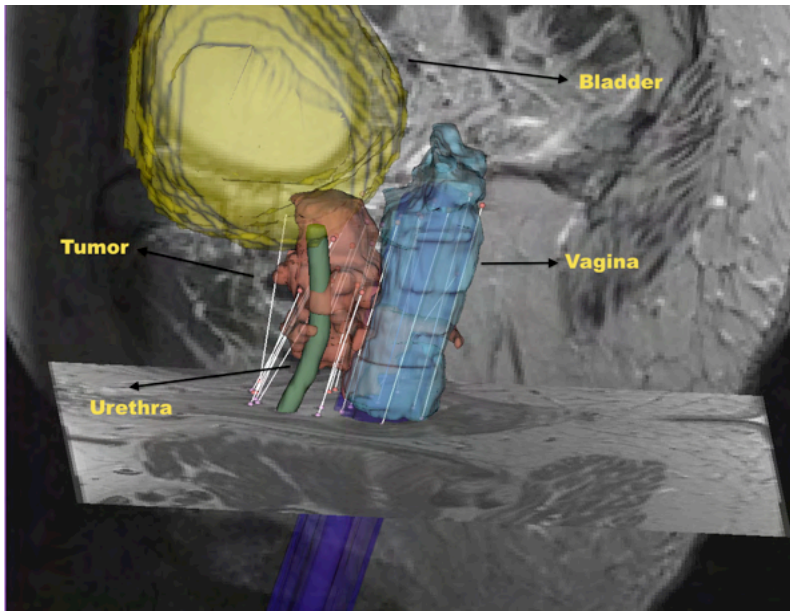


Efforts for optimizing this workflow by automating the segmentation of the obturator, template, catheters, tumor, and OARs in the MRI images are currently underway.

## Results and Conclusion

A concept has been developed and prototyped using 3D Slicer for image-processing-based guidance during interstitial gynecologic brachytherapy catheter placement. This has been tested retrospectively, under IRB approval, on data obtained from the first AMIGO gynecologic brachytherapy procedure performed on September 9, 2011. Preliminary results indicate that the prospective use of this guidance workflow in AMIGO will provide a useful means to increase efficiency in interstitial brachytherapy.

This work was performed with partial support from NIH grants R03EB013792, P41RR019703, and P41RR013218.

## References

1. Gynecologic Radiation Therapy: Novel Approaches to Image-Guidance and Management. Akila N. Viswanathan, Christian Kirisits, Beth E. Erickson, and Richard Pötter. Springer. ISBN-13: 978-3540689546
2. 3D Slicer software website http://www.slicer.org

# Predictive Outcome of Cervical Cancer Treatment Using Tumor Volume and Tumor Regression Rate during Radiation Therapy on Sequential Magnetic Resonance Imaging

Kanokpis Townamchai MD, Tina Kapur PhD , Radhika Tibrewal BS Akila Viswanathan MD, MPH
Brigham and Women's Hospital, Dana Farber Cancer Center, Harvard Medical School, Boston, MA, USA
Corresponding author: aviswanathan@lroc.harvard.edu

**Purpose**: Treatment of locally advanced cervical cancer consists of concurrent chemotherapy and external beam radiation therapy (EBRT) followed by brachytherapy [1]. The tumor size and tumor regression during radiation therapy treatment have been shown to predict outcomes of cervical cancer treatment [2]. Magnetic resonance imaging (MRI) provides a precise imaging tool for evaluation in pre- and post- treatment. The goal of this project is to assess the feasibility of assessing the tumor volume and tumor regression rate on magnetic resonance images at our institution.

**Methods:** Patient Population: A total of 126 patients were treated for cervical cancer at the Brigham and Women's/Dana-Farber Cancer Institute (BWH/DFCI) from 2005-2010. All patients had an MRI at diagnosis, prior to starting any radiation therapy (MRI1). In this study, eight patients with locally advanced cervical cancer that had an additional MRI after completing external beam radiation or at the first brachytherapy fraction (MRI2) were included. MRI Images: T2 weighted MRI with slice thickness 4mm in axial, sagittal and coronal planes were used. Contouring and Measurements: The gross tumor volume (GTV) was evaluated by two measuring methods. In the first method, the GTV was contoured in each axial image slice using the Editor module of the free and open source software platform 3D Slicer [3], and volumes were calculated using the Statistics module. In the second method, an ellipsoidal approximation to the volume was computed. 3D Slicer was used to measure the greatest diameter in three orthogonal planes (D1,D2,D3) and the volume of the ellipsoid was calculated as $E=D1xD2xD3x\pi/6$. Tumor volumes were measured pre and post EBRT as MRI1 and MRI2 ($V1_M$,$V1_E$, $V2_M$,$V2_E$). The tumor regression rate was calculated by [1-(V2/V1)] x100. All parameters were correlated with the outcome of treatment including recurrence and death.

**Results:** For this study, eight locally advanced cervical cancer patients were selected including three patients who had recurrence to determine whether tumor volume was predictive of recurrence. Stages included IB1 (1), IIA (1), IIB (4), IIIB (1), and IVA (1). Median follow-up time was 22.4 months (range (rg), 10.6-65.6). Mean tumor volumes $V1_M$,$V1_E$, $V2_M$ and $V2_E$ were 63.07 $cm^3$ (rg, 8.4-200), 59.25 $cm^3$ (rg, 8.3-129.3), 7.9 $cm^3$ (rg, 0-13.71) and 6.8 $cm^3$ (rg, 0-13.29) respectively. Tumor regression rates pre- and post-EBRT were 81 (rg, 47-100) and 80.7 (rg,34.97-100). Sites of first recurrence include the cervix, left pelvic lymph node, and mediastinal lymph nodes. T-tests of volumes showed no difference between tumor volume pre and post EBRT in both volume measurement methods. There was no difference of tumor volume at diagnosis and after external beam radiation therapy between patients with and without recurrence or death. A tumor regression rate of greater than 85% corresponded to a 100% tumor control, while tumor regression rates less than 85% corresponded to only 25% tumor control (Chi-square,$p<0.05$)

**Conclusion:** Based on this preliminary study, tumor regression before and after EBRT is predictive of recurrence. This quantification of the relationship between tumor measurement parameters and outcomes will be continued with 3T MRI in AMIGO at BWH/DFCI, and will be expanded to include Diffusion Weighted MRI images.

## References

1. Gynecologic Radiation Therapy: Novel Approaches to Image-Guidance and Management. Akila N. Viswanathan, Christian Kirisits, Beth E. Erickson, and Richard Pötter. Springer. ISBN-13: 978-3540689546
2. Mayr NA, Taoka T, Yuh WT, et al. Method and timing of tumor volume measurement for outcome prediction in cervical cancer using magnetic resonance imaging. *Int J Radiat Oncol Biol Phys.* Jan 1 2002;52(1):14-22.
3. 3D Slicer software website http://www.slicer.org

**The use of Interactive, Real-time, Three-dimensional (3D) Volumetric Visualization for Image Guided assistance in the Brachytherapy Needle Placement for Advanced Gynecological Malignancies**

[1]E. Brian Butler, M.D., [1]Paul E. Sovelius, Jr., [1]Nancy Huynh, [2]Tri Dinh, M.D., [2]Alan Kaplan, M.D.

The Methodist Hospital, [1]Department of Radiation Oncology and [2]Department of Obstetrics and Gynecology

**Purpose/Objective(s):** It is often difficult to predetermine needle length to target, proximity to bowel, vascularity (in relation to the needle path), and bony interference when performing a needle implant for advance gynecological malignancies. Needle placement can often require laparoscopic guidance. Three-dimensional, interactive, measurable volumetric software utilized by other subspecialties, i.e.: cardiovascular interventions is evaluated to see if it can accomplish this task.
**Materials/Method:** A patient with a vaginal recurrence of endometrial carcinoma status post exenteration with bowel adherent to tumor preventing the use of laparoscopic guidance was evaluated for brachytherapy needle placement utilizing interactive, 3D volumetric, image guided visualization. CTA study (computer tomographic angiography) was fused with a PET imaging study was used to define and refine target. Acquisition of the CTA data set occurred at .625 mm slices as compared to standard of care routine 2-5 mm acquisition, in an effort to improve 3D targeted path. Acquisition at .625 mm adds no additional dose of radiation to the patient and measurably improves 3D targeting and volume visualization. Skin to target distance, template to target distance, and ideal measured placement and trajectory of needles were predetermined prior to going to the operating room. The image-guided volume metrics were recorded on an iPad for additional insight during the intra-operative procedure. The only diagnostic imaging available in the operating room was fluoroscopy. Postoperative CT imaging verified needle placement with standard of care 3D treatment plan analysis.
**Results:** Needle placement was within 1-2mm of ideal placement. There was no boney obstruction of the needle, perforation of the bowel, or any vascular penetration of the of the needles. This was verified clinically and radiographically by postoperative imaging.
**Conclusion:** Three-dimensional volumetric reconstructive software can assist the radiation oncologist in preplanning brachytherapy needle placement in advanced gynecological malignancies. In order to optimize the 3D volumetric reconstruction process the radiation oncologist needs to understand that CT data sets are routinely acquired at .625 mm slice thickness but are routinely stored at 5mm thickness on PACS or other storage devices. The technology of interactive image guided 3D volume reconstruction and visualization needs to be evaluated in a larger number of patients.

# Bladder Segmentation for Interstitial Gynecologic Brachytherapy with the Nugget-Cut Approach

Jan Egger, Ph.D.[1,2,3], Akila Viswanathan, MD, MPH [1], Tina Kapur, Ph.D.[1]
[1] Brigham and Women's Hospital and Harvard Medical School, Boston, MA, USA
[2] Dept. of Math. and Computer Science, University of Marburg, Marburg, Germany
[3] Dept. of Neurosurgery, University of Marburg, Marburg, Germany

**Purpose** – Gynecologic malignancies, which include cervical, endometrial, and vaginal/vulvar cancers, are the 4th leading cause of death in women in the US, with 83,750 new cases in the US in 2010 and 26,930 deaths per year [1]. Treatment consists of concurrent chemotherapy and external beam radiation followed by brachytherapy. The clinical practice of brachytherapy is well characterized using five components: 1) Applicator Choice and Insertion Techniques 2) Imaging Protocol 3) Contouring Protocol 4) Treatment Planning 5) Dose and Fractionation. Details of each institutional experience are provided in the textbook of Viswanathan et al. [2] and its references. With this work we want to support the time consuming Contouring Protocol, more precise the segmentation of the bladder.

**Methods** – Our overall method starts by setting up a directed 3D graph from a user-defined seed point that is located inside the bladder. To set up the graph, the method samples along rays that are sent through the surface points of a polyhedron with the seed point as the center. The sampled points are the nodes $n \in V$ of the graph $G(V,E)$ and $e \in E$ is the corresponding set of edges. There are edges between the nodes and edges that connect the nodes to a source $s$ and a sink $t$. After the graph has been constructed, the minimal cost closed set on the graph is computed via a polynomial time s-t cut [3], creating the segmentation of the object.

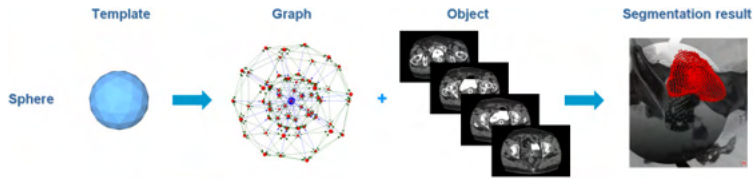


**Results** – For testing the presented segmentation method we used a C++ implementation within the medical prototyping platform MeVisLab (see http://www.mevislab.de). The overall segmentation – sending rays, graph construction and mincut computation – in our implementation took about one second on an Intel Core i5-750 CPU, 4x2.66 GHz, 8 GB RAM, Windows XP Professional x64 Version, Version 2003, SP 2. The left image shows the segmentation result of a bladder (red) on a 2D slice with the user-defined seed point (blue) located inside the bladder. The image in the middle visualizes a triangulated model of the segmented bladder (yellow/green) faded into the Computed Tomography (CT) dataset. The image on the right displays the 3D mask of the bladder (red).

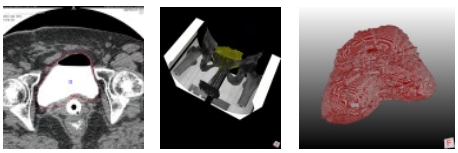

**Conclusions** – In this contribution, we present a segmentation method for the bladder. The method is based on an algorithm we developed recently in a previous work where the novel segmentation scheme was successfully used for segmentation of glioblastoma multiforme (GBM) and provided an average Dice Similarity Coefficient (DSC) of 80% [4]. For bladder segmentation, the original scheme was used, creating a directed 3D-graph within two steps: sending rays through the surface points of a polyhedron and sampling the graph's nodes along every ray. The center of the polyhedron was user-defined and located inside the bladder. Then, the minimal cost closed set on the graph is computed via a polynomial time s-t-cut, creating an optimal segmentation of the bladder's boundary and volume.

**References**

[1] American Cancer Society, *Cancer Statistics 2010.* http://www.cancer.org/acs/groups/content/@epidemiologysurveilance/documents/document/acspc-026238.pdf accessed Oct. 4, 2011

[2] A. N. Viswanathan, C. Kirisits, B. E. Erickson, R. Pötter. *Gynecologic Radiation Therapy: Novel Approaches to Image-Guidance and Management*. Springer Press, ISBN-13: 978-3540689546, 2010.

[3] Y. Boykov, V. Kolmogorov. *An Experimental Comparison of Min-Cut/Max-Flow Algorithms for Energy Minimization in Vision*. IEEE Transactions on Pattern Analysis and Machine Intelligence, 26(9), pp. 1124-1137, 2004.

[4] J. Egger, M. H. A. Bauer, D. Kuhnt, B. Carl, C. Kappus, B. Freisleben, Ch. Nimsky. *Nugget-Cut: A Segmentation Scheme for Spherically- and Elliptically-Shaped 3D Objects*. In: 32nd Annual Symposium of the German Association for Pattern Recognition (DAGM), LNCS 6376, pp. 383–392, Springer Press, Darmstadt, Germany, Sep. 2010.

# Posters on Technology for IGT

1. A Method for Solving the Correspondence Problem for an n-Camera Navigation System for Image Guided Therapy
   Jan Egger, Ph.D., Bernd Freisleben, Ph.D., Radhika Tibrewal, B.Sc., Christopher Nimsky, M.D., Ph.D., Tina Kapur, Ph.D. Brigham and Women's Hospital and Harvard Medical School, Boston, MA, University of Marburg, Marburg, Germany

2. ProbeSight: Video Cameras on an Ultrasound Probe for Computer Vision of the Patient's Exterior
   J. Galeotti, J. Wang, S. Horvath, M. Siegel, G. Stetten, Carnegie Mellon University, University of Pittsburgh.

3. A Fully Automatic Calibration Technique for Real-time 3D Ultrasound Using Mathematical Fiducials
   Elvis C.S. Chen, Jonathan McLeod, Pencilla Lang, Feng Li, and Terry M. Peters, Robarts Research Institute, London Ontario, The University of Western Ontario, London, Ontario

4. Hand Held Force Magnifier with Magnetically Stabilized Bidirectional Distal Force Sensor
   G. Stetten, R. Lee, Bing Wu, J. Galeotti, R. Klatzky, M. Siegel, Ralph Hollis, University of Pittsburgh, Carnegie Mellon University

5. PLUS: An open-source toolkit for developing ultrasound-guided intervention systems.
   Andras Lasso, Tamas Heffter, Csaba Pinter, Tamas Ungi, Thomas K. Chen, Alexis Boucharin, and Gabor Fichtinger Queen's University, Laboratory for Percutaneous Surgery, Kingston ON, Canada

6. Simulating the Imaging Operating Suite of the future. From angiography to multimodal image-guidance: framework and pilot models.
   Fabiola Fernández-Gutiérrez, Graeme Houston, Malgorzata Wolska-Krawczyk, Ole Jacob Elle, Arno Buecker3, Andreas Melzer .Intitute for Medical Science and Technology, University of Dundee, Dundee, Scotland, UK, Ninewells Hospital, Dundee, Scotland, UK, Saarland University Hospital, Homburg, Germany, The Intervention Centre, Oslo University Hospital, Oslo, Norway

7. Shadie: A Domain Specific Language for Quantitative Volumetric Visualization in Radiotherapy.
   John Wolfgang PhD, Milos Hasan PhD, Hanspeter Pfister, Georgy TY Chen. Harvard Medical School, Massachusetts General Hospital, Boston, MA, Berkeley University, Department of Computer Science, Berkeley, CA, Harvard School for Engineering and Applied Sciences, Cambridge, MA

# A Method for Solving the Correspondence Problem for an n-Camera Navigation System for Image Guided Therapy

Jan Egger, Ph.D.[1,2,3], Bernd Freisleben, Ph.D. [2], Radhika Tibrewal, B.Sc.[1],
Christopher Nimsky, M.D., Ph.D.[3], Tina Kapur, Ph.D.[1]
[1] Brigham and Women's Hospital and Harvard Medical School, Boston, MA, USA
[2] Dept. of Math. and Computer Science, University of Marburg, Marburg, Germany
[3] Dept. of Neurosurgery, University of Marburg, Marburg, Germany

**Purpose** – Precise navigation or tracking is a key component of image-guided procedures including biopsy, surgery, and radiation therapy. Users of optical navigation systems (that typically comprise of a pair of stereoscopic cameras) are well aware that having multiple cameras covering the field of view significantly facilitates workflow by minimizing the disruption of line of sight between the cameras and the tracked instruments. An algorithmic challenge in the use of an *n*-camera system for triangulation is the correspondence problem between the $n \cdot (n-1)/2$ resulting different binocular camera systems, and we describe a method for solving it.

**Methods** – We setup a tetra-optical camera system [1] and used five fiducial markers to localize an object (Fig. 1) or a patient in 3-space. If all fiducial markers are visible to all cameras, and correspondences between them are not known, up to 25 solutions are possible for a camera pair, and 125 for 6 camera pairs (or 4 cameras). Narrowing these to a single solution or knowledge of correspondences between the points leads to a unique solution and is the focus of this work.

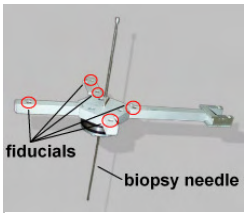

Figure 1

In a pin-hole camera geometry all image points on one epipolar line correspond to points on a single epipolar line in the second image [2]. If a point in 3-space is visible in *m* images, then the intersection of the *m* resulting epipolar lines is used to reconstruct its 3D coordinates. Because of measurement errors, the lines often do not intersect in a point, and in our algorithm, we develop an efficient method for determining the approximate intersection points of these line clusters. In the case when $m=2$, we compute center point of the minimal distance between the lines. When $m > 3$, we compute the pairwise center points, and average the point cloud of centers thus obtained. The resulting points are matched with the (known) tracker or patient model via translation and rotation [3].

**Results** – For evaluation we performed navigation in several scenarios using a tetra-optical camera system. We used standard CCD video cameras (Teli CS8320BC) and LEDs with wavelength of 890±45 nm. The correspondence algorithm was able to recover 3-space coordinates in all experiments, and repeated position measurements of the same position and orientation of the models could be reproduced within 0.5 mm. To accomplish the repeatability evaluation, we fixed the models to a robot (Mitsubishi RV-E2) with a positioning accuracy of ca. 0.4 mm [4].

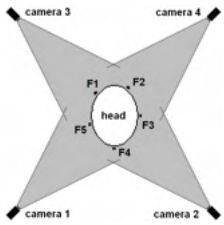

Figure 2

**Conclusions** – We have introduced an algorithm for solving the correspondence problem for a multi-camera navigation system that can be used to track patient or instrument position in an operating or interventional suite. Compared to using a single stereo pair, a multi-camera navigation system allows a significantly larger field of view and is more robust to occlusions caused by breach of line of sight. Such a system is being planned for the **A**dvanced ***M**ultimodality **I**mage **G**uided **O**perating* (*AMIGO*) Suite of the ***N**ational **C**enter for **I**mage **G**uided **T**herapy* (*NCIGT*) funded in part by the NIH Grant P41RR019703 [5].

### References

[1] D. Richter, F. La Torre, J. Egger, G. Straßmann. *Tetraoptical Camera System for Medical Navigation*. Proceedings of the 17th International EURASIP Conference BIOSIGNAL, Brno, Czech Republic, pp. 270-272, Vutium Press, June 2004.

[2] B.K.P. Horn. *Robot Vision*. The MIT Press McGraw-Hill Book Company, 1986.

[3] J. Egger. Fractioned 3D Recognition of Landmarks with a Tetraoptical Camera System (in German). Diploma thesis in Computer Science, University of Wiesbaden, Germany, 103 pages, 2004.

[4] D. Richter, J. Egger, G. Straßmann. *An Algorithm to Determine the Position of Patients and Biopsy-Needles with a Tetraoptical Camera System* (in German). Proceedings of Bildverarbeitung für die Medizin (BVM), Hamburg, Germany, pp. 316-320, Springer Press, 2006.

[5] National Center for Image Guided Therapy (NCIGT), *Advanced Multimodality Image Guided Operating (AMIGO) Suite* funded by NIH Grant P41RR019703 (http://www.ncigt.org/pages/AMIGO)

# ProbeSight: Video Cameras on an Ultrasound Probe for Computer Vision of the Patient's Exterior

**J. Galeotti[1], J. Wang[2], S. Horvath[1], M. Siegel[1], G. Stetten[1,2,3]**

[1] Robotics Institute, Carnegie Mellon University;
[2] Department of Biomedical Engineering, Carnegie Mellon University;
[3] Department of Bioengineering, University of Pittsburgh;

## Purpose

Medical ultrasound typically deals with the interior of the patient, with the exterior left to that original medical imaging modality, direct human vision. For the human operator scanning the patient, the view of the external anatomy is essential for correctly locating the ultrasound probe on the body and making sense of the resulting ultrasound images in their proper anatomical context. We are now interested in giving vision to the transducer, by mounting video cameras directly onto the ultrasound probe. This could eventually lead to automated analysis of the ultrasound data within its anatomical context, as derived from an ultrasound probe with its own visual input about the patient's exterior.

## Methods

Our present embodiment of this concept consists of an ultrasound probe with two color-video cameras mounted on it, with software capable of locating the surface of an ultrasound phantom using stereo disparity between the two video images. The separate viewpoints of cameras allow triangulation of the 3D coordinates of observed points, revealing both the shape and position of the surface relative to the ultrasound probe in 3D in real time. We use OpenGL's real-time rendering to display both the 3D surface and the ultrasound data slice, each displayed in the correct spatial relationship relative to the other. Most recently, we have added the use of 2D optical flow to establish temporal correspondences for the tracked 3D points across successive video frames, which will enable tracking the full 3D movement between the probe and the patient's exterior. We have performed initial testing of our system using an ultrasound phantom, upon which a sheet of checkerboard tracing paper has been laid in order to add visible features to the phantom. The tracing paper was saturated with ultrasound gel so as not to interfere with the passage of ultrasound.

## Results

We have successfully demonstrated real-time 3D rendering of the phantom's surface with the ultrasound data superimposed at its correct relative location. The RMS error for our system's distance measurements is ±1 mm. We are also accurately tracking points on the surface over time, and are now working to track the probe's trajectory over time. In the future, we will additionally use structured-light to improve our stereo system's robustness, enabling us to move from a flat phantom to the curved, deformable surface of human skin.

## Conclusions

We believe this research represents important preliminary steps towards a clinically useful approach in merging visual and ultrasound data in real time as the ultrasound probe is moved over the surface of the patient. Eventually, automated analysis of these registered data sets may permit the scanner and its associated computational apparatus to interpret the ultrasound data within its anatomical context, much as the human operator does today.

**Elvis C.S. Chen**[1], Jonathan McLeod[2], Pencilla Lang[2], Feng Li[2], and Terry M. Peters[1,2]
1) Robarts Research Institute, London Ontario, Canada
2) The University of Western Ontario, London, Ontario, Canada

# A Fully Automatic Calibration Technique for Real-time 3D Ultrasound Using Mathematical Fiducials

## Purpose

An automatic calibration technique for Real-Time 3D Ultrasound (RT-3DUS) is presented. Based on a planes-based calibration phantom and the concept of mathematical fiducials, this technique avoided the difficult task of manually identifying fiducials and achieved a Target Registration Error (TRE) of 2.9mm.

## Methods

A calibration phantom in a roof-top configuration consisting of 4 non-parallel planes sloping from a horizontal floor was designed and constructed. The intersection of any 3 adjacent planes is a point, thus the roof-top phantom provides 6 intersection fiducials for the purpose of calibration. Eight hemispherical divots were rigidly attached to the phantom as fiducials for the purpose of registration. A microCT scan of the phantom was obtained with the geometry of the phantom (and location of divots) as determined in CT serving as the ground truth. A magnetic Dynamic Reference Body (DRB) was rigidly attached to both the phantom and the US probe.

An automatic segmentation procedure was developed to segment the surface of the phantom. Based on the RANSAC approach, equations of planes were fitted to the surface of the phantom for all US/CT volumes. Location of the fiducials were solved mathematically.

To calibrate, divots were first digitized in the tracker coordinate frame, allowing the tracker/CT to be co-registered. For each acquired US volume, the 6 intersection points in the US volumes were computed, and the calibration parameters were obtained by solving for the anisotropically-scaled Orthogonal Procrustes Problem between the US/CT fiducials. A hemispherical divot attached to the phantom was used as a target for the TRE assessment.

## Results

APhilips X7-2t (2-7MHz) 3D TEE probe was tracked with an Aurora (NDI, Canada) magnetic tracking system. A total of 12 tracked US volumes of the phantom and 7 US volumes containing a divot in the roof-top phantom were acquired. The intersection fiducials computed from each tracked US volume were concatenated into a single point set and the calibration parameters were solved. The mean TRE assessed using the 7 acquired US volumes was 2.9mm.

## Conclusions

A calibration technique for RE-3DUS is presented. The novelty of the proposed technique is 1) the planes-based phantom that allows automatic segmentation of the phantom geometry, and 2) the concept of the mathematical fiducials for calibration. The presented technique achieved a comparable accuracy (2.9mm) to other relevant works.

# Hand Held Force Magnifier with Magnetically Stabilized Bidirectional Distal Force Sensor

**G. Stetten[1,2,3], R. Lee[3], Bing Wu[4], J. Galeotti[2], R. Klatzky[4], M. Siegel[2], Ralph Hollis[2]**

[1] Department of Bioengineering, University of Pittsburgh;
[2] Robotics Institute, Carnegie Mellon University;
[3] Department of Biomedical Engineering, Carnegie Mellon University;
[4] Department of Psychology, Carnegie Mellon University;

## Purpose

A need exists for improvement in the perception of forces by the sense of touch when using tools to perform delicate procedures. This is especially crucial in microsurgery, where surgeons routinely repair tiny blood vessels under a microscope that are far too delicate to be felt by the hand of the surgeon, and ophthalmological surgery where delicate membranes are peeled off the retina using visual feedback alone.

## Methods

We present a novel and relatively simple method for magnifying forces perceived by an operator using a tool, which we call the Hand Held Force Magnifier (HHFM). A sensor measures the force between the tip of a tool and its handle held by the operator's fingers. This measurement is used to create a proportionally greater force between the handle and a brace attached to the operator's hand, providing an enhanced perception of the force between the tip of the tool and a target. We have designed and conducted experiments with an initial prototype (Model-1), which magnifies pushing forces measured directly at the tip of the tool by means of a simple analog circuit. A second prototype (Model-2) uses a magnet based pre-load force and stabilization system to permit both push and pull forces at the tip to be measured proximally within the handle. The Model-2 integrates a computer using LabView™ to permit more complex controls such as stabilization and automatic calibration.

## Results

Both the Model-1 and Model-2 are completely hand-held and can thus be easily manipulated to a wide variety of locations and orientations. The Model-1 sufficed for preliminary psychophysical evaluation, using a magnetically levitated haptics device from Butterfly Haptics™. The results showed that the HHFM could significantly enhance the users' perception of force and stiffness. The observed perceptual gain was close to the physical gain for detecting forces at threshold level, but slightly underestimated when judging stiffness and supra-threshold forces because of the saturation of the HHFM output. The new Model-2 provides a closer approximation to an actual surgical tool, because it permits both pulling and pushing at a smaller tip, which no longer contains the force sensor, thus simplifying a wide variety of possible tip designs for actual surgical utility.

## Conclusions

Previous research using a robotic arm to produce force magnification has advantages in terms of stability, especially when encountering extremely small forces, but these systems suffer from constraints on the range of motion. Magnifying forces using the HHFM may provide the surgeon with an improved ability to perform delicate surgical procedures while preserving the flexibility of a hand-held instrument.

# PLUS: An open-source toolkit for developing ultrasound-guided intervention systems

Andras Lasso, Tamas Heffter, Csaba Pinter, Tamas Ungi, Thomas K. Chen, Alexis Boucharin, and Gabor Fichtinger
*Queen's University, Laboratory for Percutaneous Surgery, Kingston ON, Canada*

**Purpose**

Ultrasound-guided intervention systems require the integration of many hardware and software components, such as ultrasound scanner, position tracking device, data processing algorithms, and visualization software. The objective of this work is to provide a free and sharable software platform – PLUS (Public software Library for UltraSound) – to facilitate rapid prototyping of ultrasound-guided intervention systems for translational clinical research.

**Methods**

Our solution is based on the open-source SynchroGrab library that implemented tracked ultrasound capturing and 3D reconstruction using a few hardware devices. This monolithic library was redesigned into a modular toolkit, modules were thoroughly tested and enhanced. A Double-N phantom based spatial calibration and change-detection based temporal calibration algorithms were added. Support for Ascension electromagnetic tracker and digitally encoded brachytherapy steppers were added. Standard data formats are used for streaming (OpenIGTLink) and storage (MetaIO image format with additional custom fields for each ultrasound frame). All hardware and software configuration settings are described in a single XML file. Building of the application is fully automated, uses CMake to download and build all required software libraries (ITK, VTK, QT, OpenIGTLink) and it supports building modules for 3D Slicer. Automatic tests are executed using CTest after each submitted software change to verify the main functionalities of the toolkit. Test results are submitted to a CDash web-based dashboard. Source control, documentation, issue tracking are all integrated and managed on a public website.

**Results**

PLUS currently supports RF and B-mode ultrasound acquisition using Ultrasonix devices and any B-mode image acquisition on any other imaging device using frame-grabber. Position tracking is supported for NDI Certus, Ascension 3DG trackers, and the CIVCO, CMS Accuseed, and Burdette Medical Systems brachytherapy steppers. Several example applications were developed for tracked ultrasound capturing, calibration, real-time display, and streaming. The toolkit is used by research groups at Queen's University, University of British Columbia, and Robarts Research Institute for prototyping prostate and spine intervention applications. The toolkit has a BSD-type license, which allows free usage and modification. The source code will be published at https://www.assembla.com/spaces/plus/ in October 2011.

**Conclusions**

The proposed toolkit has proven to be useful for developing for ultrasound-guided intervention systems. We are looking forward to seeing more research groups using, improving, and extending PLUS after its public release.

**TITLE:** Simulating the Imaging Operating Suite of the future. From angiography to multimodal image-guidance: framework and pilot models.

**AUTHORS**: Fabiola Fernández-Gutiérrez[1], Graeme Houston[2], Malgorzata Wolska-Krawczyk[3], Ole Jacob Elle[4], Arno Buecker[3], Andreas Melzer[1]
[1]Intitute for Medical Science and Technology, University of Dundee, Dundee, Scotland, UK
[2]Ninewells Hospital, Dundee, Scotland, UK
[3]Saarland University Hospital, Homburg, Germany
[4]The Intervention Centre, Oslo University Hospital, Oslo, Norway

**ABSTRACT SECTIONS**

**PURPOSE:** The integration of different imaging techniques such as MRI, PET/CT, X-Ray or ultrasound into an Imaging Operating System (IOS) has become a new challenge for the future of minimally invasive surgery. In this work, part of the European IIIOS project (Integrated Interventional Imaging Operating System), numerical modelling and computer simulation will be used to optimise ergonomics and workflow design. In the paper are the methods we followed in order to describe detailed workflow.

**METHODS:** Data collection is being undertaken from radiology and cardiology departments in Ninewells Hospital (Dundee, UK). Collaborations with The Intervention Centre at Rikshospitalet (Oslo, Norway) and the Saarland University Hospital (Homburg, Germany) allow also obtaining data from different scenarios and interventions. The data is collected via the use of templates and through attendance to the interventions, as the level of detail we require is not usually available to that level. For workflow description, we chose to use role activity diagrams (RADs). This technique indicates roles and interactions and has the capability to show decision points and sub-tasks within a unique diagram. Once flow is described, the different steps are identified. This information, matched with data collected, is analysed statistically to determine the distributions that represent each step. The last part is the model implementation for simulation using Delmia Quest.

**RESULTS:** A 4-week data set (125 interventions) has been collected from Ninewells' cardiology department and is being analysed statistically. Other 20 data records from assorted procedures have been collected from the centres mentioned. The first set of interventions is being modelled using role activity diagrams. Models of current scenarios are being implemented and 2 pilot models of the multi-modal imaging facilities in the Institute for Medical Science and Technology and the Clinical Research Centre (Dundee, UK) have already been developed for testing using Quest.

**CONCLUSION:** The detailed data collected will allow us to build appropriate and complete models for the interventions studied. Focusing on cardiovascular and endovascular procedures, we intend to overcome two challenges: to optimise existing workflow in those scenarios, and to give guidelines for ergonomic workflow design and for the development of new procedures under multi-modal imaging guidance, towards the design of the IOS of the future.

# Shadie: A Domain Specific Language for Quantitative Volumetric Visualization in Radiotherapy



John Wolfgang PhD[1], Milos Hasan PhD[2], Hanspeter Pfister[3], Georgy TY Chen[1]
[1]Harvard Medical School, Massachusetts General Hospital, Boston, MA
[2]Berkeley University, Department of Computer Science, Berkeley, CA
[3]Harvard School for Engineering and Applied Sciences, Cambridge, MA

**Purpose:** The goal of radiation therapy is to deliver maximal radiation dose to tumor cells while minimizing dose to normal, healthy tissue. Much of the recent progress towards this goal has been focused on multi-modality image-guided radiotherapy, where regular imaging of tumor position and function allows for improvement of this therapeutic ratio for modern treatment. The high influx of image data from new techniques creates a clinical implementation issue, where the prescribed treatment is modified efficiently utilizing all the image data gathered. This work employs a implementation of volume rendering for the presentation of patient image data. Employing custom shader algorithms within a GPU-based renderer, relevant clinical information may be easily projected in the volume rendered image, naturally of higher bandwidth than the traditional 2D “slice-wise" visualization approaches. Furthermore, our approach is more flexible than existing volume renderers, allowing for computation and visualization of radiation-specific quantities directly in the renderer.

**Methods:** GPUs, allow for the implementation of efficient, highly parallel algorithms on relatively inexpensive, easily available graphics cards. Shadie is completely parallel, relying on this GPU infrastructure to provide real time interactive quantitative visualization. The rendering engine takes care of data I/O, GPU initialization, CPU-GPU communication, data interpolation, user interface and a number of other tasks that generally require an expert software engineer; on the other hand, the mathematical function that defines the visualization (which we term the shader) is fully exposed to the user and can be written without advanced GPU programming expertise. .

**Results:** Shaders have been written to illustrate several issues concerning radiotherapy. Figure 1 illustrates interactively calculated cell survival probabilities based on a 4DCT motion study of a thoracic tumor treated with MV photons. This shader implements the standard Linear-Quadradic model to illustrate the clinical implications of changes to fractionation size and frequency. Figure 2 demonstrates the quantitative power of Shadie, where radiation dose is calculated “on-the-fly” as the user changes treatment parameters. The 3D static problem, taking many hours of experienced user time is reduced to seconds and easily incorporates 4D and multi-modality data, currently not available to commercial planning systems.

**Conclusions:** Shadie provides an efficient means to incorporate multiple image data sets for clinical assessment to aid in image-guided radiotherapy treatment. Use of a Domain Specific Language such as Shadie allows easy adaptation to a number of visualization problems in radiotherapy. With a minimum of training, clinicians can alter shaders to provide new custom views, illustrating clinical issues and enhance treatment outcomes.

Figure 1 (right): Probability of tumor survival for 1, 5 and 10 fractions. Pure red corresponds to 10% probability, pure blue indicates 0% probability. After 5 fractions (middle), there is significant variation in tumor cell survival

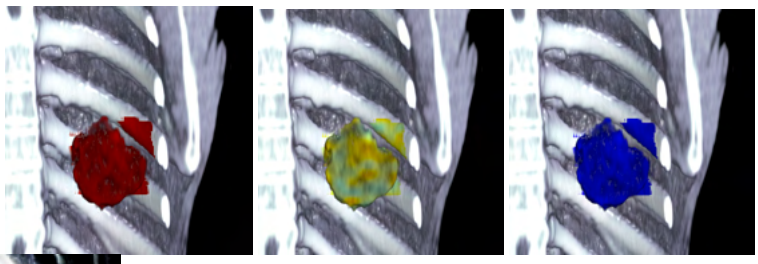

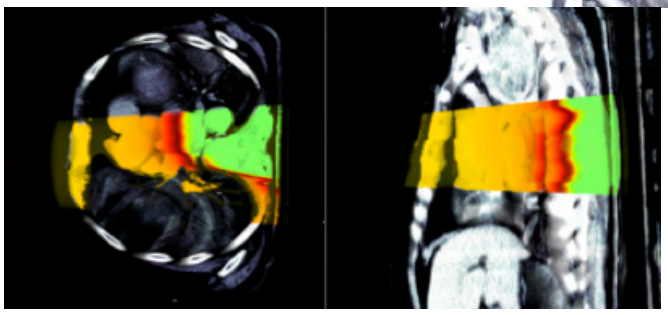

Figure 2 (left) Proton Pristine Bragg peak dose axial and sagittal view. Red = maximum dose, Green = zero dose. Modified pencil beam implemented in shadie used to interactively recalculate/display dose as user alters treatment margins and port (beam angle/rotational isocenter)

# Posters on Pulmonary IGT

1. GPU Accelerated Distance Map Classification for 2D/3D CT/X-ray Registration on Image Guided Bronchoscopy
   Di Xu, Sheng Xu, Daniel A. Herzka, Rex C. Yung, Martin Bergtholdt, Luis F. Gutiérrez, Elliot R. McVeigh, Johns Hopkins School of Medicine, Philips Research North America, Philips Research Europe, Germany, Philips Healthcare, USA.

2. A Respiratory Motion Compensation Algorithm for Image-Guided Percutaneous Lung Intervention.
   T. He1, Z. Xue, K. Lu, S.T. Wong. The Methodist Hospital Research Institute, Weill Cornell Medical College, Houston, TX and PhilipsResearch North America, Briarcliff Manor, NY

3. CT Fluoroscopy-Guided Percutaneous Lung Intervention with Fast Respiratory Motion Compensation and Registration.
   P Su, Z. Xue, K. Lu, J. Yang, S.T. Wong. The Methodist Hospital Research Institute, Weill Cornell Medical College, Houston, TX, Philips Research North America, Briarcliff Manor, NY, School of Automation, Northwestern Polytechnical
   University, Xi'an, China

4. Multimodality Image-Guided On-The-Spot Lung Intervention and Results on VX2 Rabbit Model.
   Z. Xue, K. Wong, T. He, M. Valdivia y Alvarado, K. Lu, S.T. Wong
   The Methodist Hospital Research Institute, Weill Cornell Medical College, Houston, TX, Philips Research North America, Briarcliff Manor, NY

# GPU Accelerated Distance Map Classification for 2D/3D CT/X-ray Registration on Image Guided Bronchoscopy

*Di Xu[1], Sheng Xu[2], Daniel A. Herzka[1], Rex C. Yung[3], Martin Bergtholdt[4],Luis F. Gutiérrez[5], Elliot R. McVeigh[1]*

**1. Dept. of Biomedical Engineering, Johns Hopkins School of Medicine, USA; 2. Dept. of Image Guided Technology, Philips Research North America, USA; 3. Pulmonary Oncology, Johns Hopkins School of Medicine, USA; 4. Department of Digital Imaging, Philips Research Europe, Germany; 5. Image Guided Interventions, Philips Healthcare, USA**

**Purpose:** 2D X-ray fluoroscopy is used to guide bronchoscopies of peripheral pulmonary lesions (PPLs). Airways and nodules to be biopsied are not easily visualized due to poor image contrast. Therefore, transbronchial biopsy of PPLs is often carried out blindly, which degrades diagnostic yield.[1] One possible solution is to improve intraprocedural guidance by superimposing lesions and airways segmented from a preoperative 3D CT onto the 2D fluoroscopy images. This work demonstrates a 2D/3D interactive real-time registration process taking advantage of graphic processing units (GPUs) to reduce the latency in visualization.

**Methods:** Stereo X-ray images are co-registered with CT images by extracting a bone mesh based on the intensity of the bony structures in the 3D CT dataset, and projecting it onto virtual image planes to mimic the X-ray images (Fig 1a).[2] The edge points obtained from bony structures in the X-ray images and from projected images are categorized into eight groups based on their image gradient orientations (Fig 1b).[3] An Euclidean distance map[4] is generated for each group of X-ray image edges. In the distance map, each pixel stores the distance to the closest edge as an intensity value, avoiding further time consuming distance calculations. The distances between edge points of the same class from the X-ray and projected images are summed up. An average distance among the 8 directional classes is then output to the Powell optimizer[5] to search for the best match between the CT and X-ray images. The online calculation from mesh projection to the metric calculation is parallelized in the GPU, where each mesh triangle is processed independently, and all triangles are summed to compute the final metric used to assess registration. Validation experiments were carried out on a 48-core 128GB RAM computer with NVIDIA Quadro FX 3800 GPU (NVIDIA, USA), a non-GPU-accelerated registration method based on the use of image intensities in digitally reconstructed radiograph (DRR) and gradient difference metrics[6] was also implemented for robustness comparison. To calculate registration error (RE) as the distance between current and gold standard CT positions, gold standard positions are determined by fiducial markers (phantom) and expert reader inspection (clinical).[7] Start and end registration errors (SRE and ERE, respectively) are used to determine the convergence of registration experiments (ERE<5mm) and the difficulty of the convergence (scored by SRE), respectively. Both qualitative and quantitative evaluations were carried out on phantom and clinical data (*N=8* patients).

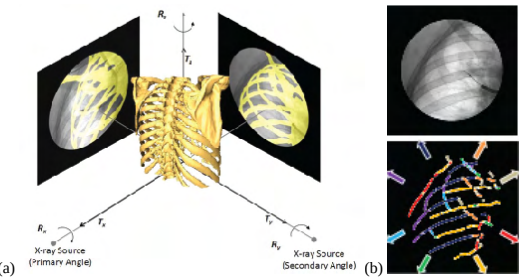


(a) (b)

**Figure 1:** Mesh projection and edge classification illustration. (a) The virtual meshes of the ribs and spine (yellow 3D rendering) from CT images are projected onto two virtual planes (yellow overlay), and superimposed on stereo X-ray images. The projected images and corresponding X-ray images (Fig 2b, bottom) are processed with a Canny edge detector.[9] The edges are classified into 8 groups depending on image gradient orientations. The 8 directional arrows illustrate the mean image gradient orientations of their corresponding edge group (Fig 2b, top) where each edge group and its corresponding arrow are labeled as a distinct

**Results:** Images from a sample case are shown in Fig 2. Qualitative evaluation showed a superior registration convergence rate: proposed method 86% vs. 67% DRR-based method with SRE<30mm (p=0.001); proposed method 70% vs. 0% DRR-based method with 30mm<SRE<120mm (p<0.00001). The registration accuracy for the proposed method was 4.2±0.5mm and 3.9±2.3 mm for phantoms and patients, respectively. The GPU accelerated registration run-time for patient data was 4.0±2.2 sec vs. 481.3±258.5 for the non-GPU-accelerated registration, for trials with 30mm<SRE<120mm.[8]

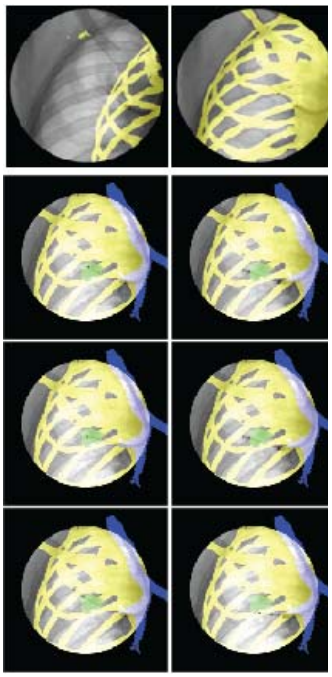

**Figure 2 (Upper left):** X-ray fluoro images acquired from a clinical PLL procedure. Yellow bone meshes from CT are overlaid on the fluoro image. Retrospective registration adapts from the initial position (left, SRE 41mm) to the final position (right, ERE 3mm) in ~3.5 seconds accelerated by GPU.

**Figure 3 (Lower left):** Fluoro images retrospectively overlaid with structures segmented from CT after registration: target lesion (green), bronchus (blue), bone (yellow). The biopsy instrument tip is highlighted by a red dot. In these six sample images, the bronchoscopist attempted to obtain biopsies by proceeding down alternative airways. Among a broad range of positions, 4/6 biopsies were unlikely to yield diagnostic samples as demonstrated by the registered structures.

**Conclusions:** The proposed algorithm shows significant improvement in convergence rate of difficult registration cases, when SRE is large. GPU acceleration improves registration speed to an acceptable level (~4sec) for intra-procedural guidance. Distance map classification using gradient orientation at edge points is an effective method for improving the convergence rate and robustness of the registration while reducing computational load. The proposed algorithm demonstrates a framework for extending the use of distance transforms in 2D-3D registration. Although the algorithm does not compensate for respiratory motion, a rough alignment between the CT and X-ray images provide sufficient information for the bronchoscopist to exclude the incorrect airway branches for device guidance, shown in Fig 3.This is in contrast to today's standard procedure, where no CT overlay is used and the bronchoscopist can only decide where to biopsy based on experience.

**References:**[1]Baaklini et al, Chest 2000 117: 1049; [2]Xu et al, CARS 2010; [3] Xu et al, EMBS 2010: 3715; [4]Sundar et al, Proc. SPIE 2006 6141: 7; [5] Powell et al, Lec. Notes in Math.1978 630: 144; [6] Turgeon et al, Med. Phys. 2005 32: 3737; [7] Van de Kraats et al, TMI 2005 24: 1177; [8] Xu et al, ISBI 2010: 1945; [9] Canny, IEEE Trans. on Patter.Analy. Mach. Intell. 1986 8: 679.

# A Respiratory Motion Compensation Algorithm for Image-Guided Percutaneous Lung Intervention

T. He[1], Z. Xue[1*], K. Lu[2], S.T. Wong[1]

[1]The Methodist Hospital Research Institute, Weill Cornell Medical College, Houston, TX and [2]Philips Research North America, Briarcliff Manor, NY

Email: zxue@tmhs.org

**Purpose.** Percutaneous lung intervention is a common procedure for lung tumor biopsy, ablation, and other local treatments. With new device tracking and imaging techniques in computer-aided intervention, more efficient and safer procedures can be achieved. In applications where real-time 3D imaging is not available, motion compensation plays an important role to visualize the real-time tracked interventional device in estimated dynamic anatomical images. The objective of this work is to estimate such motion compensated CT images that match the patient's anatomy through chest surface sensors.

**Methods**. The electromagnetic (EM) tracked needle can be visualized in a pre-procedural CT by registering the two coordinate systems in percutaneous lung intervention. Since the static pre-procedural CT does not reflect the patient's dynamic anatomy especially respiratory motion, patient-specific serial CT images are estimated from real-time chest sensors. A joint PCA-based statistical model is constructed to characterize relationship between 4DCT and chest respiratory signals from a number of patients (in the template space after image registration). Then, such model is utilized as prior knowledge to estimate the patient-specific serial CTs, given a static 3D pre-procedural CT and the real-time chest surface sensor signals. The estimated serial CT images cover the entire respiratory cycle of the patient whose 4DCT are not available and are visualized in real-time based on the real-time tracked chest surface sensor signals for guiding the interventional procedure.

**Results.** 4DCT data from thirty patients were used to evaluate our motion compensation method using leave-one-out strategy quantitatively. Each time 29 subjects were used to train the model and the left out subject was used for testing. Five chest surface points were manually picked from the first time-point and automatically mapped onto the subsequent images using image registration. The differences between the lung field surfaces of the estimated 4DCTs and the real 4DCTs were calculated as the accuracy of the proposed algorithm. The results showed that average lung field surface distance across all the 30 experiments was 2mm.

**Conclusions.** A motion compensation method is proposed to estimate the dynamic anatomical images of patients from the pre-procedural CT and real-time tracked sensor signals during the procedure. Simulation results using 4DCT images from 30 patients showed accurate estimation of the lung motion. We are planning further online clinical validation on patients under the proved institutional IRB.

# CT Fluoroscopy-Guided Percutaneous Lung Intervention with Fast Respiratory Motion Compensation and Registration

P Su[1], Z. Xue[1*], K. Lu[2], J. Yang[3], S.T. Wong[1]

[1]The Methodist Hospital Research Institute, Weill Cornell Medical College, Houston, TX, [2]Philips Research North America, Briarcliff Manor, NY, [3]School of Automation, Northwestern Polytechnical University, Xi'an, China

Email: zxue@tmhs.org

**Purpose.** CT-fluoroscopy (CTF) is an efficient imaging method for guiding percutaneous lung interventions. During CTF-guided biopsy procedure, four or more axial sectional images are captured in a very short time period to provide nearly real-time feedback to advise adjustment of the needle as it is advanced towards the target lesion while the patient is holding breath. This procedure may require repetitive scans and cause unnecessary radiation exposure to clinicians and patients. To better utilize CTF guidance, we propose a fast CT-CTF registration with embedded respiratory motion model to adapt to the patient's anatomy during intervention. Electromagnetic (EM) tracking is then used to track and visualize the device for guidance.

**Methods**. Patient-specific serial CT images are first estimated from real-time chest sensors under EM tracking. When an intra-procedural CTF is captured, the respiratory phase can be determined by matching the CTF with the estimated serial CT images using least squares differences. Then the CT-CTF registration is performed to warp the CT image onto the CTF space by considering a combined deformation: first deforming the inhale CT image onto the estimated CT that best matches the respiratory phase, and then deforming onto CTF. This process requires a fast computation to satisfy intra-procedural guidance while the patient is holding breath. With the EM-guided system, the tracked needle can be displayed in the deformed 3D CT image for guiding the intervention. Currently the table needs to be moved out of the gantry so that EM tracking can be used. The procedure is repeated till the tumor is targeted.

**Results.** Two sets of experiments were carried out to evaluate the proposed algorithm using 4DCT datasets from 30 subjects. For each subject, three images: exhale, inhale, and an intermediate phase in between were used. Four slices from the intermediate phase was cut to simulate CTF images. The first experiment evaluated the performance without motion compensation, and the second experiment validated the algorithm with motion compensation. The quantitative results showed that the latter yielded smaller estimation errors than the conventional registration algorithm (e.g. FSL). The fast implementation of the algorithm allows generating the 3DCT to match patient's anatomy within two second.

**Conclusions.** A new CTF-guided intervention workflow is proposed in this work. With pre-procedural exhale and inhale CT scans, it is possible to estimate a series of CT images at different respiratory phases and warp the best motion compensated data to the CTF. This allows a ~15 second time window for interventional radiologists to advance the needle with 3D image guidance during the breath holding.

# Multimodality Image-Guided On-The-Spot Lung Intervention and Results on VX2 Rabbit Model

Z. Xue[1*], K. Wong[1], T. He[1], M. Valdivia y Alvarado[1], K. Lu[2], S.T. Wong[1]

[1]The Methodist Hospital Research Institute, Weill Cornell Medical College, Houston, TX, [2]Philips Research North America, Briarcliff Manor, NY

**Purpose**

Lung cancer is the leading cause of cancer-related death in the US, with more than half peripheral cases. Although Computed Tomography (CT) has been used to detect early staged peripheral lung cancer, image-guided biopsy is often necessary to help confirm diagnosis. Currently this intervention procedure is guided by repetitive CT, which is time consuming and with high radiation exposure. The objective of our study is to develop a Minimally Invasive Multimodality Image-Guided (MIMIG) interventional system to help guide the biopsy needle to the lesion, to confirm diagnosis with molecular imaging and to allows on-the-spot diagnosis of early staged lung cancer.

**Methods**

The MIMIG system uses CT images and electromagnetic (EM) tracking to help interventional radiologists target the lesion efficiently. Using the software developed, pulmonary vessels, airways, as well as nodules can be segmented and visualized for surgical planning. The needle is inserted into the lesion under image guidance. A fiber-optic probe coupled with optical molecular imaging contrast agents, IntegriSense 680 (PerkinElmer Inc., MA) for $\alpha_v\beta_3$ integrin labeling, to confirm the existence of cancerous tissues in situ at microscopic resolution through confocal microendoscopy. The MIMIG system was evaluated using rabbit model with VX2 lung cancer to evaluate the targeting accuracy, guidance efficiency, and performance of molecular imaging.

**Results**

Using the system, we evaluated the targeting accuracy for VX2 rabbit lung tumor model. 12 rabbits were used in the experiments, and we achieved an average targeting accuracy of 3.3mm. Eight rabbits were undergoing optical imaging experiments, and the IntegriSense signals within VX2 tumor were found at least two folds of normal lung tissue. Finally, the presence of VX2 tumor cells and IntegriSense 680 was confirmed in all animals by immunohistochemical staining and confocal microscopy.

**Conclusions**

The MIMIG system enables efficient and accurate image guidance for percutaneous lung intervention and enables effective in situ fluorescence molecular imaging for on-the-spot lung cancer diagnosis. The results suggest the great potential of applying the system in human trials in the future if an optical molecular imaging agent is approved by the Food and Drug Administration (FDA). The MIMIG system is also useful in current clinical settings where accurate image-guided biopsy is needed.

# Posters on Neurosurgical IGT

1. MRI-guided stereotactic aspiration of brain abscesses with use of optical navigator
   Yubo Lü, Chengli Li, Ming Liu, Jan Fritz2, John A. Carrino, Lebin Wu, Bin Zhao, Shandong University, Jinan, China, Johns Hopkins University School of Medicine, Baltimore, MD

2. Intraoperative Targeting, Trajectory Planning, Device Insertion and Infusion Monitoring with Real-Time MRI
   Walter F. Block, Ethan K. Brodsky, Andy L. Alexander, Ben P. Grabow, Sam A. Hurley, Chris D. Ross, Karl A. Sillay, University of Wisconsin, Madison, WI, Engineering Resources Group, Inc., Pembroke Pines, FL, inseRT inc, a MRI therapeutic development company

3. Fiber tract detection using fMRI-DTI landmark distance atlases.
   Lauren J. O'Donnell, Laura Rigolo, Isaiah Norton, Carl-Fredrik Westin, Alexandra J. Golby Brigham and Women's Hospital, Boston MA, Harvard Medical School

# **Title:** MRI-guided stereotactic aspiration of brain abscesses with use of optical navigator

**Authors:** Yubo Lü[1, 2], Chengli Li[1], Ming Liu[1], Jan Fritz[2], John A. Carrino[2], Lebin Wu[1], Bin Zhao[1]

**Affiliations:**

1. Yubo Lü, Chengli Li, Ming Liu, Lebin Wu, Bin Zhao: Shandong Medical Imaging Research Institute, Shandong University，324 Jingwu Road, Jinan, China 250021

2. Yubo Lü, Jan Fritz, John A. Carrino: Russell H. Morgan Department of Radiology and Radiological Science, Johns Hopkins University School of Medicine, 600 N Wolfe St., Baltimore, MD 21287.

**Corresponding Author:** Chengli Li, Shandong Medical Imaging Research Institute, Shandong University，324 Jingwu Road, Jinan, China 250021, lichenglichina@mail.com, phone: 053185186713.

**Purpose:** Imaging-guided aspiration is considered an ideal choice in the management of brain abscesses. The purpose of this study was to evaluate the safety and efficacy of an open-configuration MRI system in performing the procedure.
**Methods:** 13 brain abscesses in 11 patients were treated with percutaneous aspiration. All procedures were performed solely under MRI guidance with a 0.23-T open-configuration MRI scanner with optical tracking. FFE with enhancement and CBASS images were used for needle and lesion localization. Clinical and imaging follow-up was at 1 week, 1 month, 3 months and 6 months. The changes of abscess, MRI features and clinical symptoms were recorded. Descriptive statistical analysis was performed.
**Results:** MRI-guided stereotactic aspirations were performed successfully in all cases without serious complications. External drainage tubes were successfully placed in three large abscesses. The sequences met the need of near real time scanning and monitoring. The mean operating time was 70 min (range 45-100 min). Follow-up MRI at 1 week after the procedure showed average reduction of abscesses by 60% (2.1/3.5). And the abscesses continued to get smaller by up to 89.7% (3.14/3.5) at 1 month follow-up. All cavities resolved at the end of the 6 months follow-up period. The recovery rate was 100% for fever, headache, vomiting, papilledema, meningismus, altered sensorium, 75% (3/4) for hemiparesis, and 83.3% (5/6) for epilepsy.
**Conclusion:** Punctures of brain abscesses with subsequent aspiration can be performed safely and accurately by monitoring the procedure using an open interventional MRI system.

# Intraoperative Targeting, Trajectory Planning, Device Insertion and Infusion Monitoring with Real-Time MRI

Walter F. Block[1,3], Ethan K. Brodsky[1,3], Andy L. Alexander[1,3], Ben P. Grabow[1], Sam A. Hurley[1], Chris D. Ross[3], Karl A. Sillay[1,3]
[1]University of Wisconsin, Madison, WI USA; [2]Engineering Resources Group, Inc., Pembroke Pines, FL, USA
[3]inseRT inc, a MRI therapeutic development company

**Purpose** MR guidance can enhance and/or enable several intraoperative surgical procedures [1-3], particularly with therapy and drug delivery related to Parkinson's disease (PD). However, development of these technologies is complicated by the need for task-oriented visualization of 2D and 3D datasets, flexible real-time image processing pathways, and interfaces with proprietary scanner hardware. We present initial work on a system for MR-guided and monitored convection enhanced delivery (CED) of intracerebral infusions.

**Methods** The system provides rapid aiming of an FDA-approved MR-visible trajectory guide, monitoring of the insertion of an FDA-approved rigid catheter, and infusion of MR-visible agents. This system was developed as a set of plug-ins for the RTHawk MR development environment (HeartVista; Palo Alto, CA) [4] and Vurtigo visualization environment (Sunnybrook HSC, Toronto, Canada) [5]. Together, these platforms compose an extensible architecture that simplifies the development of real-time applications.

A rigid, fused silica catheter was aimed and inserted through the Navigus pivot-point-based aiming system (Medtronics; Minneapolis, MN), which includes a ball-joint pivot base and a MR-visible external trajectory guide. Testing was conducted using a GE Healthcare 1.5 T Signa scanner, targeting the putamen in ex-vivo non-human primate brains.

The system uses a high-resolution 3D scan as a roadmap from which a neurosurgeon manually selects a brain target and device pivot point. The system then automatically calculates four real-time imaging planes that guide the neurosurgeon while aligning the yaw and pitch of the trajectory. Once aligned, the catheter is advanced to the indicated depth, while being monitored with real-time MR. Dilute MR contrast was then injected under pressure through the catheter. Multiple monitoring planes can be visualized simultaneously using a $T_1$-weighted GRE sequence that acquires a 20 cm FOV with 0.8 mm resolution at 1.4 s per slice.

**Results** Initial trials show that the catheter can be inserted such that the tip is within 1.5 mm of the target. Device insertion times dropped to 15 minutes while previous manual methods took up to 90 minutes.

**Conclusions** The system provides an intuitive method for reliable planning, alignment, and insertion of devices within a brain. The platform will be extended to merge mapping of the putamen vasculature to aid in catheter placement and quantitative T1 imaging for infusion mapping.

**Acknowledgements:** We acknowledge the support of the Kinetics Foundation and GE Healthcare for this research.

**References** [1] Martin AJ, et al., MRM 54(5):1107 ('05) [2] Bankiewicz, et al., Exp Neurol. 2000 Jul;164(1):2-14. [3] Richardson et al. Mol Ther. 2011 Jun;19(6):1048-57. [4] Santos JM, et al., Proc. IEEE EMBS 26:1048 ('04) [5] Pintilie S, et al., Proc. ISMRM 19:6887 ('11)

**Fiber tract detection using fMRI-DTI landmark distance atlases**

Lauren J. O'Donnell, Laura Rigolo, Isaiah Norton, Carl-Fredrik Westin, and Alexandra J. Golby

Golby Lab, Dept. Neurosurgery, BWH
Lab for Mathematics in Imaging, Dept. Radiology, BWH
Harvard Medical School

**Purpose**:
Motivated by the fact that a white matter tract and related cortical areas are likely to displace together in the presence of a mass lesion (brain tumor), in this work we propose a rotation and translation invariant model that represents the spatial relationship between fiber tracts and anatomic and functional landmarks. This landmark distance (LD) model can be used for detection of fiber tracts. We performed two experiments to assess the robustness of the LD model to brain displacements caused by mass lesions.

**Methods**:
5 healthy control right-handed subjects and 3 patients with brain tumors were studied. fMRI was acquired during the following tasks: antonym generation, noun categorization, left and right hand clench, left and right foot toe wiggle, and lip pursing. Structural (SPGR) and diffusion weighted images (EPI) were acquired. 10 fMRI peaks (vision, hand, foot, and lip motor for each hemisphere, and putative Broca's and Wernicke's areas) and 5 anatomical landmarks (in anterior/posterior corpus callosum, anterior commissure, and cerebral peduncles) were selected for each subject using 3D Slicer. We constructed landmark distance atlas (LDA) models from the normal controls using distances between their fiber tracts (arcuate fasciculus or AF and corticospinal tract or CST) and fMRI/anatomical landmarks.

We proposed 4 distance measures for use in detecting tracts based on the LDA. In the first experiment, each LDA and measure were tested for robustness to several synthetic brain deformations of the magnitude expected due to a mass lesion. Detected tracts were compared to expected tracts to determine the most successful distance measure for tract detection. Then in the second experiment, the best performing distance measure was applied to detect tracts in the patients with mass lesions.

**Results**:
Results from experiment 1 indicate that the LDA is robust to synthetic displacements of the magnitude expected due to mass lesions: the mean fiber similarity measure across all pairs of detected and expected fibers in AF and CST was greater than 0.8. For the synthetic displacements studied, the proposed measure based on percent error was the most robust measure for tract detection. The results from the second experiment showed that for AF and CST, the LDA generalized well to a small group of patients with mass lesions.

**Conclusions**:
Our initial results demonstrate that the LD model is robust to displacement. Our results are preliminary but promising, and the method provides a new way to transfer atlas information to individual patients.

**Acknowledgements**:
NIH 1R21CA156943-01A1, P41RR019703, P01CA067165, R01MH074794, R25CA089017, R01MH092862, P41RR013218, Klarman Family Foundation, and Brain Science Foundation.

# Posters on Bone and Musco-skeletal IGT

1. Intravascular 3.0T MRI of Bone Marrow-derived Stem-Progenitor Cell Migration to Injured Arteries for Potential Repair.
   Yanfeng Meng, Feng Zhang, Bensheng Qiu, Xiaoming Yang, University of Washington

2. MR Image Overlay Adjustable Plane System for Percutaneous Musculoskeletal Interventions
   Paweena U-Thainual,Tamas Ungi, John A. Carrino, Gabor Fichtinger, Iulian Iordachita
   Queen's University, Kingston, ON, Canada,The Johns Hopkins University, Baltimore, MD

3. Perk Station image overlay improves training of facet joint injections
   Tamas Ungi, Paweena U-Thainual, Caitlin T. Yeo, Andras Lasso, Robert C. McGraw, and Gabor Fichtinger, Queen's University, Kingston ON, Canada

# Intravascular 3.0T MRI of Bone Marrow-derived Stem-Progenitor Cell Migration to Injured Arteries for Potential Repair

Yanfeng Meng, Feng Zhang, Bensheng Qiu, Xiaoming Yang

Image-Guided Biomolecular Intervention Section, Department of Radiology,

University of Washington

**Purpose:** To validate the feasibility of using intravascular 3.0T MRI to track migration of bone marrow-derived stem-progenitor cells to the injured arteries for potential cell-based repair.

**Methods:** This study consisted of two portions: (1) developing an intravascular 3T MRI technique by using an MR imaging-guidewire (MRIG), and (2) validating the feasibility of using intravascular 3T MRI to track auto-transplanted bone marrow cells (BMCs) that migrated to injured arteries. In the first portion, we produced a 0.032-inch MRIG that was made of a nitinol coaxial cable with an extended 3.2-cm inner conductor. Compared to surface coils, we first evaluated, in vitro, the functions of the MRIG using a phantom. We then used the MRIG to generate intravascular 3T MRI of ten arteries of six pigs, which were compared to surface coils (TR/TE=5000/40ms). Signal-to-noise ratios (SNR) were calculated and compared between the MRIG and surface coils. In the second portion, thirteen pigs were divided into two study groups with (i) auto-transplantation of MR-labeled BMCs; and (ii) non-labeled BMC or no cell transplantation. BMCs were extracted from the iliac crests of pigs and then labeled with a T2 contrast agent, Feridex, and/or a fluorescent tissue marker, PKH26. Before cell transplantation, the pigs underwent ultrasound-guided, endovascular balloon-mediated intimal injuries of the iliofemoral arteries. The labeled or un-labeled BMCs were then auto-transplanted back to the same pig. Three weeks later, intravascular 3T MRI was performed to detect BMCs migrated to the injured arterial sites, with subsequent MRI-histologic confirmation and correlation.

**Results:** Of the first portion experiments, intravasclar 3T MRI displayed the iliofemoral arterial walls more clearly than surface coils. The average SNR of iliofemoral arterial wall images using the MRIG was significant higher than that using the surface coils (76.22±34.76 vs. 12.63±4.25, $P<0.01$). Of the second portion experiments, intravascular 3T MRI detected clearly signal voids of the arterial walls due to Feridex/BMCs migrated to the injured arteries, which were confirmed by histology correlation.

**Conclusion:** This study has validated the feasibility of generating an intravascular 3T MRI of iliofemoral arteries and demonstrated the capability of using clinical 3T MRI to monitor autotransplantation of BM cells that migrate to the injured arteries in near-human-sized animals, which may open new avenues to effectively monitor the stem-progenitor cell-based therapy of injured arteries.

## MR Image Overlay Adjustable Plane System for Percutaneous Musculoskeletal Interventions

Paweena U-Thainual[1],Tamas Ungi[2], John A. Carrino[4], Gabor Fichtinger[2], Iulian Iordachita[3]

[1]Queen's University, Department of Mechanical and Materials Engineering, Kingston, ON, Canada
[2]Queen's University, School of Computing, Kingston, ON, Canada
[3]The Johns Hopkins University, ERC/LCSR, Baltimore, MD, US
[4]Johns Hopkins University School of Medicine, Russell H. Morgan Department of Radiology and Radiological Science, Baltimore, MD, US

* This work is supported by NIH Grants: R01 CA118371 A2 and Cancer Care Ontario

### Purpose
The 2D MR image overlay system (IOS) concept and its clinical feasibility have been evaluated and successfully proved in MSK procedures. However, IOS image plane is vertical, limiting the insertion at the scanner axial plane. In many cases of MSK procedures, such as joint arthrography and facet joint injections, the optimal access to target requires an oblique insertion plane. To overcome such problems, we have developed the *MR image overlay adjustable plane system (IOAPS).* The challenges remain due to the strong magnetic field and confined operating space.

### Methods
MR image overlay adjustable plane system (IOAPS) is an advanced version of the IOS. It has 4 degrees of freedom of motion (two translations and two rotations), manually actuated. These motions are indicated by calibrated encoders attached to the moving joints. The IOAPS consists of two main units; 1) *out-of-room unit* consisting of an interconnection box, a power control box, and a laptop and 2) *in-room unit* placed next to the MRI scanner and consisting of a fully MR-compatible monitor, linear and rotary motion encoders, a sensor control box, a transverse plane laser, an MRI-compatible keyboard, a semi-transparent mirror, and a supporting aluminum frame. The aluminum frame carries the weight of all devices and provides the motion of ±100 mm (in X-Y directions) and ±25° (around X-Y axes). The MR-compatible monitor (18-inch, RF shielded LCD monitor, Siemens Corp) allows the operator to work within 60 cm from the bore, thus minimizing table translation. The system was designed to allow for sufficient working space to execute multiple oblique needle insertions. A system workflow and calibration processes were designed.

### Results
The IOAPS has been successfully designed and built. The new system calibration is more challenging compared to IOS. Modules of the in-room unit have been tested. Technical validation of the IOAPS is currently in progress.

### Conclusions
We report the design and implementation of an MR image overlay system with adjustable imaging plane, with the objective of assisting the interventionalist in performing MR-guided needle insertion in oblique planes.

# Perk Station image overlay improves training of facet joint injections

Tamas Ungi, Paweena U-Thainual, Caitlin T. Yeo, Andras Lasso, Robert C. McGraw, and Gabor Fichtinger

*Queen's University, Kingston ON, Canada*

**Purpose**

Image guided injection into the facet joint of the spine is a skill demanding manual procedure even for operators with prior experience in needle-based medical interventions. Our hypothesis is that the augmented reality environment of the Perk Station provides trainees with a visual experience of facet joint injections that retains, and causes improvement in their performance even in the standard clinical setup without augmented reality guidance.

**Methods**

Forty medical and biomedical engineering students participated in this study as subjects on a voluntary basis. They were randomized into two groups. The Overlay group (n=20) performed four training insertions on a simulation facet joint phantom with image and laser overlay, followed by two training insertions with laser-only overlay. The Control group (n=20) was given the opportunity to practice six insertions on the same phantom with the freehand method. After the training sessions both groups participated in an evaluation session with freehand method. The needle was tracked, and its trajectory was recorded throughout both the training and the evaluation sessions. Procedure time, needle placement accuracy, and potential tissue damage were calculated off-line from the recorded needle trajectories. Interactive modules for the 3D Slicer application were developed both for the recording and the off-line evaluation of needle trajectories.

**Results**

The total needle insertion time seemed to converge to 62 s in both groups. Potential tissue damage caused by the needle was lower in the Overlay group for all insertions, and it remained significantly lower when the group performed the freehand insertion. Success rate was higher in the Overlay group when receiving additional guidance for the first six insertions, and remained higher during the freehand insertions.

**Conclusions**

Augmented reality image overlay of the Perk Station during training improves the performance of medical trainees even when they perform freehand facet joint injections after the training session. Augmented and virtual reality simulators have a great potential in the teaching of needle-based medical procedures.

FRIENDS OF AMIGO

July 2011, Issue 2

*Advanced Multimodality Image Guided Operating Suite*

# BWH Unveils "Unprecedented Opportunity and One-Of-A-Kind Setting"

On May 4, 2011, Brigham and Women's leapt into the future of image guided therapy with the much anticipated unveiling of the AMIGO suite. After years in the making, AMIGO was finally ready to open its doors to the world. Inside this space, cutting-edge surgical procedures will be introduced, tested and perfected for the benefit of patients througout the world.

There was a palpable air of anticipation on the morning of the ribbon-cutting ceremony. With the event scheduled to start at noon, AMIGO's ambassadors and tour guides – people like Flow Coordinator Sean Jackson and Head Nurse Angela Kanan – bustled about, making sure the space would be shown in its finest to the day's visiting dignitaries. Director of Surgical Services and Program Development and AMIGO Administrator, Rachel Rosenblum, conferred with Suzanne Leidel, the Development Office's Event Coordinator, to review the planned activities one last time and make sure everything was in place. Anticipation spiked when Suzanne's event team hung a royal blue ribbon across the doorway leading to AMIGO's PET/CT room.

On the main floor of the Shapiro Cardiovascular Center, Danielle Chamberlain, Executive Assistant to Ferenc A. Jolesz, MD and Clare M. Tempany, co-Directors of the AMIGO surgical interventional suite, draped spotless white linen over the table where she would be checking in guests and having them complete the MR safety screening to be able to enter the suite. Around 11 o'clock, the first guests started to arrive. Befitting the magnitude of AMIGO's anticipated impact on surgical care, the ribbon-cutting brought together some of the most influential people in the field of Image Guided Therapy. All told, close to 100 guests attended the ribbon-cutting.

As they arrived, the guests were put into small groups for guided tours of the three-room AMIGO facility. During one of the tours, Neurosurgeon and AMIGO Associate Medical Director Alexandra Golby, MD, spoke about the collaborative spirit that imbues everything about the AMIGO suite. The multidisciplinary nature of the project was critical in the planning stages, and will continue to be key to AMIGO's success.

"From the beginning, this has been a multidisciplinary project, relying on expertise from clinicians, engineers, medical physicists, project managers, architects, contractors and facility supervisors," Dr. Golby said. "And our expertise here at the Brigham will continue to drive us in this area. Everyone from nurses and technicians, to people in the research community, brings a huge amount of expertise that is critical to AMIGO's success."

When it was time for the speaking portion of the event to start, a handful of the guests remained in the suite itself. The rest watched from the control room, where screens displayed live images taken on AMIGO's custom built A/V system. Steven E. Seltzer, MD, the Master of Ceremonies, stood in front of the blue ribbon and introduced the day's speakers: BWH President Betsy Nabel, MD, Dr. Tempany and Dr. Jolesz.

Speaking first, Dr. Nabel highlighted hospital leadership's on-going institutional support for AMIGO. The work that will take place in the suite will maintain the Brigham's leading international profile in the field of image guided therapy.

"The availability of advanced imaging modalities in AMIGO's highly integrated environment represents an unprecedented opportunity and a one-of-a-kind setting," said Dr. Nabel. "The investment in AMIGO further reflects BWH's commitment to providing the highest quality health care to patients and their families and to expanding the boundaries of medicine through research."

Dr. Tempany spoke next, sharing her appreciation for what the project team accomplished.

"I want to thank you all for being here for this special day. To get to where we are, celebrating the opening of the AMIGO suite, took years of planning and the unwavering focus and invaluable contributions of dozens of colleagues and co-workers," said Dr. Tempany. "Knowing the work you all poured into this project, I hope you all hold your heads a little higher today. You have helped to create a space where image guided therapies will be tested and perfected and to be put into practice for the benefit of patients around the world."

Dr. Jolesz was the final speaker *(turn to page 4 for the full text of Dr. Jolesz's thank you speech)*. Roundly considered the forefather of image guided therapy, it was his vision that pushed the project through the many challenges encountered along the way. The result is a first-of-its-kind surgical space.

"This is the first suite in the world to bring all of these imaging modalities into one integrated operating room," said Dr. Jolesz. "The three-room complex that you see today will be used by a multidisciplinary team of radiologists, surgeons, engineers, computer scientists and physicists. While the construction is over, the innovation is just beginning."

# The AMIGO Suite Equipment Array

**MRI: Siemens 3T Verio 70 cm Wide Bore**: This ceiling-mounted MRI moves into the operating room and over the patient for pre- or intraoperative imaging. Its 3T field strength arms clinicians with the highest resolution MR imaging possible.

**PET/CT: Siemens mCT 40 Slice/4 Ring**: Combining structural and functional imaging, the dual PET and CT scanner will be used as a stand-alone system and in pre- and intraoperative circumstances under research protocols to better locate and characterize disease and any needed treatment. This PET/CT will also be the device used for the BWH to investigate new radiotracers, under research protocols, that have never before used in medicine. The BWH's nearby Cyclotron can produce these agents for safe intravenous administration.

**BrainLAB Navigation**: This neurosurgical system uses a GPS-like device to track hand-held tools. MRI and PET/CT images are registered to the patient's coordinate system and interactively viewed based on where in the body the clinician is pointing with a tool.

**Zeiss Pentero Surgical Microscope**: Used in delicate brain tumor resections and vascular surgery, the scope is equipped with a feature to visualize dyes in the blood stream that help to identify blood vessels. AMIGO clinicians can track the scope with the BrainLAB navigation system to display MRI or PET/CT images in the focal plane of the scope.

**Integra Ultrasonic Aspirator**: Used in delicate brain tumor resection, AMIGO researchers plan to capture the intact cells liberated by this device and analyze them to determine if any tumor tissue remains in the brain following an intervention.

**IntraMedical Imaging Node Seeker and Beta Probe**: This device assesses whether a surgical procedure has been fully completed by detecting traces of a radioactive isotope that is injected into the bloodstream after a tumor is removed. If radiation is detected from the excised tumor specimen, the surgeon can conclude that there is still tumor in the body and surgery should continue.

**Visualase Medical Laser**: This laser will be used to remove cancerous tumors and diseased tissues. A laser fiber is placed through the skin into the target, and real-time MR images let the interventionist monitor the devices heat deposition to determine when the target is successfully treated.

**Galil Medical Cryohit**: Used for intervention with cold temperatures, a needle-like probe is placed into the tumor through the skin. Radiologists monitor the frozen area of tissue with either MRI and/or CT as targeted tissue is destroyed.

**B-K Medical Systems Ultrasound**: Unlike conventional ultrasound systems, the B-K Medical Systems device has unique probes that can go inside the abdomen to aid in endoscopic-guided surgery or through an opening in the skull or the sinuses to aid in brain tumor resection.

**Siemens S2000 Ultrasound**: For all other ultrasound applications, the Siemens S2000 will be used for both tumor identification and targeting.

**Sentinelle Medical (Hologic) Aegis Navigation Workstation:** This system enables the clinician to track probes from either of the ultrasound systems. Previously-acquired MRI or PET/CT images can be displayed in the same plane as the real-time ultrasound image.

**Sentinelle Medical (Hologic) Aegis Ultrasound**: This device will enhance MR image quality for interventional treatment of prostate and cervical cancer.

**Robin Medical Endoscout:** Using dynamic magnetic fields produced during MR imaging to track needles and probes, this device gives clinicians the ability to visualize device location on MR images when the patient is inside the scanner, facilitating real-time MRI-guided procedures.

**Northern Digital Polaris Vicra Optical Tracking System, Aurora Electromagnetic Measurement System and Ascension Technology 3D Guidance MedSAFE Electronic Unit**: These systems allow BWH researchers to build navigation applications based on the in-house image processing software, which is called the 3D Slicer.

**Cardiac Equipment:** While intra-procedural MRI is the novel aspect of catheter-based MRI-guided cardiac ablation, which is why it finds a home in AMIGO, much specialized cardiac equipment must join it to allow for successful outcomes. These devices and components include: a **St. Jude Medical Mapping and Navigation System** that enables the clinician to identify the source of the arrhythmia and guide the catheter to the target location; a **Fischer Bloom Stimulator** that is used to pace the heart in conjunction with the **GE CardioLab Hemodynamic** recording system that is used to monitor the heart to determine when the ablation is complete. **Boston Scientific** and **Stockert** RF ablation generators will both be used for their unique abilities to deliver therapeutic energy to the target heart tissue. Boston Scientific and **Siemens Intra-Cardiac Echo** will be used to visualize the myriad of catheters in the chambers of the heart. Finally, **OptoAcoustics MRI Compatible Communication Headsets** will facilitate communication between the clinicians and the technologists' operating equipment in the control room.
**In Vivo Vital Signs Monitor** and **GE Datex-Ohmeda Anesthesia Gas Delivery Machine**: These systems are both MRI-compatible and are critical in caring for the patient during operations.

**AMIGO Infrastructure:** ETS-Lindgren provided shielding for use of the MRI in the suite and provided the industry's widest doors to enable the MRI scanner to travel between the MRI room and the OR. Nelco provided the rooms' lead shielding to safely use radioisotopes for PET imaging and x-ray for CT and angiography imaging. Trumpf provided the AMIGO OR's lights and booms. The lights are LED, providing a range of light colors to suit a particular surgery without generating heat that could make it uncomfortable for clinicians and other staff.

The video integration is provided by **Black Diamond Video**. Images can be routed to monitors in our control room or procedures room via a touchscreen. Recording and streaming is also possible. The most important aspect of the Black Diamond system is that it solves a critical space problem. These same touchscreens become the user interface for several different workstations that would not have all fit in the packed control rooms. A 56" monitor suspended from a boom creates a montage of images from different sources to visualize all available information at a glance.